# ATTACHMENT 1: SITE-SPECIFIC SEISMIC HAZARD STUDY

SUSITNA-WATANA HYDRO

*Clean, reliable energy for the next 100 years.*

**Report**
**15-03-REP**
**v0.0**

# Susitna-Watana Hydroelectric Project
# Site-Specific Seismic Hazard Study Summary Report
***(Attachment 1 to Study Completion Report 16.6)***

**AEA11-022**


***Prepared for:***
**Alaska Energy Authority**
813 West Northern Lights Blvd.
Anchorage, AK 99503

***Prepared by:***
**MWH**
1835 South Bragaw St., Suite 350
Anchorage, AK 99508


**October 2015**

[This page intentional blank]

# TABLE OF CONTENTS

# LIST OF FIGURES

# LIST OF TABLES

# LIST OF ACRONYMS, ABBREVIATIONS, AND DEFINITIONS

| Abbreviation | Definition |
|---|---|
| AEA | Alaska Energy Authority |
| AEC | Alaska Earthquake Center |
| AFE | Annual Frequency of Exceedance |
| ASZ | Alaskan Subduction Zone |
| BC | British Columbia |
| BOC | Board of Consultants |
| DEM | Digital Earth Model |
| DGGS | Alaska Department of Geological & Geophysical Surveys |
| DSHA | Deterministic Seismic Hazard Assessment |
| FERC | Federal Energy Regulatory Commission |
| ft | Foot |
| GF | Geologic Feature |
| GMPE | Ground Motion Prediction Equations |
| in | Inch |
| INSAR | Interferometric Synthetic Aperture Radar |
| ILP | Integrated Licensing Process |
| IMASW | Interferometric Multichannel Analysis of Surface Waves |
| ISR | Initial Study Report |
| Ka | Kiloannum |
| km | Kilometer |
| LiDAR | Light Detection and Ranging |
| m | Meter |
| M | Magnitude |
| mm | Millimeter |
| Mmax | Maximum Magnitude |
| Mw | Moment Magnitude |
| MCE | Maximum Credible Earthquake |
| MDE | Maximum Design Earthquake |
| mi | Mile |
| NFFTB | Northern Frontal Fold and Thrust Belt |
| NGA | Next Generation Attenuation |

| Abbreviation | Definition |
|---|---|
| OBE | Operating Basis Earthquake |
| OSL | Optically-Stimulated Luminescence |
| PHA | Peak Horizontal Acceleration |
| PRM | Project River Mile |
| PSHA | Probabilistic Seismic Hazard Assessment |
| RCC | Roller Compacted Concrete |
| RSP | Revised Study Plan |
| RTS | Reservoir Triggered Seismicity |
| SA | Spectral acceleration |
| SAB | Southern Alaska Block |
| sec | Second |
| SPD | Study Plan Determination |
| UHS | Uniform Hazard Spectra |
| USACE | United States Army Corps of Engineers |
| USGS | United States Geological Survey |
| Vs | Shear Wave Velocity |
| Vs30 | Average Shear Wave Velocity in the Top 100 Feet (30 Meters) |
| WCC | Woodward Clyde Consultants (AECOM) |

# EXECUTIVE SUMMARY

The proposed Susitna-Watana Dam is a hydroelectric power development project planned for the upper Susitna River. As proposed, the project would involve the construction of a dam, reservoir and power facilities on the Susitna River at project river mile (PRM) 187, approximately 34 miles upstream of Devils Canyon. The current proposed project is a curved gravity dam, approximately 705 ft. high, constructed using the roller compacted concrete (RCC) methodology.

The proposed Watana Dam is regulated by the Federal Energy Regulatory Commission (FERC). This study was performed at the request of AEA in accordance with the FERC Engineering Guidelines for the Evaluation of Hydropower Projects (FERC, 2014) and a Draft version of Chapter 13, Evaluation of Earthquake Ground Motions (Idriss & Archuleta, 2007) guidelines, and with direction from the FERC.

The purpose of this report is to provide FERC with the finalized Section 16.6 of the RSP for the current licensing initiative which was filed on December 14, 2012. Section 16.6 is described as the Site-Specific Seismic Hazard Study and focuses on conducting deterministic and probabilistic seismic hazard evaluations to estimate earthquake ground motion parameters at the Project site, assessing the risk at the site and the loads that the Project facilities would be subject to during and following seismic events, and proposing design criteria for Project facilities and structures considering the risk level This report is a compilation of technical memorandums, reports and the Engineering Feasibility Report:

- Fugro Consultants, Inc., (FCL), (2012), Seismic Hazard Characterization and Ground Motion Analyses for the Susitna-Watana Dam Site Area, prepared for Alaska Energy Authority, Technical Memorandum No. 4, Dated February 24, 2012, 146 pages and 4 Appendices.

- Fugro Consultants, Inc., (FCL), (2013), Lineament Mapping and Analysis for the Susitna-Watana Dam Site, prepared for Alaska Energy Authority, Technical Memorandum No. 8, Dated March 27, 2013, 61 pages plus figures, plates, and 1 appendix.

- MWH, (2013a), Preliminary Reservoir Triggered Seismicity, prepared for Alaska Energy Authority, Technical Memorandum No. 10 v3.0, Dated March 29, 2013, 95 pages.

- MWH, (2013b), Preliminary Reservoir Slope Stability Assessment, prepared for Alaska Energy Authority, Technical Memorandum No. 12, Dated September 18, 2013, 43 pages and 3 Attachments.

- MWH, (2014a), Briefing Document – Discussion of MCE and OBE, prepared for Alaska Energy Authority, Technical Memorandum No. 14-13-BD, Dated April 30, 2014, 6 pages.

- MWH, (2014c), Engineering Feasibility Report for the Susitna-Watana Dam, prepared for Alaska Energy Authority, December 2014.

- Fugro Consultants, Inc. (FCL) (2014a). Watana Seismic Network Station Vs30 Measurements for the Susitna-Watana Dam Site, prepared for Alaska Energy Authority, Technical Memorandum No. 14-12-TM, Dated March 20, 2014, 51 pages and 1 Appendix.

- Fugro Consultants, Inc., (FCL), (2014b), Revised Intraslab Model and PSHA Sensitivity Results for the Susitna-Watana Dam Site Area, prepared for Alaska Energy Authority, Technical Memorandum No. 14-11-TM, Dated April 25, 2014, 31 pages.

- Fugro Consultants, Inc., (FCL), (2014c), Seismic Network 2013 Annual Seismicity Report for the Susitna-Watana Dam Site Area, prepared for Alaska Energy Authority, Technical Memorandum No. 14-06-REP, Dated March 14, 2015, 40 pages.

- Fugro Consultants, Inc., (FCL), (2015a), Crustal Seismic Source Evaluation for the Susitna-Watana Dam Site, prepared for Alaska Energy Authority, Report No. 14-33-REP, Dated May 2015, 141 pages and 3 Appendices.

- Fugro Consultants, Inc., (FCL), (2015b), Seismic Network 2014 Annual Seismicity Report for the Susitna-Watana Dam Site Area, prepared for Alaska Energy Authority, Technical Memorandum No. 14-32-REP, Dated March 31, 2015, 55 pages.

- Alaska Earthquake Information Center (AEC). (2015), Susitna-Watana Seismic Monitoring Project: January –June 2015 Report, prepared for the Alaska Energy Authority, September 2015, 43 pages.

This report summarizes our current investigations and engineering to date, however given the iterative nature of these reports some initial studies have not incorporated results from subsequent studies.

An initial seismic hazard characterization and ground motion analysis for the proposed Project site, this technical memorandum includes the seismotectonic setting, historical seismicity, seismic source characterization, applicable ground motion prediction equations, probabilistic seismic hazard analysis (PSHA), and deterministic seismic hazard analysis (DSHA) (Fugro, 2012). Subsequent lineament mapping and analysis was based on digital imagery as well as the

seismic sources identified in the initial seismic hazard analysis (Fugro, 2013). Focused studies were then performed for the local crustal seismic sources / faults (Fugro, 2015a) and the subduction intraslab (Fugro, 2014b).

A long-term earthquake monitoring system was created in August-September 2012, and expanded in 2013. Details regarding the earthquake event data are documented in various reports (Fugro, 2014c, 2015b; AEC, 2015). The earthquake monitoring system was installed to monitor earthquake activity and to record strong shaking of the ground in the Project area during moderate to strong earthquakes. Data obtained from this monitoring system has been used to refine the intraslab model (Fugro, 2014b), check the source characterization of background sources (Fugro, 2015a), define the focal mechanisms for the larger detected earthquakes, and provide a background level of seismicity to monitor reservoir triggered seismicity (RTS).

Studies regarding earthquake hazards such as RTS, a dam site area fault rupture, and reservoir rim slope stability were also performed. Current literature and empirical relationships were used to evaluate the potential for RTS (MWH, 2013a). Site investigations were performed which included: LiDAR (Light Detection and Ranging), INSAR (Interferometric Synthetic Aperture Radar), geologic mapping, drilling and in situ testing, instrumentation installation and monitoring, and laboratory testing. These site investigations were used to update the terrain units and complete a preliminary evaluation of the reservoir rim slope stability (MWH, 2013b) and also provide necessary data to evaluate the dam site area fault rupture evaluation, included in the Crustal Source Evaluation (Fugro, 2015a).

For Watana Dam, maximum credible earthquake (MCE) ground motions were estimated following FERC guidelines using deterministic seismic hazard analysis (DSHA), while the maximum design earthquake (MDE) was defined based on the 5,000-year return period ground motions from a probabilistic seismic hazard analysis (PSHA). The operating basis earthquake (OBE) was selected to be the 500 year return period from the PSHA. Table ES-1 summarizes the peak ground acceleration resulting from the MCE, MDE and OBE (see additional details regarding the seismic design criteria in MWH, 2014a, 2014b).

**Table ES-1. Peak Ground Acceleration Values for the MCE, MDE and OBE**

| CASE | DESIGN EVENT | PGA |
|---|---|---|
| MCE | Deterministic | 0.81g |
| MDE | 5,000-yr Return Period | 0.66g |
| OBE | 500-yr Return Period | 0.27g |

Finally, the report concludes with a discussion on the design response spectra and the development of time histories. Additional details on the development of time histories can be found in the Engineering Feasibility Report (MWH, 2014b; Appendix B6).

# 1. INTRODUCTION

## 1.1. Background

The purpose of this report is to develop an assessment of the seismic hazard potential relating to the Watana Dam which is part of the Susitna-Watana hydroelectric project (FERC Project No. 14241) located in Matanuska Borough, Alaska.

The Susitna- Watana hydroelectric project ("Project") will be a major development on the Susitna River some 120 mi (193 km) north and east of Anchorage and about 75 mi (121 km) south of Fairbanks.

As proposed, the project would involve the construction of a dam, reservoir and power facilities on the Susitna River at Project river mile (PRM) 187, approximately 34 miles (55 km) upstream of Devils Canyon.

An application for a FERC license for the Susitna-Watana hydroelectric project was submitted to FERC under FERC number P-7114 in 1983, with the application being subsequently amended under the same number in 1985. That application was withdrawn in March 1986.

The current proposed project is significantly smaller than that previously proposed, but includes a curved gravity dam - of a height of approximately 705 ft. (215 m) – constructed using the roller compacted concrete (RCC) methodology. This choice of dam was made after comparison of an Earth Core Rockfill dam, a Concrete Faced Rockfill dam, and a Roller Compacted Concrete dam.

As part of the current licensing initiative, on December 14, 2012, Alaska Energy Authority (AEA) filed with the Federal Energy Regulatory Commission (FERC or Commission) its Revised Study Plan (RSP), which included 58 individual study plans. Section 16.6 of the RSP described the Site-Specific Seismic Hazard Study. This Study Plan focuses on conducting deterministic and probabilistic seismic hazard evaluations to estimate earthquake ground motion parameters at the Project site, assessing the risk at the site and the loads that the Project facilities would be subject to during and following seismic events, and proposing design criteria for Project facilities and structures considering the risk level. RSP 16.6 provided goals, objectives, and proposed methods for data collection regarding seismic hazards.

On February 1, 2013, FERC staff issued its study plan determination (February 1 SPD) for 44 of the 58 studies, approving 31 studies as filed and 13 with modifications. RSP Section 16.6 was one of the 31 study plans approved with no modifications.

Following the first study season, FERC's regulations for the Integrated Licensing Process (ILP) required AEA to "prepare and file with the Commission an initial study report describing its overall progress in implementing the study plan, schedule and the data collected, including an explanation of any variance from the study plan and schedule." (18 CFR 5.15(c)(1)) An Initial Study Report (ISR) on the Site Specific Seismic Hazard Study was prepared in accordance with FERC's ILP regulations and detailed AEA's status in implementing the study, as set forth in the FERC-approved RSP.

*This document records the completed initial Site Specific Seismic Hazard Study for feasibility and licensing. For detailed design, certain studies would be undertaken to incorporate additional data to be collected and update the seismic hazard analysis. Tasks may include:*

- *Update the crustal seismic source characterization based on new data obtained for design of the project (rock structure and shear wave measurements at the dam site)*
- *Update the ASZ and worldwide subduction zone data will be needed to develop appropriate weighting of uncertain parameters such as Mmax*
- *Subduction fault model and source characterization*
- *Revise areal source zones with recorded seismicity*
- *Update probabilistic seismic hazard analysis (PSHA)*
- *Update ground motion prediction equations (GMPE)*
  - *NGA West2*
  - *Subduction*

## 1.2. Regulators

The proposed Watana Dam is regulated by the Federal Energy Regulatory Commission (FERC). The Watana Dam has been evaluated using FERC Engineering Guidelines for the Evaluation of Hydropower Projects (FERC, 2011). Guidance for the evaluation of seismic hazards is provided under a Draft version of Chapter 13, Evaluation of Earthquake Ground Motions (Idriss & Archuleta, 2007). These guidelines were released for review and further development by the FERC, but have been used for several years in draft form. The regulatory process for seismic hazard evaluation defined by the FERC specifies that both probabilistic and deterministic evaluations be conducted. This study was performed at the request of AEA in accordance with these guidelines, and with direction from the FERC.

The "Maximum Design Earthquake" (MDE) may be selected between the 2,500 year event and the maximum credible earthquake (MCE). The dam and appurtenances must also be designed to resist the Operating Basis earthquake (OBE) representing the ground motions or fault movements from an earthquake considered to have a reasonable probability of occurring during the functional life-time of the project. All critical elements of the project (such as dam,

appurtenant structures, reservoir rim, and equipment) should be designed to remain functional during the OBE, and any resulting damage should be easily repairable in a limited time. For a Class I dam, the OBE can be defined based on probabilistic evaluations, with the level of risk (probability that the magnitude of ground motion will be exceeded during a particular length of time) as a probabilistic event with a return period between 150 and 250 years or greater return frequency.

For Watana Dam, MCE ground motions were estimated following FERC guidelines using deterministic seismic hazard analysis (DSHA), while the MDE was defined based on the 5,000-year return period ground motions from a probabilistic seismic hazard analysis (PSHA). The OBE was selected to be the 500 year return period from the PSHA.

## 1.3. Objective

The goals of this study were to conduct deterministic and probabilistic seismic hazard evaluations to estimate earthquake ground motion parameters at the Project site, assess the risk at the site and the loads that the Project facilities would be subject to during and following seismic events, and propose design criteria for Project facilities and structures considering the risk level. The intent of the study is to fulfill specific objectives including, but not limited to the following:

- Identify the seismic sources along which future earthquakes are likely to occur, including the potential for reservoir-triggered seismicity;
- Characterization of the degree of activity, style of faulting, maximum magnitudes, and recurrence information of each seismic source;
- Develop maps and tables depicting the spatial and geometric relations of the faults and seismic source zones together with specific distance parameters to evaluate ground motion parameters from each source;
- Assemble available historical and instrumental seismicity data for the region, including maximum and minimum depth of events;
- Determine the distance and orientation of each fault with respect to the site;
- Estimate the earthquake ground motions at the proposed dam site, updating previous studies to include changes in practice and methodology since the 1980s;
- Propose the seismic design criteria for the site; and,

- Use the appointed Board of Consultants (BOC) for independent technical review and guidance during development of site-specific studies.

The Supporting Design Report prepared for the FERC license application will include the seismic criteria determined herein, and the results of dam stability analysis under seismic loading.

## 1.4. Study Area

The study area for the seismic hazard evaluation was necessarily large in order to include potentially significant seismic sources throughout the region. The study area encompassed subduction-related sources (i.e. plate interface between the North American and Pacific Plates, which was the source of the 1964 earthquake, the epicenter of which is a significant distance south of the Project, and intraslab sources within the down-going Pacific Plate) and all applicable Quaternary crustal seismic sources within about 62 miles (100 kilometers) of the site (Figure 1-1). Crustal seismic sources beyond these distances are not expected to provide significant ground motion contributions at the dam site relative to nearby sources. A more focused study area included the dam site and reservoir areas. The study area thus included much of the Talkeetna block and surrounding fault zones such as the Denali; Castle Mountain; Northern Foothills fold and thrust fault zone; inferred Talkeetna fault; and Broad Pass Fault.

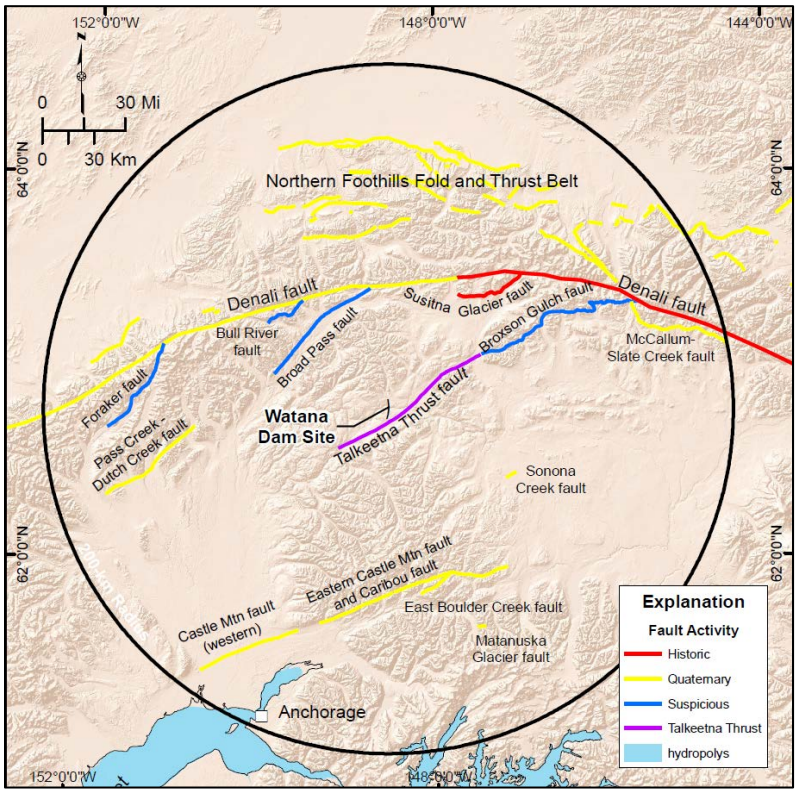


**Figure 1-1. South-Central Alaska Regional Faults**

## 1.5. Limitations

This report is presented to provide an evaluation of the site specific seismic hazards and their potential effect on the design and economic construction of the proposed project. The analyses, conclusions, and recommendations contained in this report are based on 1) the project site conditions as they existed at the time of this evaluation, 2) review of readily available existing data and information obtained from public and private sources, 3) the degree to which unconsolidated sediments mantle bedrock, 4) the duration of seismic event monitoring, and 5) the project layout described herein. In the event that there are any changes in the nature, design or location of the project, if additional subsurface data and seismic event data are obtained or any future additions are planned, the conclusions and recommendations contained in this report will need to be reevaluated by MWH in light of the proposed changes or additional information obtained.

# 2. GEOLOGIC SETTING, SEISMOTECTONIC SETTING AND SEISMICITY

## 2.1. Regional Geologic Setting

The tectonic evolution of south-central Alaska is defined by long-term plate convergence, with Mesozoic (i.e., Jurassic-Cretaceous) collisions of the Wrangellia composite terrane to North America. The Wrangellia composite terrane itself is an accretion of the Peninsular terrane to the Wrangellia terrane. The Wrangellia terrane generally consists of late Paleozoic flood basalts and meta volcanic rocks; the Peninsular terrane consists of Mesozoic (Jurassic) arc volcanics, metasediments, and plutons. The two terranes originated well south (~30° latitude) of their current position and were sutured together in the Late Jurassic (Csejtey, et al., 1978). The Wrangellia composite terrane, in turn, was accreted onto North America in the mid- to late-Cretaceous when the southern plate margin of North America was roughly along the position of the Denali fault. Between the converging Wrangellia composite terrane and North America was a marine basin (Kahiltna Basin) that accumulated syn-collisional Jurassic-Cretaceous sedimentation shed from the southeast direction (Kalbas, Ridgway, & and Gehrels, 2007). The northeast-striking Talkeetna fault, located approximately 3.5 miles (5.6 km southeast of the Watana dam site, is the eastern boundary of the Wrangellia composite terrane, with the Jurassic-Cretaceous sedimentary rocks (i.e., Kahiltna Basin deposits) on the northwest of the fault and the Wrangellia composite terrane rocks to the southeast of the fault (Figure 2-1 and Figure 2-2). Thus, in terms of terrane accretion, the region of crust south of the Denali fault and northeast of the Talkeetna fault is a large suture zone that narrows to the east, reflecting oblique plate convergence and the long-term closing of the Kahiltna Basin. The rocks that formed in the Kahiltna Basin have been uplifted through the Cenozoic, making up much of the Alaska Range and northwestern Talkeetna Mountains and forming a structural inversion. Essentially, formerly low-lying areas (i.e., basins) have now become high topography (i.e. mountains) as a result of plate convergence and mountain-building uplift along generally northeast trending folds and thrust faults.

Jurassic plutonism from melting of the oceanic subducting slab formed the batholitic complex of the southeastern Talkeetna Mountains (Nelson 2009) by intruding into the Peninsular terrane (Figure 2-2, map unit TKg). Subsequent uplift initiated northeast-directed sedimentation within proto-Kahiltna Basin in what is now the northeastern Talkeetna Mountains (Kalbas, Ridgway, & and Gehrels, 2007). Kahiltna Basin sediments continued to accumulate during the Cretaceous as westward sediment transport on fluvial, shallow marine and submarine fan depositional environments. The Kahiltna assemblage is about 1.9 to 3.1 miles thick (3 to 5 km), and consists of turbidite sequences, chert, mudstone, sandstone, and greywackes that comprise eight distinct lithofacies (Kalbas, Ridgway, & and Gehrels, 2007). Progression in the understanding of the

relationships between the terrane units and tectonics has allowed a deeper understanding about the Kahiltna Basin rocks and their significance as a recorder of long-term tectonic deformation, in contrast to previous interpretations that generalized the complex stratigraphic unit as "argillite" or "flysch".

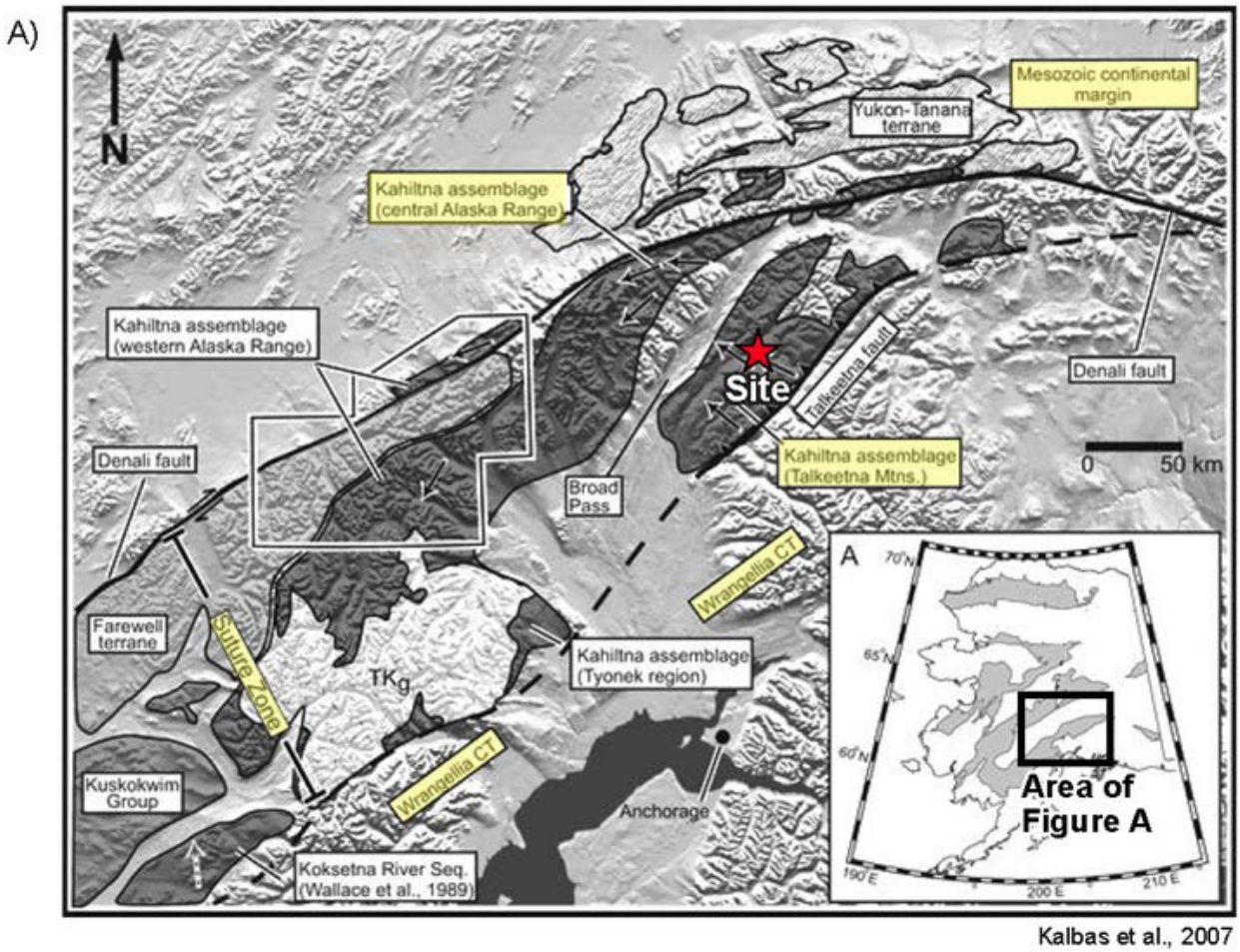


**Figure 2-1. Regional Tectonic Terranes and Basins – Part 1 of 2**

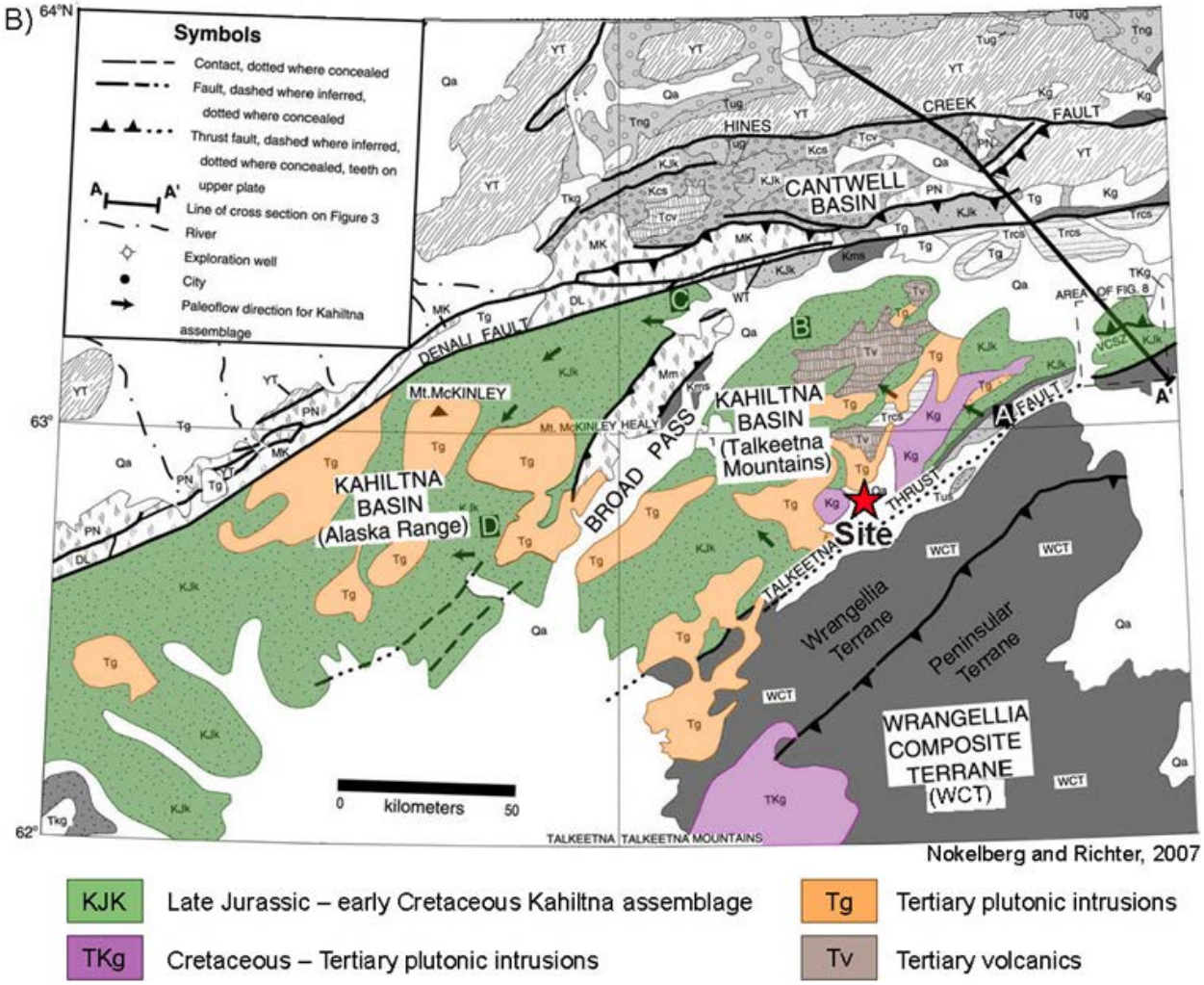


**Figure 2-2. Regional Tectonic Terranes and Basins Part 2 of 2**

Oblique subduction of an oceanic spreading center during Paleocene to early Eocene initiated magmatism and formation of short-lived northwest trending extensional (normal) faults shown in Figure 2-3 (Ridgway K. , Trop, Glen, and O'Neill, & eds., 2007). Included in these volcanics are the Cantwell and Jack River volcanic fields dated at 55 to 60 Ma, and 50 to 56 Ma, respectively shown in Figure 2-4 (Cole, Layer, Hooks, & and Turner, 2007). To the southeast, volcanic flows that overlie and cap the Talkeetna fault are dated at 50 Ma (Csejtey, et al., 1978). Thus, Tertiary magmatic intrusions punctuate the Kahiltna Basin assemblage and, the Wrangellia composite terrane, and the Talkeetna fault (Figure 2-2).

Regional crustal rotation of southern Alaska took place sometime in the early to mid-Tertiary, with rotation of 30 to 50 degrees in the counterclockwise direction accommodated by the dextral Denali and Castle Mountain faults to the north and south, respectively. Consequently, regional

transpressive deformation occurred during middle Eocene to Oligocene time, generating narrow fault-bounded basins along major strike slip faults as well as northeast trending folds (Trop & Ridgway, 2007). The Watana Creek basin probably was formed during this time as the Talkeetna fault re-activated as a strike slip structure from the changing crustal stress orientations (Figure 2-3 and Figure 2-4).

Post-Eocene tectonic growth of southern Alaska is controlled by the oblique collision of the Yakutat terrane, probably 15 to 10 Ma, with construction of continental magmatic arcs (i.e., the Wrangell volcanic field) from subduction of the Yakutat microplate, and development of large coastal mountain ranges (e.g., St. Elias Mountains). The collision of the Yakutat microplate is considered to have substantial influence on the deformation and counterclockwise rotation in the interior of south-central Alaska (Haeussler P. , 2008). Subduction of the Pacific plate continued beneath North America from Eocene onwards, with growth of the Aleutian Islands from three main pulses of arc-wide magmatism occurring at 38 to 29 Ma, 16 to 11 Ma, and 6 to 0 Ma (Jicha, Scholl, Singer, Yogodzinski, & Kay, 2006).

Since the latest Cenozoic through today, south-central Alaska has experienced rapid rates of tectonic deformation driven by the obliquely convergent northwestward motion of the Pacific Plate relative to the North American Plate. In this region, the Pacific Plate is converging with North American Plate at a rate of 2.1 inches per year (in/yr)(54 millimeters per year (mm/yr)) at a slightly oblique angle (Demets & Dixon, 1999) (Carver & Plafker, 2008). Consequently, rates and magnitudes of seismicity are also accordingly high. In southern and southeastern Alaska, the oblique convergent plate motion is accommodated by subduction of the Pacific Plate along the Alaska-Aleutian megathrust trench, and dextral (right-lateral) transform faulting along the Queen Charlotte and Fairweather fault zones. Transpressional deformation primarily is accommodated by dextral slip along the Denali and Castle Mountain faults, as well as by horizontal crustal shortening to the north of the Denali fault.

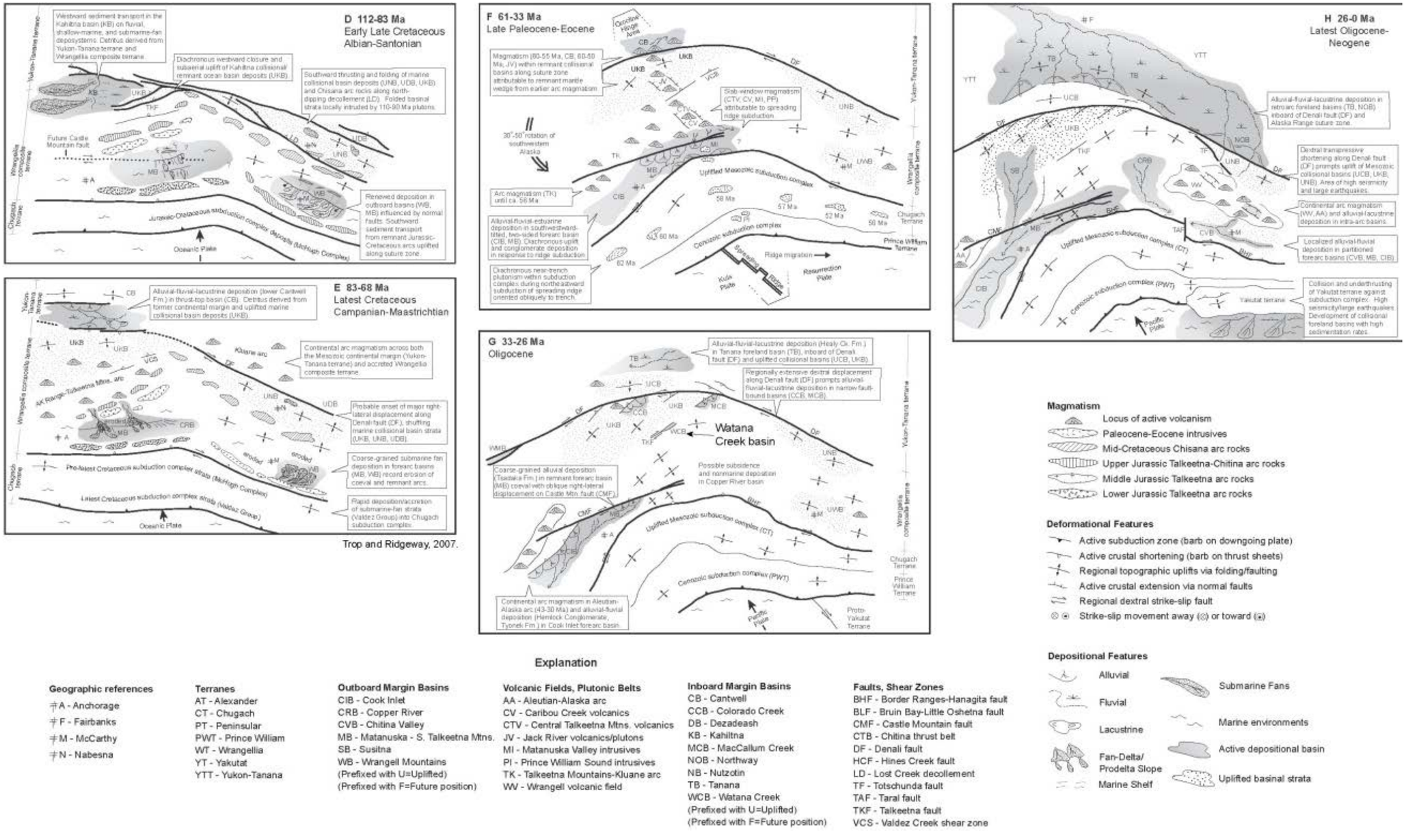


**Figure 2-3. Schematic Evolution of South-Central Alaska**

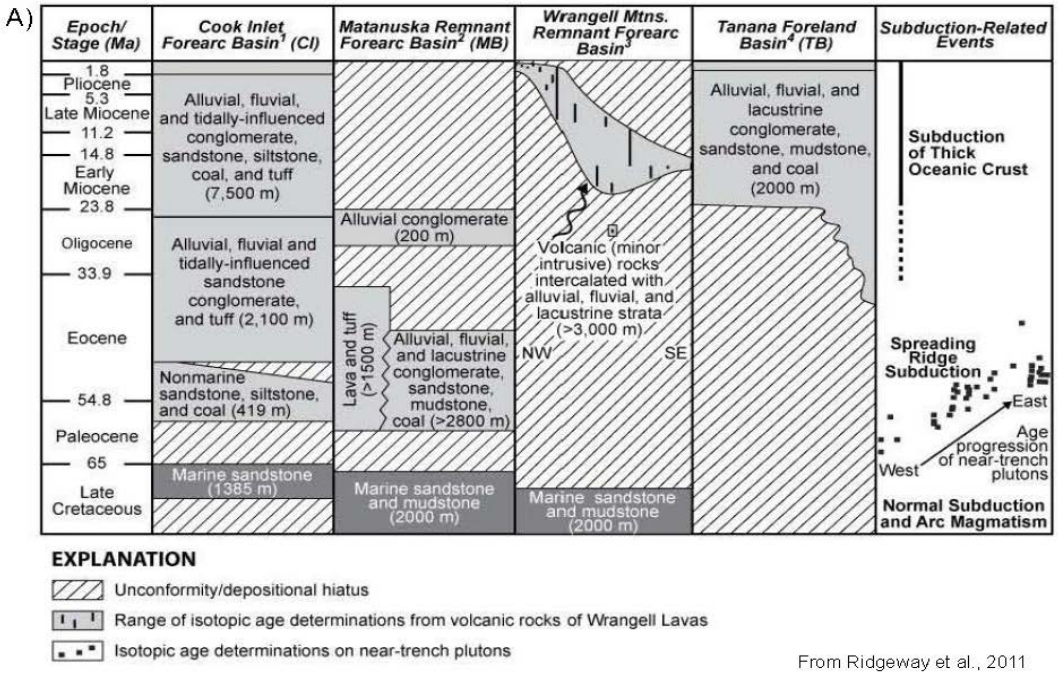


From Ridgeway et al., 2011

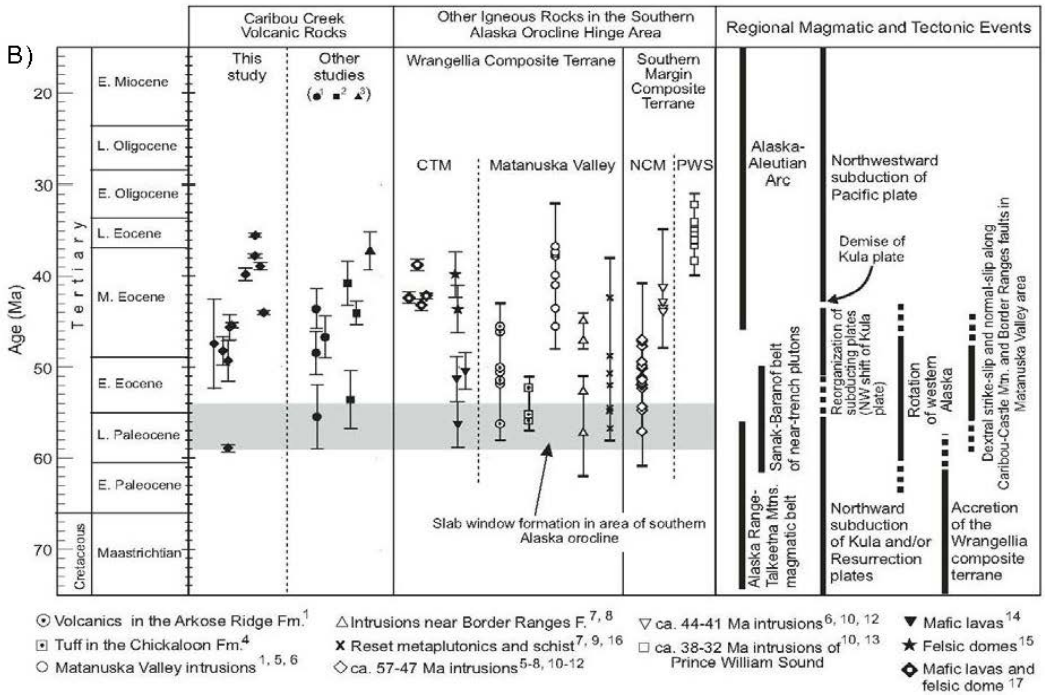


From Cole et al., 2007

Age-event diagram showing radiometric ages of volcanic rocks in the Caribou Creek volcanic field.

**Figure 2-4. Correlations of Cenozoic Tectonic, Magmatic, and Sedimentary Events in South-Central Alaska**

The regional magmatism described above directly forms the rocks that make up the dam site though plutonic intrusions and volcanism. Multiple ages of early Cenozoic (i.e., Tertiary) volcanics intruded the Kahiltna formation, as well as the Wrangellia Terrain rocks and the Talkeetna suture zone (e.g., (Wilson, Schmoll, Haeussler, Schmidt, Yehle, & Labay, 2009)). The rocks present at the dam site range in mineralogical composition and texture, including diorite intrusions, andesite, and felsic dikes and, to a lesser extent, mafic volcanic extrusive rocks (Acres, 1982b). Previous geologic mapping reveals that the volcanic rocks have a complex field relationship at the dam site with intrusive and extrusive rocks often occurring proximal to each other with gradational contacts. A range of mineralogical variability within intrusional bodies is relatively common (U.S. Army Corps of Engineers (USACE), 1979). Review of rock core drilled for the project (Golder Associates, Inc., 2013), (MWH, 2014) as well as inspection of field outcrops confirms the complexity of the igneous history. Both andesite and diorite rocks include a wide range of textures and compositions. In some instances, diorite bodies locally are cut by felsic dikes. In both outcrop and core samples, inclusions of diorite have been observed within the andesite. No dikes were found cutting the andesite, suggesting it is the youngest volcanic unit at the site based on these cross cutting relationships ( (Acres, 1982a); p. 6-7). The intrusions likely occurred sometime between 50 to 60 Ma, the field observations and relationships confirm multiple ages (or, episodes) of volcanism, intrusion, or flows of which the specific chronology has yet to be defined. Mapping by Csejtey et al. (1978) suggests that the dam site rocks could be of the order of 58 Ma; however, these dates were not collected on rock at the dam site. Rock samples were collected during 2014 field investigations that may be suitable for absolute dating purposes to establish site geochronology.

## 2.2. Regional Structure

The geologic mapping transect along the Susitna River, extending through the Watana dam site area, suggests that the site area lies within a relatively coherent crustal block of Kahiltna assemblage sedimentary rocks which are overall gently tilted to the northwest, moderately folded, and intruded by multiple early to mid-Tertiary plutonic and volcanic rocks (Figure 2-5 and Figure 2-6). The Watana dam site area lies within an area of Tertiary intrusive rocks. Kahiltna assemblage rocks and additional intrusive rocks downstream of the Watana dam site near the confluence of the Tsusena Creek and Susitna River appear structurally congruent, with an apparent absence of major cross-cutting structure or extensive penetrative deformation. There are likewise no significant expressions of vertical uplift or tectonics along the Susitna River transect, downstream of the Talkeetna fault and Watana Creek basin.

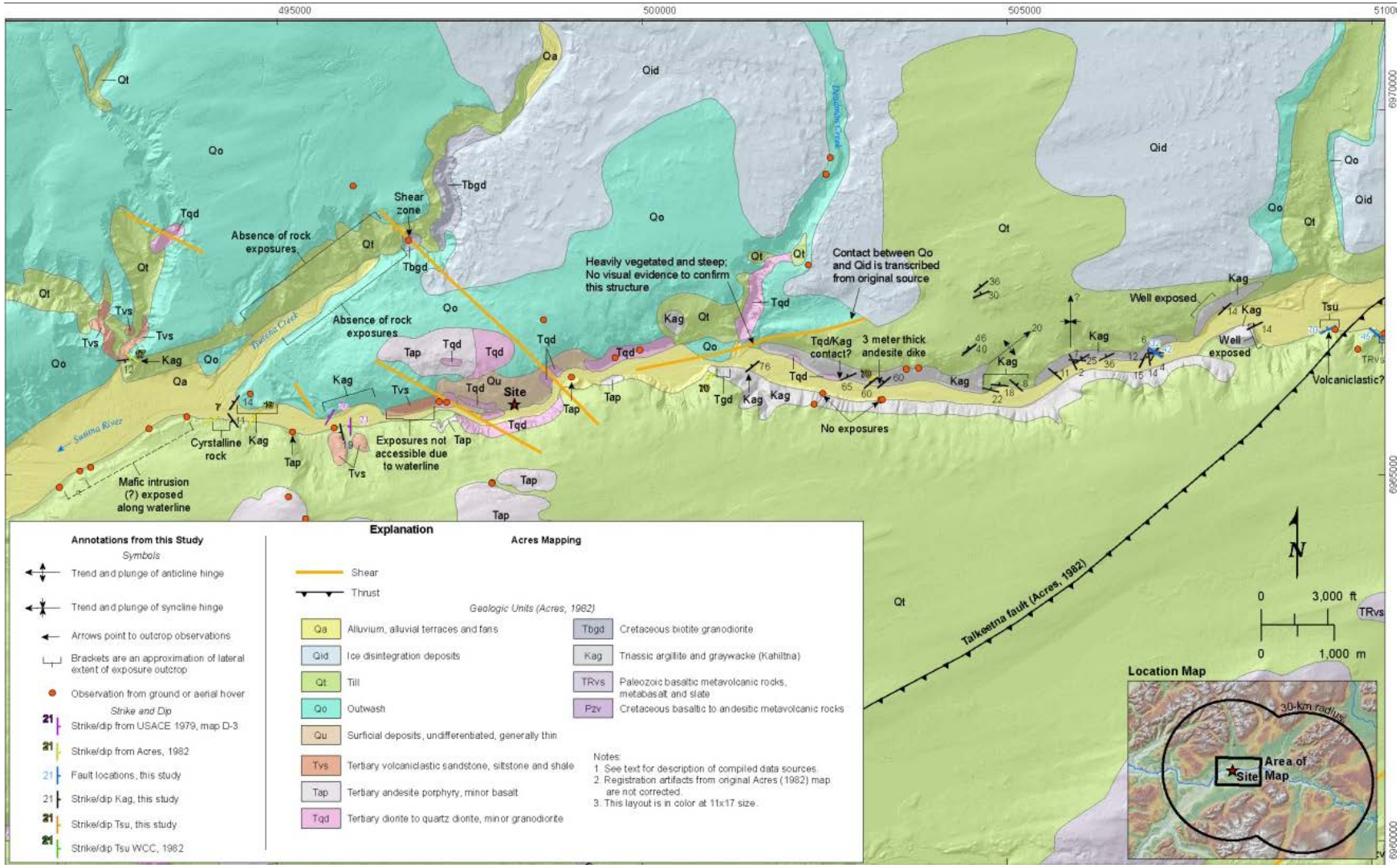


**Figure 2-5. Geologic Map Updated With Observations from 2014**

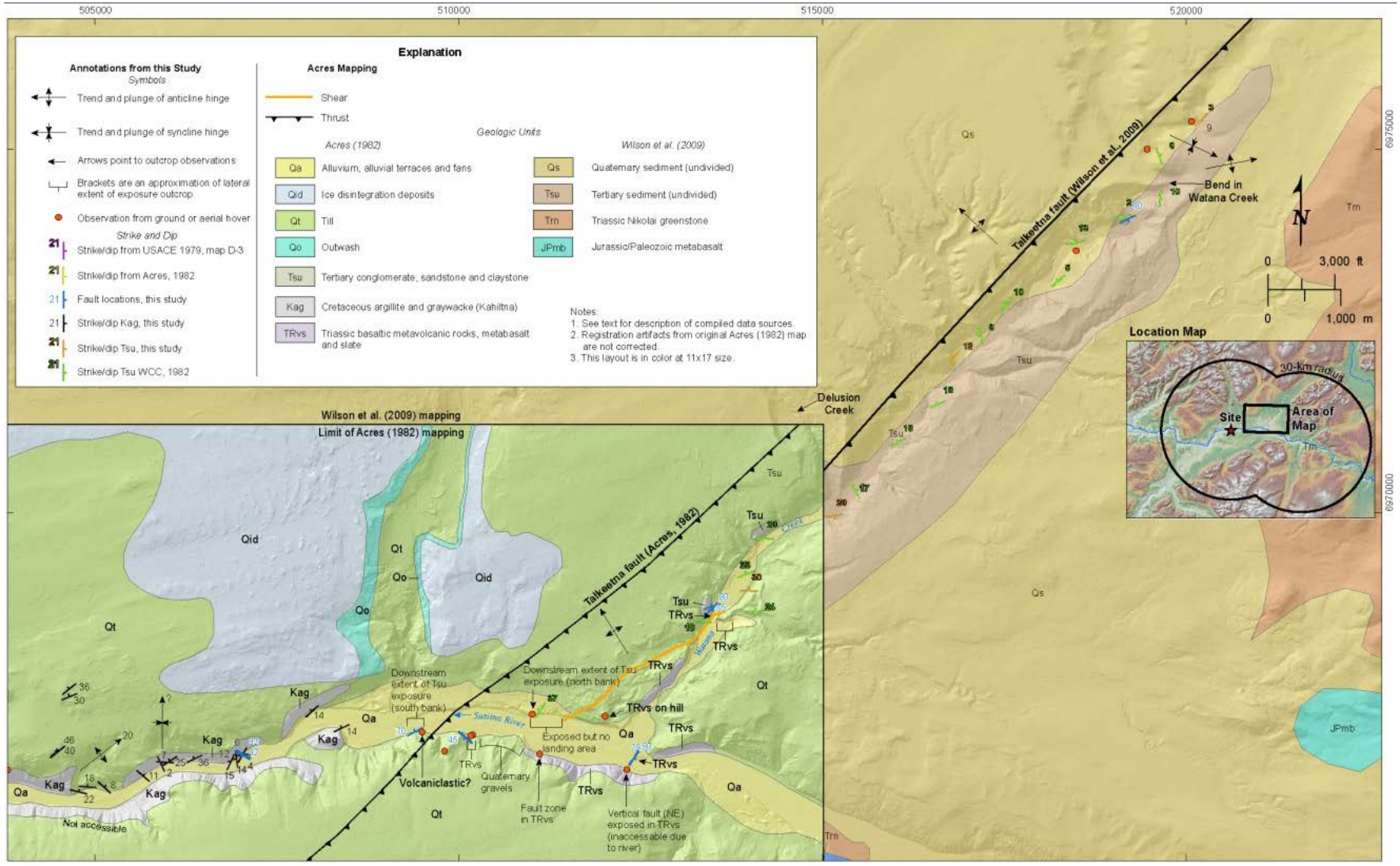


**Figure 2-6. Geologic Map Updated With Observations from 2014**

## 2.3. Seismotectonics

South-central Alaska experiences significant tectonic deformation and seismicity driven by the oblique convergent northwest motion of the Pacific Plate relative to the North American Plate. The Talkeetna Mountains formed as a direct result of the convergence of these plates as the Pacific Plate was subducted below the North American Plate as shown in Figure 2-7.

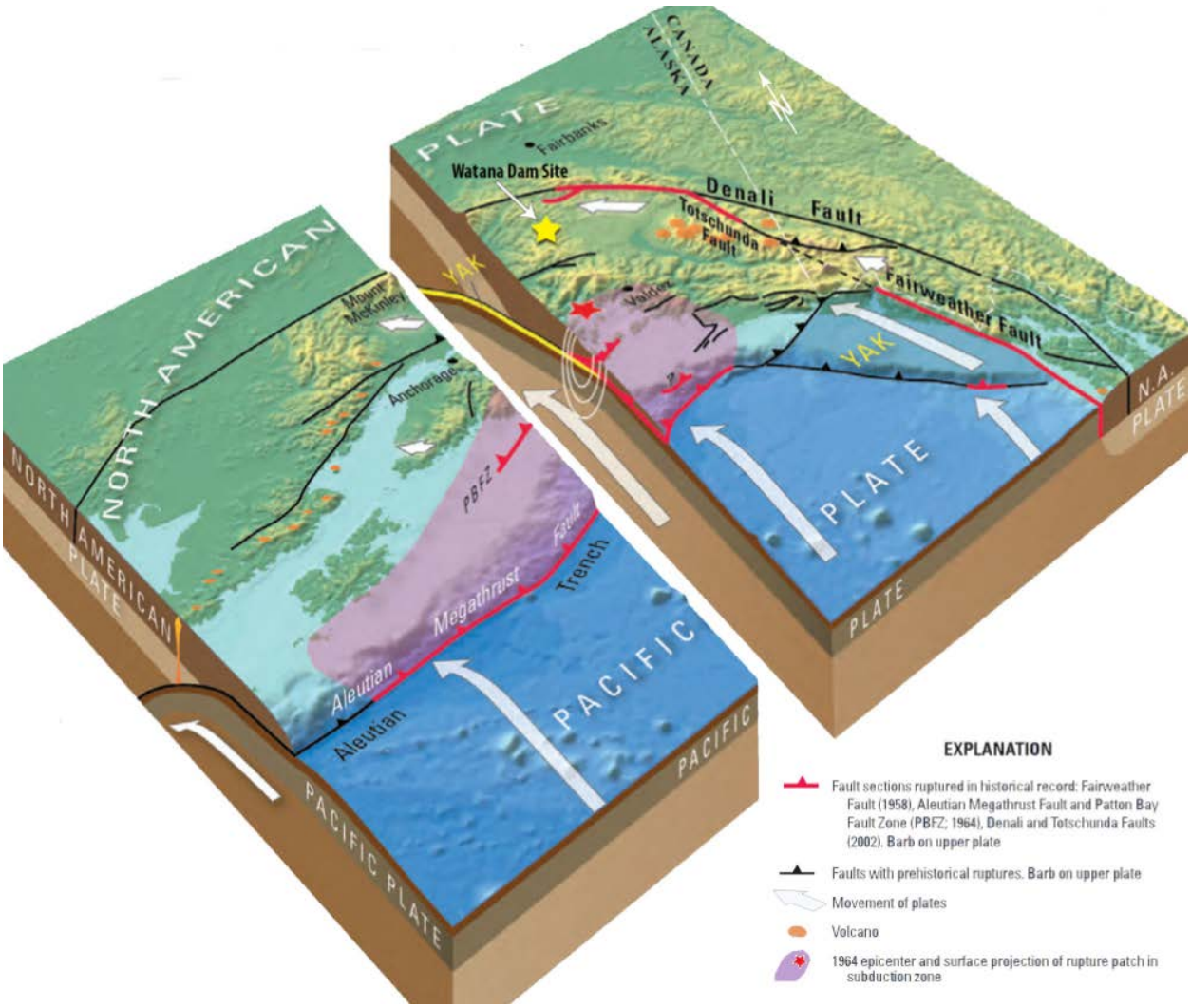


**Figure 2-7. Tectonic Setting of South-Central Alaska During the 1964 Earthquake (modified from (Brocher, et al., 2014)**

The Alaska-Aleutian subduction zone is one of the longest and most tectonically active plate boundaries in the world. It extends for nearly 2,500 miles (4,000 km) from south-central Alaska to the Kamchatka peninsula, and has produced some of the world's strongest earthquakes – such as the 1964 magnitude (M) 9.2 Great Alaskan (or Good Friday) earthquake. The subduction zone has three tectonic regimes: continental subduction in the east, an island arc along the central Aleutian volcanic chain, and oblique subduction and transform tectonics in the west (Nishenko & Jacob, 1990). The eastern continental subduction zone, in the vicinity of Prince William Sound, is significant in the evaluation of the seismic hazards at the Watana Dam site. In this region, the Pacific Plate is converging with the North American Plate at a rate of 2.1 in/yr (54 mm/yr) at a slightly oblique angle ( (Demets & Dixon, 1999); (Carver & Plafker, 2008)).

It has been recognized that the Alaska-Aleutian subduction zone is segmented in central Alaska, and may be broken into independent fragments (Ratchkovski & Hansen, 2002). In addition, it has been recognized that the Alaskan-Aleutian subduction zone's eastern termination lies within 100 km northeast of the Susitna-Watana site (Fuis, et al., 2008). The precise location and geometric character of the slab edge are not well determined. Ruppert and Hansen (2010), define three major sections of the slab, which they termed the McKinley, Kenai, and Kodiak Blocks. The dam site is located within the McKinley Block as shown in Figure 2-8, this figure was developed based on the work performed and will be discussed later in this report. A schematic of the subducting slab, which has a shallow dip (Carver & Plafker, 2008) and a typical forearc basin is shown on Figure 2-7. Small-magnitude seismicity observed from Susitna-Watana seismograph network data occurs within a 7.6 mi (12.3 km) thickness at the top of the slab as shown in Figure 2-9. In central Alaska, the slab is approximately 30.5 mi (50 km) thick (Zhao, Christensen, & Pulpan, 1995). Larger (M 7+) slab earthquakes are likely to rupture deeper into the slab than the zone defined by the recorded microseismic event in Figure 2-9.

Further south, transform motion along the eastern edge of the subducting slab is accommodated by the Fairweather and Queen Charlotte (not shown) fault zones.

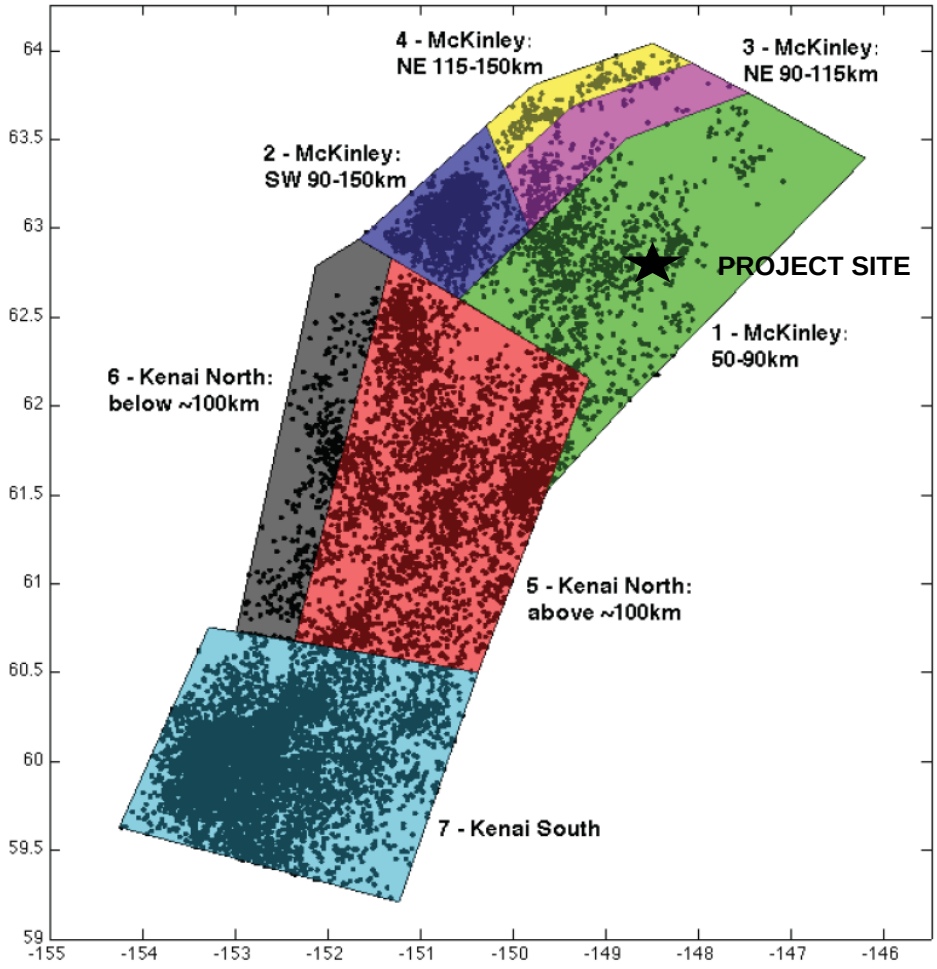


**Figure 2-8. Map View of Slab Planes**

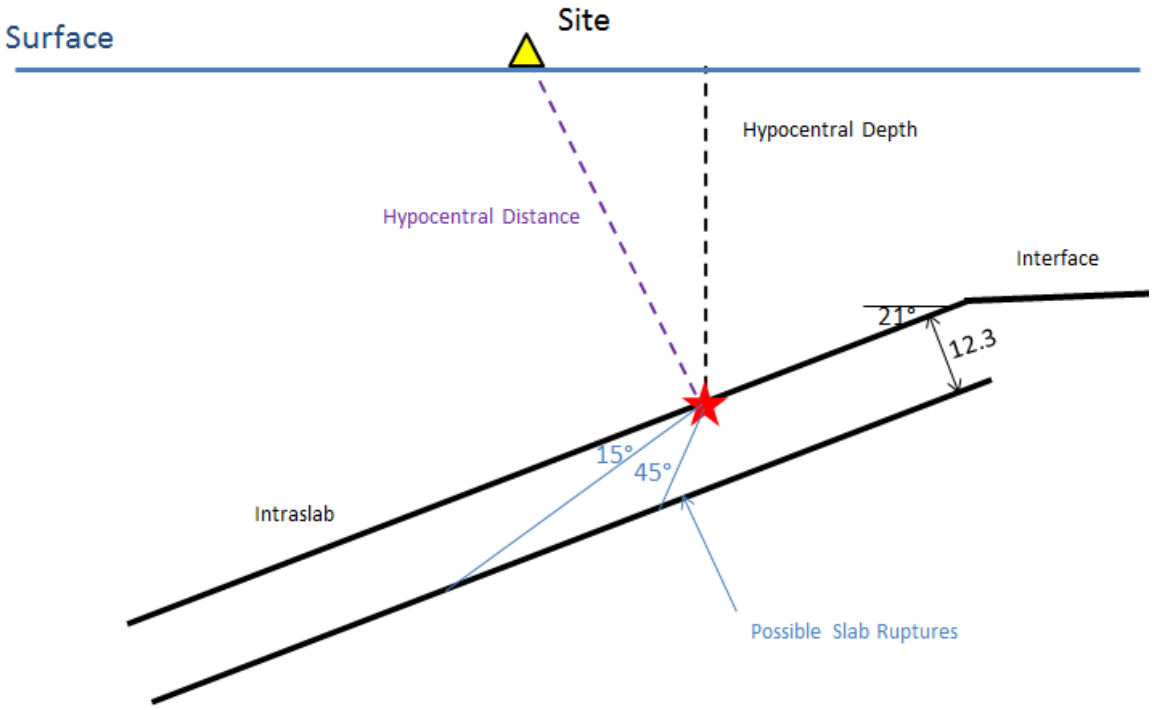


**Figure 2-9. Schematic Showing Subducting Slab Geometry**

The dam site is located within a distinct geologic domain referred to as the Talkeetna block. The Talkeetna block is bounded by the Denali fault system to the north, the Castle Mountain fault to the south, the Wrangell Mountains to the east and the northern Aleutians and Tordrillo Mountains volcanic ranges to the west (Figure 2-1). Major stress is released along the Denali and Castle Mountains bounding faults during earthquakes resulting in movement (i.e., strain). However, it is less clear how stress and strain are accommodated to the east and west. There is a relative absence of large historical earthquakes within the Talkeetna block as well as a lack of mapped faults with documented Quaternary displacement ( (Koehler, 2013); (Koehler R. , Farrell, Burns, & and Combellick, 2012) ). The absence of earthquakes and mapped Quaternary faults within the block implies that the block is behaving rigidly with little to no internal deformation.

The Talkeetna suture zone refers to the broad area of crust northwest of the Talkeetna thrust fault and south of the Denali fault (labeled in Figure 2-1.) Glen et al. (2007) describe the Talkeetna suture zone as a deep crustal structure bounding the northwestern edge of the Wrangellia Terrane; thus the Talkeetna fault is the southeastern boundary of the suture zone.

The Denali fault predominantly shows right-lateral, strike-slip fault motion; and in plan the fault has an arcuate shape and defines the northern margin of the Talkeetna block as shown in Figure 2-1.

The Denali fault has been a major structural component of Alaska since it formed during the Late Jurassic to early Cretaceous Period (Ridgway K. D., Trop, Nokleberg, Davidson, & Eastham, 2002). Offsets of 56 Ma metamorphic and intrusive rocks suggests at least 249 mi (400 km) of total right lateral displacement (Nokleberg, Jones, & Silberling, 1985). Offset is also constrained in the Denali region where the 38 million year old Mt. Foraker pluton is displaced 24 mi (38 km) from the McGonagal Pluton (Reed & Lanphere, 1974).

In 2002, movement on the Denali fault produced an M 7.9 earthquake, the largest strike-slip earthquake to occur in North America in almost 150 years (Eberhart-Phillips, et al., 2003). Detailed studies of offset glacial features along the fault following the earthquake have demonstrated a westward decrease in the Quaternary slip rate along the fault ( (Matmon, et al., 2006); (Mériaux, et al., 2009)), as shown in Figure 2-10.

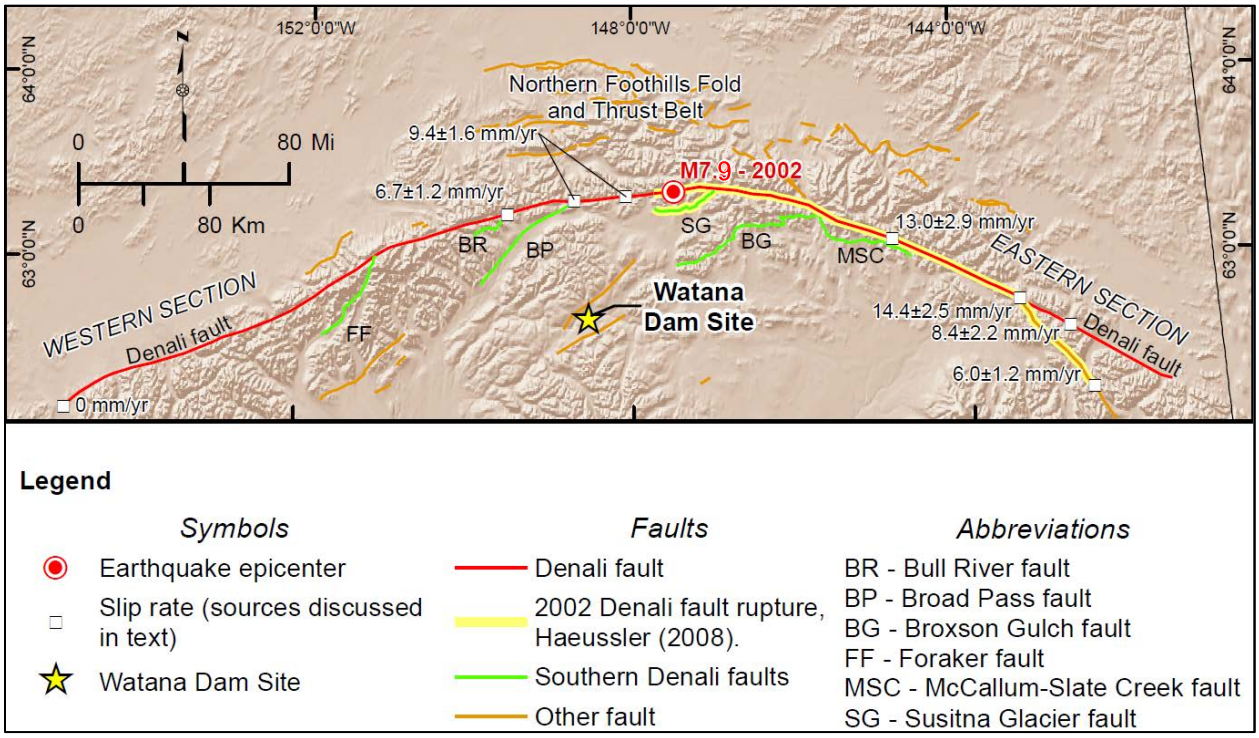


**Figure 2-10. Denali Fault Characterization**

Along the north and south sides of the Denali fault lie two zones of deformation. To the north is the Northern Foothills Fold and Thrust Belt (NFFTB), a zone of variably dipping, but generally Quaternary thrust faults and folds that accommodates transpressional deformation along the north side of the Alaska Range (Figure 2-10). The westward reduction in Denali fault slip rate is considered to be predominantly the result of strain partitioning onto the NFFTB ( (Haeussler P. , An overview of the neotectonics of interior Alaska—Far-field deformation from the Yakutat Microplate collision, 2008); (Mériaux, et al., 2009) ).

The other zone of deformation adjacent to the Denali fault lies south of the fault where several thrust faults splay from the Denali fault's central section as shown on Figure 2-10. Most of these faults are recognized as Tertiary terrane-bounding features in which Mesozoic or Paleozoic rocks are thrust over Tertiary sediments and volcanics (Haeussler P. , 2008). Rupture along the previously unmapped Susitna Glacier thrust fault during the 2002 Denali fault earthquake highlighted the potential for seismogenic activity in this area, in contrast to the relatively sparse mapping of Quaternary faults south of the Denali fault. This concept is well expressed in the Neotectonic Map of Alaska fault explanatory note (Plafker, Gilpin, & Lahr, Neotectonic map of Alaska, 1994).

The Castle Mountain fault defines the southern margin of the Talkeetna block. This fault is described by some as a dextral oblique strike-slip fault whose western segment is defined by a 39 mi (62 km) long Holocene fault scarp. Recent field and LiDAR-based geomorphic observations by Koehler et al. (2014) support the inference that the Castle Mountain fault is a high angle oblique reverse fault. The eastern section is primarily evident in bedrock, and there is no indication of Holocene surface rupture as shown in Figure 2-11. Paleoseismic studies, by Haeussler et al. (2002), on the western section demonstrate four earthquakes on the fault in the past 2,800 years, with a recurrence interval of approximately 700 years. More recent work by Koehler et al. (2014), suggest only two earthquakes in the Holocene indicating that the recurrence interval could be longer than previously thought. Despite the apparent lack of Holocene surface rupture on the eastern section, this section of the fault is spatially associated with historic seismicity as high as M 5.7 (Lahr, Page, Stephens, & Fogleman, 1986).

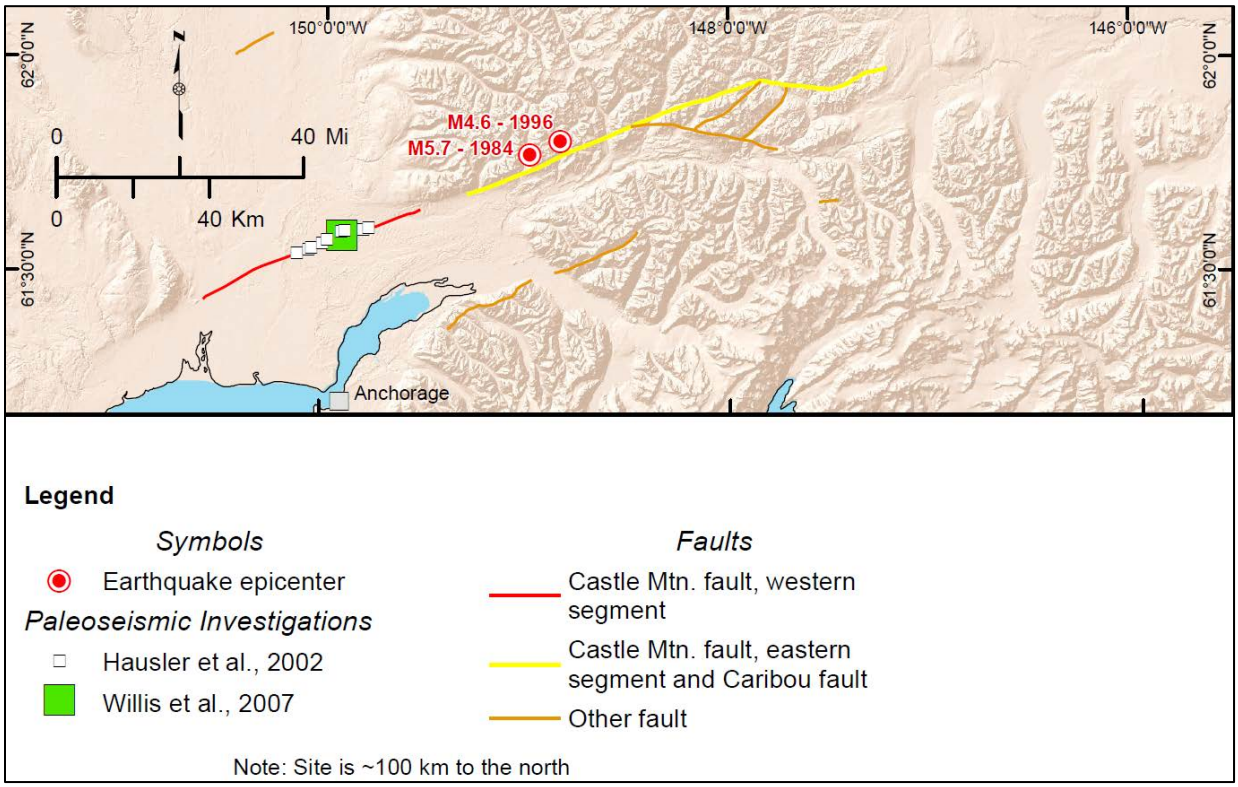


**Figure 2-11. Castle Mountain Fault Characterization**

## 2.4. Historical Seismicity

The region within the 124 mi (200 km) radius of the Watana dam site is seismically active as indicated by the occurrence of earthquakes with a magnitude greater than or equal to M 5 (AEC seismicity catalog). The greatest number of these are deep (> 25 mi (40 km) depth) events with magnitudes up to M 7.1, that likely are associated with the subducting Pacific Plate, and a smaller number of events to the southeast that likely are associated with tectonic under-plating of the Yakutat block. The remaining events are crustal earthquakes occurring at depths of about 19 mi (30 km) or less. The largest of those crustal earthquakes is the 2002 M 7.9 Denali fault earthquake (initiated on the Susitna Glacier fault), with an epicenter approximately 59 mi (95 km) from the dam site. Several of the M ≥ 5 events are associated with the Denali fault including: the M 6.7 foreshock of the 2002 earthquake (Nenana Mountain earthquake), several 2002-2003 aftershocks up to M 5.8, and six additional events up to M 6.4.

Events up to M 7.2 are located in the Northern foothills fold and thrust belt and the Minto Flats seismic zone. The Northern foothills fold and thrust belt includes the Kantishna seismic cluster, the Northern foothills thrust, and the Molybdenum Ridge fault (Figure 2-12). An M 5.7 event in 1984 is associated with the Castle Mountain fault (Lahr, Page, Stephens, & Fogleman, 1986).

Many events cannot be spatially correlated with a documented Quaternary fault, including an M 7.2 earthquake in 1912.

Seven historical earthquakes are documented within 31 mi (50 km) of the site (AEC catalog). Four of these earthquakes occurred at depths between 30 to 60 mi (49 to 97 km), which places them within the subducting slab. The largest slab event within 31 mi (50 km) of the site has a magnitude of M 5.4. Three earthquakes are located at upper crustal depths (13-22 mi [21-36 km]), the largest of which has a magnitude of M 6.2. These three earthquakes occurred between 1929 and 1933, and spatially are not associated with any known Quaternary fault, though they may be inaccurately located, or have poor depth control, due to the lack of regional seismograph stations at that time.

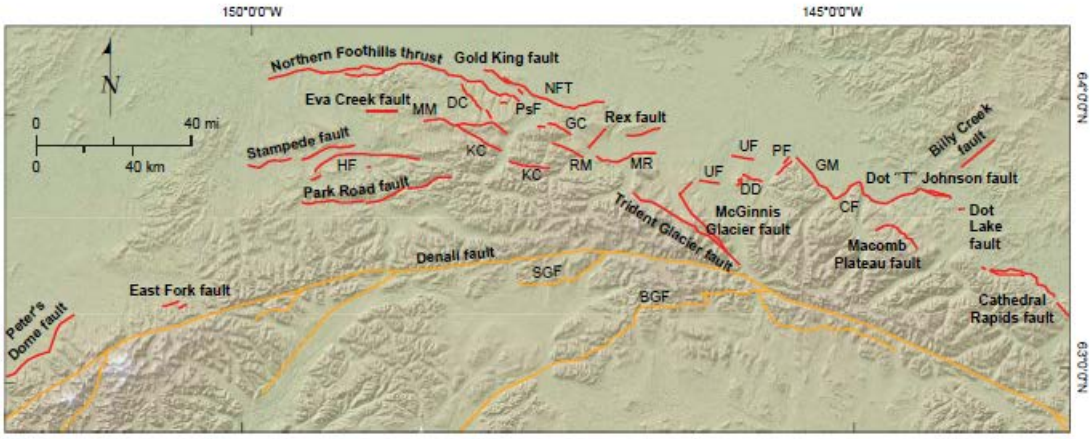


**Key to Abbreviations**

BGF – Broxson Gulch fault
CF – Canteen fault
DC – Ditch Creek fault
DD – Donnelly Dome fault
GC – Glacier Creek fault
GM – Granite Mountain fault
HF – Healy Creek fault
KC – Kansas Creek fault
MM – Mystic Mountain fault
MR – Molybdenum Ridge fault
NFT – Northern Foothills Thrust
PF – Panoramic fault
PsF – Potts fault
RM – Red Mountain fault
SGF – Susitna Glacier fault
UF – Unnamed fault

**Figure 2-12. Northern Foothills Fold and Thrust Belt**

### 2.4.1. 2002 Denali Fault Earthquake

The M 7.9 2002 Denali fault earthquake is the largest onshore strike-slip earthquake in North America in the past 150 years (Eberhart-Phillips, et al., 2003). The earthquake initiated on the previously unmapped Susitna Glacier thrust fault (Figure 2-10) with a 30 mi (48 km) surface

rupture and up to 36 ft. (11 m) of displacement (Crone, Personius, Craw, Haeussler, & Staft, 2004). The earthquake then propagated eastward rupturing 140 mi (226 km) of the central Denali fault and 41 mi (66 km) of the Totschunda fault. Average slip along the Denali fault was approximately 16 ft. (5 m), with a maximum slip of 29 ft. (8.8 m) west of the junction with the Totschunda fault (Haeussler, et al., 2004). The earthquake caused no fatalities and minimal damage to infrastructure, likely due to the sparse population density near the fault. The estimated intensity of the earthquake at the Watana Dam site was Modified Mercalli scale VI (USGS, 2003).

### 2.4.2. 1964 Great Alaskan Earthquake

The M 9.2, March 28, 1964 Great Alaskan earthquake had an epicenter directly south of the 124 mile (200 km) radius site region; however, the subsurface rupture area extends nearly beneath the site region (Figure 2-13). The isoseismal map of the event shows the Watana Dam site experienced ground shaking with Modified Mercalli scale VII intensity (Stover & Coffman, 1993). The earthquake is the second largest recorded in the world since instrumental recordings began in the late 1800s (the one larger event was the 1960 M9.5 Chilean earthquake).

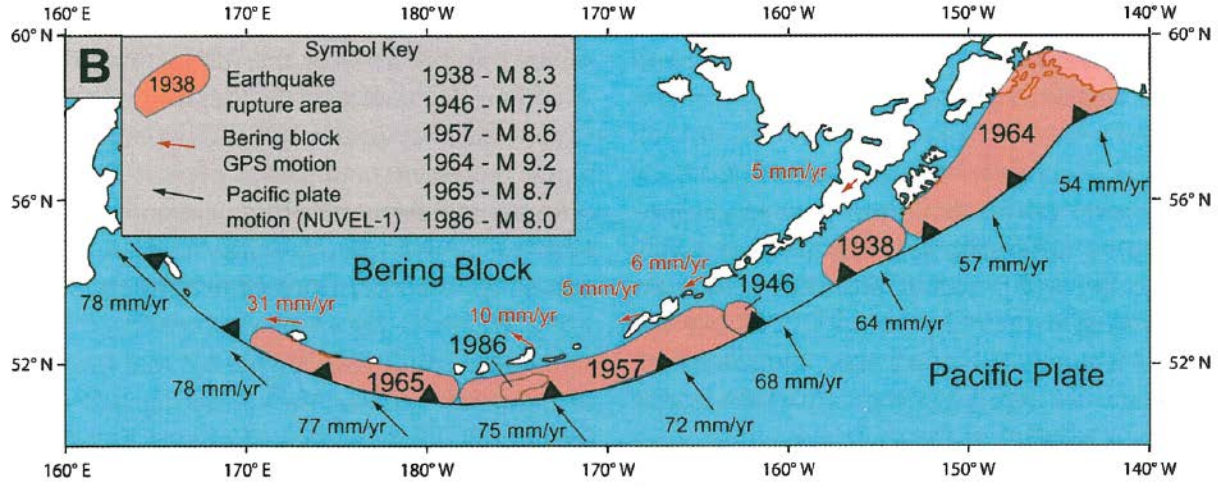


Motion of the Pacific Plate relative to North America is indicated by black arrows. Red arrows show motion of the Bering Block relative to North America.

From Carver and Plafker (2008)

**Figure 2-13. Rupture Areas for Historical Alaskan Subduction Zone Earthquakes**

The 1964 earthquake ruptured approximately 500 mi (800 km) of the Aleutian megathrust with left-lateral reverse-slip motion, and produced approximately 66 ft. (20 m) of maximum displacement (Christensen & Beck, 1994). The earthquake was felt over 700,000 square miles in Alaska and Canada (Hake & Cloud, 1966) with an intensity of MM VII estimated at the Watana

Dam site (Stover & Coffman, 1993). Coseismic vertical displacements affected an area of about 200,000 square miles. Prince William Sound experienced up to 38 ft. (11.5 meters) of uplift, and 7.5 ft. (2.3 meters) of inland subsidence (relative to sea level) occurred (Plafker, 1969). Fifteen fatalities were attributed to the earthquake and 113 fatalities from the ensuing tsunami. In Anchorage, the earthquake destroyed structures up to 6-stories high and triggered numerous destructive landslides.

### 2.4.3. 1912 Delta River Earthquake

A widely felt 1912 earthquake, commonly referred to as the Delta River earthquake, was relocated by Doser (2004) to a location within 6 mi (10 km) of the Denali fault, though with 95% error bounds of about 62 mi (100 km) in the east-west direction and 44 mi (70 km) north to south. Carver et al. (2004) interpreted healed tree damage as having resulted from surface deformation during the 1912 event. However, paleoseismic studies at several sites along the Denali fault do not show any evidence for a surface rupturing 1912 event ( (Schwartz & (DFEWG), 2003); (Plafker, Carver, Cluff, & and Metz, 2006); (Koehler, Personius, Schwarz, Haeussler, & Seitz, 2011b) ). Therefore, the event is considered as being unassociated with a particular known crustal fault.

## 2.5. Susitna-Watana Seismic Network

An earthquake monitoring network was created in August-September 2012, and expanded in 2013. The system was installed to monitor earthquake activity and to record strong shaking of the ground in the Project area during moderate to strong earthquakes. The entire network system at build-out consisted of four 6-component strong motion and broadband stations, three 3-component broadband stations, and a GPS station, co-located with a 6-component seismograph station at the dam site.

The monitoring network remained in operation through mid-June 2015. The system coverage is within about 31 mi (50 km) of the proposed dam site – all as shown on Figure 2-14. Data for the analysis of seismic events in the Project area were obtained in real-time for processing, and archived by IRIS (Incorporated Research Institutions for Seismology). The seismograph stations were operated as part of the Alaska Seismographic Network by the Alaska Earthquake Information Center (AEC). These seismograph stations have increased the station density in the region, leading to greater magnitude and detection capabilities, a decrease in magnitude of completeness, and greater location accuracy. The increase in recorded events has led to a better picture of shallow crustal seismicity and intraslab seismicity associated with the subducting Pacific Plate below the proposed dam site. Due to funding constraints, stations WAT2, WAT3, WAT4, and WAT5 were removed in mid-June, 2015.

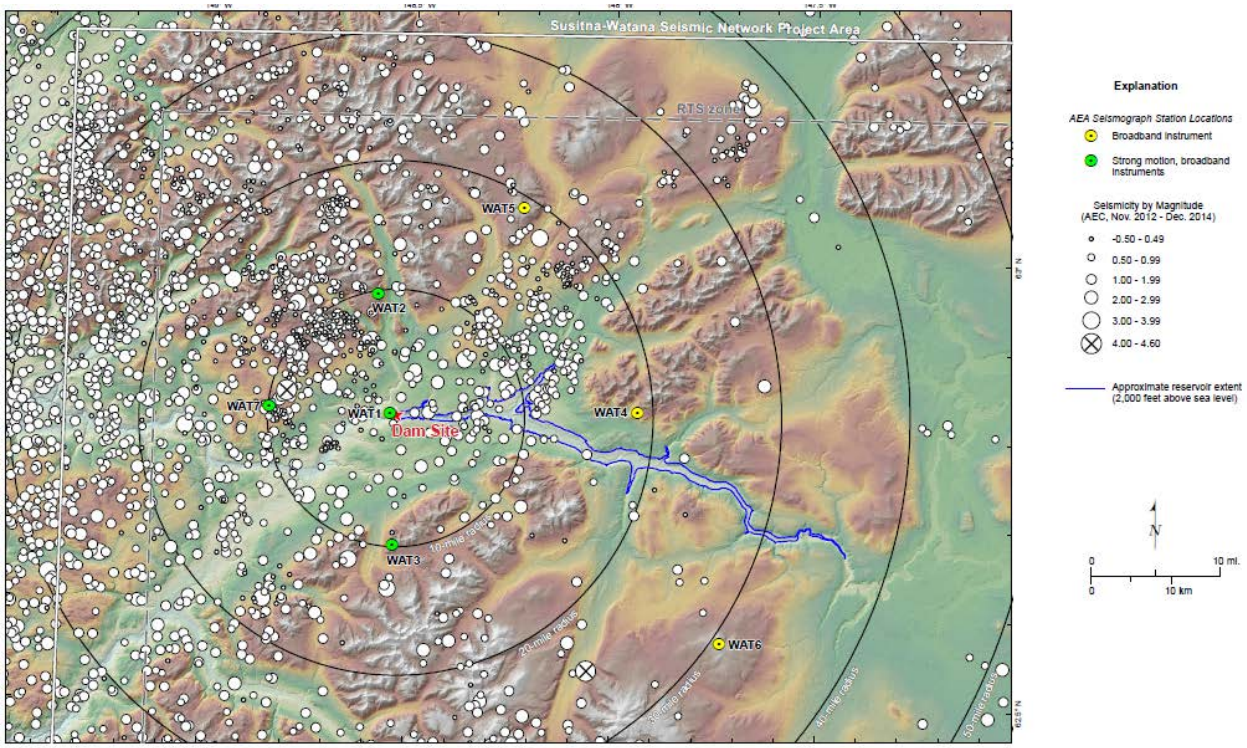


**Figure 2-14. Susitna-Watana Seismic Network Location Plan and November 16, 2012 through December 31, 2014 Seismic Events**

From November 16, 2012 to the end of 2014 the earthquake monitoring system has recorded a total of 2,523 earthquakes which were located within a region roughly 50 mi (80 km) east-west and 30 mi (50 km) north-south of the site.

The earthquakes in the Project area form two distinct groups, crustal events between 0 and 25 km depth and intermediate depth events below 18.6 mi (30 km) in the subducting Pacific plate. This can be seen clearly in the cross-section (Figure 2-15).

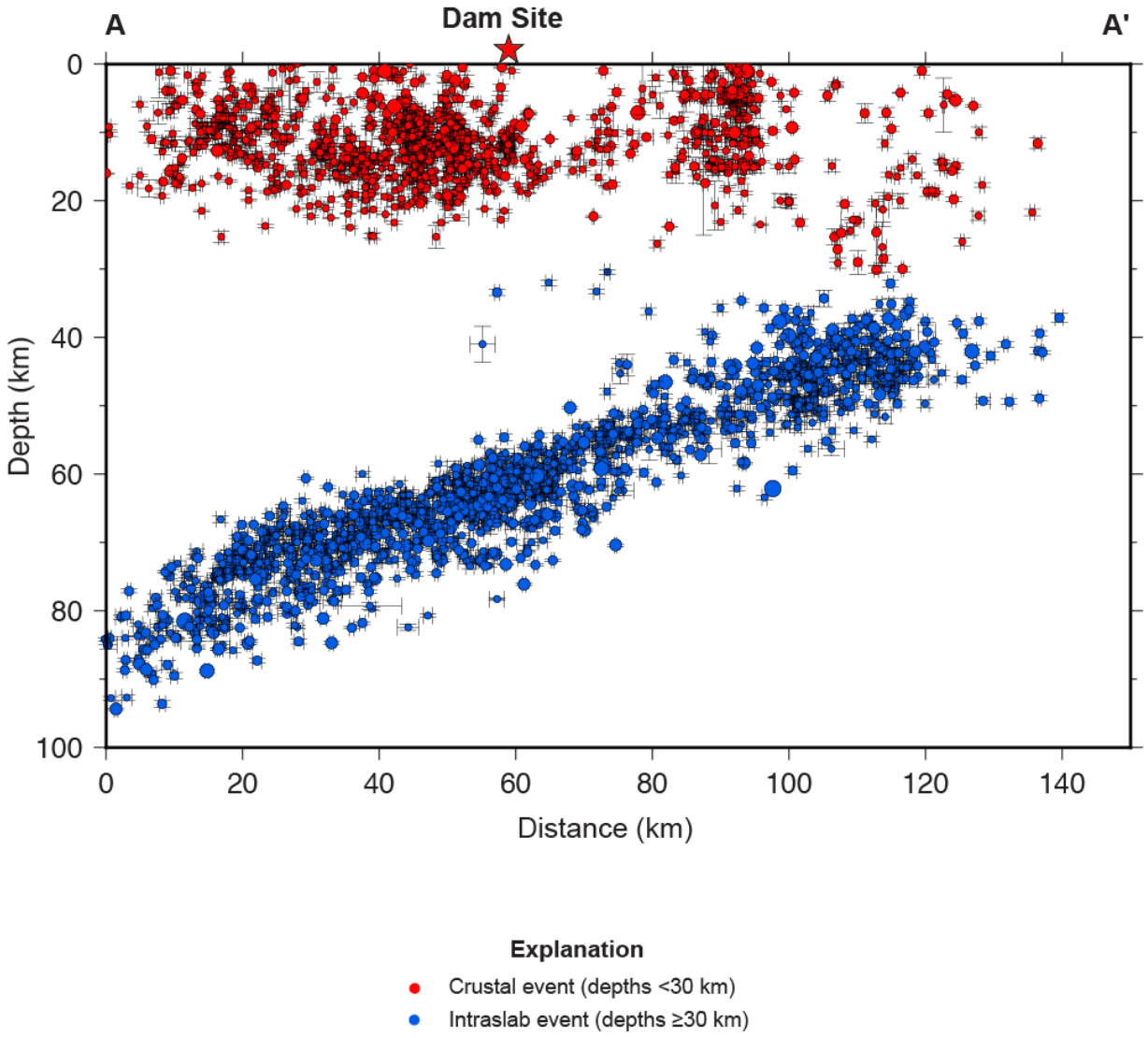


**Figure 2-15. NNW-SSE-Oriented Cross Section Showing Seismicity from November 16, 2012 through December 31, 2014**

Since network installation, the largest earthquake within the subducting plate, a magnitude 4.6 earthquake, occurred on November 29, 2014 at a depth of 37.9 mi (62 km) and located 39.5 km (24.5 miles) ESE of the dam site. The largest earthquake magnitude within the crust, magnitude 3.8, occurred on July 24, 2013 at a depth of 6.9 mi (11.1 km) and was located 8.8 mi (14.2 km) NW of the dam site. About 10 small aftershocks (M=0.9-2.3) were located within a few days of the 3.8 event.

Details of seismicity patterns, rates, and focal mechanisms refer to reports by Fugro (2015a) and AEC (2015).

# 3. PRELIMINARY SEISMIC HAZARD ANALYSIS APPROACH

At the beginning of the studies recorded in this report, a preliminary deterministic and probabilistic seismic hazard evaluation was undertaken to update the seismic hazard studies from the 1980s by Woodward Clyde Consultants ( (Woodward-Clyde Consultants (WCC), 1980); (Woodward Clyde Consultants (WCC), 1982)) and R&M (2009) including an update of the site-specific seismic source model (Fugro 2012). Initial ground motion parameters were developed based on a desk-top study. The methods follow general guidance defined according to Chapter 13 of the Federal Energy Regulatory Commission's Engineering Guidelines.

The task included research, compilation, and review of relevant scientific literature, studies, and maps necessary to update the geologic and seismologic understanding of the region. This included review of the existing seismic studies and published literature and fault rupture maps following the 2002 Denali earthquake. This assignment also included contacting technical experts in the Alaskan seismotectonics to elucidate the current understanding of shallow crustal seismic sources and Quaternary faulting in the Talkeetna Terrain. Based on this literature review, a geological and seismotectonics database and library were created.

When the initial task had been completed, a comprehensive study plan approach was implemented to allow for the final deterministic and probabilistic seismic hazard assessment (DSHA, PSHA). Subtasks included the following:

- Updating evaluations of geologic, seismologic, and seismotectonic literature for the Project study area to identify data gaps and uncertainties that may require further evaluations.

- Updating seismicity catalogue for evaluation of seismicity rates, depths, magnitudes, and focal mechanisms. This includes evaluation of recent and ongoing data collected by the Alaska Seismographic Network and augmented by the additional seismic stations installed in the Project area as part of the long term earthquake monitoring program.

- Developing a seismotectonic model that identifies and characterizes seismic sources of engineering significance to the Project.

- Conducting geologic studies using newly acquired Light Detection and Ranging (LiDAR) and Interferometric Synthetic Aperture Radar (INSAR) datasets to aid in the identification and evaluation of potential seismic sources and geohazards.

- Collecting field geologic data for characterization of potential seismic sources and surface displacement hazards.

- Assessing surface fault displacement hazard to evaluate the significance (likelihood and amount) of potential ground surface displacement from faulting in the area of the Project, including beneath the dam, if such a feature is present.

- Performing sensitivity studies on selected surface tectonic features, faults and lineaments, identified and being considered as potential seismic sources of engineering significance on the design of the Project.

- Monitoring and detection of local earthquakes to understand the seismic hazards in the Project area.

The initial site specific seismic hazard for the Watana Dam site was completed on February 24, 2012 (Fugro 2012). This initial seismic hazard assessment was performed prior to acquisition of the LiDAR data, lineament mapping and analysis, evaluation of crustal seismic sources, acquisition of earthquake event data in the Project, etc. For design, the site specific seismic hazard analysis and calculations at the Watana Dam site should be revisited and further evaluation of the ASZ and worldwide subduction zone data will be needed to assess the full range and weights for larger Mmax estimates and to develop a basis for estimation of an appropriate characterization of Mmax for the intraslab source for use in deterministic evaluations.

# 4. CRUSTAL SEISMIC SOURCE EVALUATION SUMMARY

## 4.1. General

As described in Section 3, a preliminary seismic hazard source model and probabilistic ground motion assessment was prepared in 2012 based on desktop review of prior studies and recent literature (Fugro, 2012). Subsequent to the preliminary seismic hazard ground motions assessment, this study completed lineament mapping based on interpretation of recently acquired, detailed, topographic data (i.e., INSAR- and LiDAR-derived DEM data). The mapped lineaments were assembled into lineament groups, and evaluated in the office using semi-qualitative criteria to reject or select lineament groups for further investigation during the summer field season of 2013 (Fugro, 2013). In total, 22 lineament groups and three broader lineament areas were advanced to the field investigation phase that took place over parts of summer of 2013 and 2014 (Fugro, 2015a).

The purpose of the lineament mapping and crustal evaluation was two-fold:

1. to identify potential crustal seismic sources that could appreciably contribute to the seismic hazard at the proposed hydroelectric project and affect dam design; and

2. to identify faults and assess their potential for surface fault rupture at the proposed dam site area.

A primary objective of the lineament field investigation was to document and interpret available field evidence for the presence or absence of potential crustal seismogenic sources (faults) along features identified through previous lineament mapping, and evaluate the features' significance with respect to Quaternary faulting and their potential as seismic sources of significance to the Susitna-Watana Project seismic hazard evaluations. The crustal seismic source evaluation was vetted through peer-review of technical memoranda and selected field sites by the Alaska Department of Geological & Geophysical Surveys (DGGS), as well as meetings with the Board of Consultants.

## 4.2. Methods

The desktop lineament mapping and analysis report (Fugro, 2013) describes the approach and results for mapping of individual lineaments across the Project area, that is, within a 62 mi (100 km) radius from the dam site. For that effort, criteria were established to provide a basis for delineating lineament groups (that is, aggregates of individual lineaments) that appear to have sufficiently extensive lateral continuity and geomorphic expression consistent with an origin by tectonic processes. Additional criteria were developed to exclude lineament groups that were

created by erosional or depositional processes (i.e. non-tectonic lineaments), lineament groups that are chiefly related to lithologic controls (i.e., differential erosion), lineament groups that did not meet length and distance criteria, and lineaments that did not show consistent senses of displacement along strike. In total, 22 lineament groups and three broader lineament areas were advanced to further field investigation and evaluation

The selected lineament groups were assessed in the field based on geomorphological characteristics observed in the field as well as geologic relationships around the lineaments (Fugro, 2015a). As guidelines for the field teams conducting the evaluation of individual lineament groups, a series of questions were developed as an aid to focus observations made during the field investigation. To evaluate the field data, a set of questions and criteria similar to those used for evaluation of the desktop findings were developed. The principal objective of these criteria is to guide judgments regarding the lineaments' origins in order to evaluate their potential association with Quaternary faulting and potential crustal seismogenic sources.

The lineament groups were visually inspected in the field to identify positive evidence for (or against) tectonic deformation of the Quaternary deposits (as present in the field) that may overlie, or project toward, the lineaments. The ground-based geologic data collection included walking of parts of mapped lineaments, photo documentation, exposure and logging of shallow soil pits, local mapping, collection of relevant structural measurements (strike, dip), and comparison of existing geologic mapping to field exposures and findings.

Geologic observations made during this recent study included examination of prominent geologic outcrops that seem to have been un-recognized in previous mapping. This effort is intended to indicate confirmation or disagreement with existing mapping, and to provide a level of transparency as to where outcrops are present or absent, and from which locations outcrop-based interpretations are possible. Field geologic transects were completed to document styles, distributions, and extent of structural deformation sub-regionally and near the dam site. Sub-regional field transects were completed where outcrops were accessible in terms of helicopter landing sites, river water level conditions, and availability of outcrop exposures. The transects were completed chiefly along the Susitna River, Watana Creek, and to a much lesser extent, Tsusena Creek. The transect data were synthesized with regional mapping to characterize the significance of structural features such as terrane bounding faults and deformation of sedimentary strata. These observations, in turn, allow development of a conceptual tectonic model that provides a consistent framework that helps explain the presence or absence, as well as significance, of the structural geologic features at the dam site (Section 5).

## 4.3. Results

All lineament groups targeted for field work received a low-altitude aerial observation and ground inspection was completed at selected locations where features of interest were identified. Based on these investigations, the overall evaluation and grouping of the lineament groups and features are summarized in Table 4-1 below.

**Table 4-1. Summary of Lineament Groups and Areas**

| Category | Category Description | Lineament Groups |
|---|---|---|
| I | Lineament groups that were not advanced for field investigation in 2013 based on Fugro (2013) desktop evaluations. Most were not rigorously inspected during field activities. | 4, 10, 11, 13, 14, 15, 16, 18, 24, 25, North-South Features near Talkeetna River-Susitna River Confluence |
| IIa | Lineament groups evaluated during 2013-2104 field studies, and judged to be non-tectonic (dominantly erosional, depositional, or jointing/bedding in origin). No further field investigation is recommended for evaluation as potential crustal seismic sources. | 1, 2, 3a, 3b, 5, 12a, 17a, 21a, 21b, 22, 23, 26, select Reger et al. (1990) features, Susitna feature, Watana lineament |
| IIb | Lineament groups evaluated during 2013-2014 field studies, and also judged to be of non-tectonic origin, but which appear to be spatially associated with previously mapped bedrock faults. No evidence of Quaternary faulting was observed, and no field investigation work is recommended for evaluation as potential crustal seismic sources | 6, 7, 8, 9, 12b, 17b, 17c, 19, 20, Broad Pass area, Clearwater Mountains area, select Reger et al. (1990) features, Talkeetna fault at T-1 and T-2 |
| III | Lineament groups that have defensible justification based on current field investigations for consideration or inclusion as crustal seismic sources in an updated seismic source model. | 27 (Sonona Creek fault), Castle Mountain extension |

Category I includes several lineament groups not advanced for further field study based primarily on distance from the site considerations derived from the evaluations (Fugro, 2013).

Many of the lineament groups investigated are judged to be dominantly erosional in origin, or to a lesser extent, related to rock bedding or jointing, are not associated with tectonic faults, and are thus assigned to Category IIa. A second set of lineament groups do appear to be coincident with previously mapped pre-Quaternary (i.e., bedrock) faults, but are also interpreted as erosional in origin as no evidence was found for offset or deformation of Quaternary deposits or surfaces. These are assigned to Category IIb.

Category III lineaments have defensible justification for consideration or inclusion as crustal seismic sources in an updated seismic source model, and consist of lineament group 27 (Sonona Creek fault) and lineaments of the Castle Mountain extension. The results of our field investigations did not identify any specific features with evidence of late Quaternary faulting within at least 25 mi (40 km) of the Watana dam site. For most of this area, the time and

detection limits of the imagery and field investigations imply post-glacial time limits of about 12,000 to 15,000 years, and detection of surface offsets of more than about 1 m extending over several kilometers. For the area near Watana dam site where detailed LiDAR data was the basis for this evaluation, potential detection limits of surface fault displacements are much lower (about 0.5 m over several hundred meters).

For crustal seismic evaluations, the ages from regional glacial chronologic correlations imply that the vast majority of the landscape within about 62 mi (100 km) of Watana dam site was covered beneath glacial ice or glacial lakes as late as about 17 ka, with a slow reduction in ice and lake extent through 12 to 11 ka (Fugro, 2015a). The final stages of deglaciation in the middle Susitna Basin near the Watana dam site appear to be recorded by the large areas of stagnant ice deposits extending north from the Susitna River between Tsusena and Deadman Creeks (Acres, 1982b) to Tsusena Butte (Figure 4-1). Samples for optically-stimulated luminescence (OSL) dating of this last stage of deglaciation were collected in 2014 from an exposure along Deadman Creek about 2.5 mi (4 km) northeast of the Watana Dam site. The OSL ages suggest that deglaciation and stagnation of the larger Deadman Creek ice lobe in the middle Susitna River valley, and thus, geomorphic surfaces on which a record of potential surface faulting might be preserved, must be older than about 14 to 15 ka (Fugro 2015a).

Despite the apparent absence of geologic evidence for late Quaternary faulting in the broader region, updates to the seismic source model (Fugro, 2012) may consider inclusion of portions of some new sources. Such an updated source model would consider the findings and limitations from this evaluation, seismicity recorded since 2012, and other data, although some seismic sources may be constrained to very low slip rates as defined by the crustal seismic study (Fugro, 2015a).

Synthesis of regional geology and seismology, sub regional mapping transects, and site data all indicate that major faults, typical of active crustal seismic sources capable of primary surface rupture associated with major earthquakes in the contemporary tectonic environment, are absent from the Watana dam site area. The evaluation of potential crustal seismic sources has not identified any specific features with evidence of late Quaternary faulting within at least 25 miles (40 km) of the Watana dam site. This is consistent with the observations that the reservoir area is structurally coherent with lack of pervasive penetrative deformation (see also Section14.1). This is also consistent with previous fault studies completed in the dam site area.

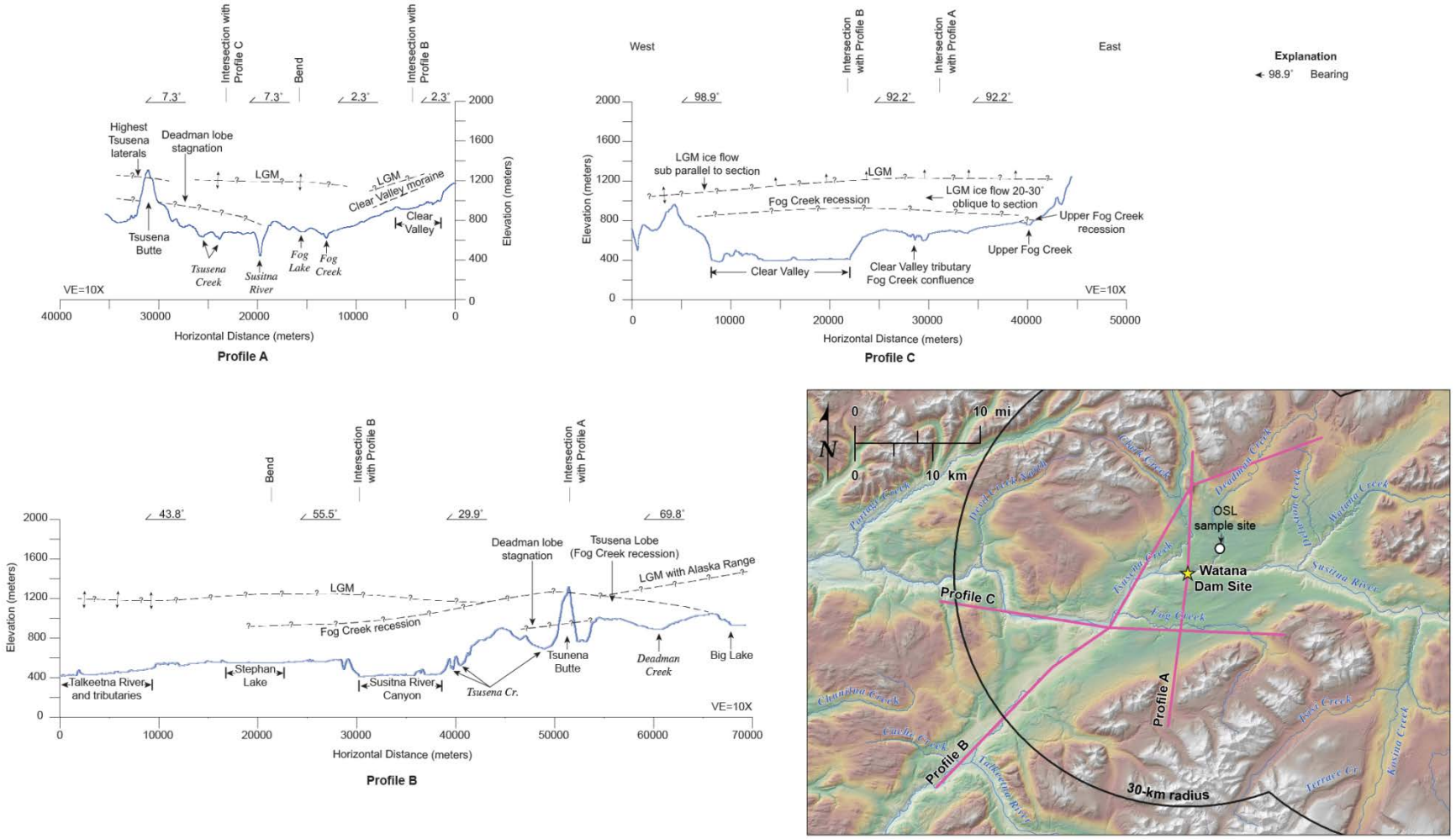


**Figure 4-1. Glacial Ice Reconstruction Profiles**

# 5. DAM SITE AREA FAULT RUPTURE EVALUATION

## 5.1.1. General

Permanent ground deformation from surface fault rupture can occur as primary, secondary, or sympathetic (triggered) rupture. Primary rupture is ground displacement associated with the main trace of a seismogenic fault. Secondary rupture is ground displacement from a fault that is structurally connected to the seismogenic fault, but is not the main seismogenic source. Sympathetic rupture is ground displacement from neither the main seismogenic source nor a secondary fault, but occurs principally from the effects of co-seismic strong ground shaking.

Potential sources of surface fault rupture hazard that were considered and characterized to the extent possible at the proposed Watana dam site consist of: 1) crustal seismic source faults with surface expression which transect the dam foundation directly or extend nearby, 2) buried or "blind" crustal seismic source faults with no direct surface expression, or 3) features, proximal to the dam site, not active in the contemporary stress regime that could be potentially reactivated through mechanisms of reservoir triggered seismicity. Each of these potential sources of surface fault rupture hazard was evaluated based on differing aspects and combinations of the existing geological, geophysical, and seismological data. Evaluation of crustal scale seismic source faults, either those with surface expression or "blind" structures, which are the source of primary or secondary fault rupture hazards underscores the importance of regional data because the source dimensions of these structures requires features with scales on the order of tens of kilometers. Evaluation of potential fault reactivation emphasizes knowledge of the existence, extent, and orientation of potential faults in the immediate site vicinity because of the potential significance to the dam. One common element for evaluation of each source of potential fault rupture hazard is the existence and characteristics of faults within the dam foundation. In an absence of known seismogenic faults at the dam site, the evaluation of fault rupture hazard focuses on the possibility of displacement along existing planes of weakness in the bedrock.

## 5.1.2. Methodology

The approach for evaluating surface rupture hazard at the dam site relies on four principal lines of independent data and analyses:

1. Assessment of the contemporary tectonic framework (stress field) of the site region as an indication of the potential for reactivation of site geologic features.

2. Geomorphic evaluation of Quaternary and post-glacial faulting (i.e., lineament mapping and analyses) to assess whether potential seismogenic faults are present near the site vicinity,

3. Field geologic transects to assess styles and patterns of structural deformation near the site, and

4. Assessment of results of site-specific investigations of geologic structure in the dam foundation.

Collectively, these four lines of independent and relatively indirect evidence are integrated to develop the evaluation of (or supporting argument for no) fault rupture hazard at the dam site. This approach is in accordance with accepted methods and practices currently used for similar evaluations on projects involving major dam projects or critical facilities that pose potential hazard to the public and environment.

The evaluation collectively considers regional tectonic history, sub-regional deformation patterns observed in Mesozoic and Cenozoic rocks around the site, emplacement of intrusions and volcanics at the dam site, crustal stress orientations from earthquake focal mechanisms, known active faulting, plate motions, and GPS data, geomorphic landform evaluations, and current understanding of geologic features at the dam site. The surface fault rupture evaluation assesses the weight of evidence in relation to three topical areas:

- The regional and subregional evidence of Quaternary faulting,

- The presence or absence of faults and large-scale shear features at the dam site proper,

- The qualitative potential for reactivation of geologic structures at the dam site within the current tectonic framework.

Regional and sub-regional evidence of Quaternary faulting through geomorphic evaluation of post-glacial faulting is the strongest argument to address late Quaternary faulting at the dam site. The evaluation of post-glacial faulting consisted of carefully inspecting and analyzing the detailed LiDAR elevation data in the dam site area (and vicinity) to identify evidence of tectonic geomorphology suggestive of faulting. In addition, field investigations were conducted to verify the results of desktop based LiDAR lineament mapping (refer to Fugro, 2015a).

Data on the potential existence and characteristics of faults and shear features in the dam foundation are discussed in the report on lineament mapping and analysis by Fugro (2013), and are further evaluated in the framework of the regional seismic source evaluations and sub-regional mapping near the dam site (Fugro, 2015a).

To evaluate the contemporary tectonic framework of the dam site, the updated information from the Susitna-Watana Seismic Network and the AEC regional network, as well as published literature, have been reviewed (AEC, 2014). This includes data on crustal stress orientations

from earthquake focal mechanisms, known active faulting, plate motions and GPS data, geomorphic landform evaluations, and current understanding of geologic features at the dam site.

### 5.1.3. Regional Evidence

The evaluation of potential crustal seismic sources has not identified any specific features with evidence of late Quaternary faulting within at least 25 mi (40 km) of the Watana dam site. Within this region, faults depicted on existing geologic maps were evaluated through field and imagery analyses for evidence of late Quaternary faulting and multiple types of imagery were reviewed to define lineaments, which were then evaluated through field investigation for evidence of potential Quaternary faulting (Fugro, 2013, 2015a). The area along the Susitna River, and extending at least 3 mi (5 km) north and south in proximity to the dam site and deeper portions of the proposed reservoir, was also imaged with high-resolution LiDAR and aerial photography. This data improved resolution and potential detection capability to reveal the geomorphic expression and thus, the existence of potential late Quaternary faults. These efforts indicate that at least over the past 12,000 to 15,000 years – the time since deglaciation of much of the area – there is no evidence for major surface-rupturing earthquakes from crustal scale seismic sources within the dam site region (25 mi (40 km) radius).

Over longer periods, the crustal seismic source evaluation also indicates an absence of significant zones of uplift or vertical deformation localized along specific surface or blind fault structures. Recurrent large earthquakes on blind faults, e.g. M ~6.5 or larger, with repeated dip slip motion over many events, eventually result in recognizable geomorphic features and topographic uplift which persists in the landscape proximal to these features. Thus, even for features with uplift rates as low as 0.004 in/yr (0.1 mm/yr), a fault slip rate associated with large earthquake recurrence approaching 10,000 years, would result in relative uplift of about 3,300 ft. (1000 m) over a period of 10 million years. For comparison, the topographic relief along the northwestern side of Mount Watana to the Fog Lakes area, taken as a proxy for maximum uplift in that area, is about 1,650 ft. (~500 m). Maximum topographic relief along even short, relatively linear sections of hills surrounding the Fog Lakes basin near the Watana dam site is primarily less than about 1,000 ft. (~300 m). For example, the Susitna Glacier fault, which was a “blind” initiating fault plane of the 2002 Denali M7.9 earthquake, ruptured the ground surface near the base of south-facing mountains that have about 1,500 ft. (~460 m) of relief. This illustrated the premise that blind or previously undetected Quaternary faults produce noticeable long-term topographic uplift near the “buried” fault tip even if the ground expression of surface rupture is not recognized. No such high-relief topography is present either at the dam site or in the site vicinity that would be a basis on which to postulate the presence of a nearby blind fault that might transect the site footprint.

The contemporary stress regime, as defined by current plate tectonic models, GPS observations, earthquake focal mechanisms, and Quaternary faulting indicates that the Watana dam site area is subject to northwest-southeast oriented sub-horizontal compressive stress associated with the long-term ongoing subduction of the Pacific Plate in south central Alaska. Crustal deformation associated with the plate interactions has been accommodated primarily along the Denali fault, as right-lateral motion, at a relatively constant rate over the past 10 million years (Freymuller, et al., 2008). Between the Denali fault and the Castle Mountain fault, geologic evidence suggests that the intervening Talkeetna Block – a region including the Watana dam site between the Copper River Basin to the east and the Susitna Basin to the west – has been relatively stable. This is consistent with the sub-regional mapping described above that indicates only gentle structural deformation (folding) and a relative paucity of penetrative faulting. Paleomagnetic data from volcanic rocks with ages of 30 to 50 million years indicates an absence of significant internal rotation or deformation within the Talkeetna Block (Figure 2-1). Likewise, the extent and distribution of these Tertiary volcanic rocks across the landscape of the Talkeetna Block argues against the existence of large-scale vertical or lateral fault displacements within the area.

Within the contemporary stress regime of the Talkeetna Block, the primary modes of tectonic deformation appear to involve right-lateral strike slip structures with east-northeast strikes (sub-parallel to the closest portion of the Denali and Castle Mountain faults), and with dip slip or compressional shortening along structures with northeast strikes or elongations (roughly perpendicular to the regional direction of crustal shortening), Figure 5-1. Structures with these orientations would be oriented roughly parallel to the overall structural grain of the pre-existing tectonic terrains and rock units within the Talkeetna Block. Secondary modes of tectonic deformation might involve left-lateral strike-slip motions along north to north-northwest striking faults, or potentially lessor amounts of extensional deformation along structures with northwest strikes. Because evidence suggests the dam site region is dominated by compression (Figure 5-1), extensional features are expected to be relatively less common and would primarily be expected as second or third order local structures, found locally in association with structural complexities of the primary east-northeast or northeast striking structures, instead of northwest-southeast trending structures that dominate the dam site (Fugro, 2015a).

### 5.1.4. Sub-Regional Geologic Transects

For evaluation of primary bedrock crustal structure, two sub-regional transects, one oriented roughly east-west along the Susitna River, and a second oriented roughly northeast-southwest along Watana Creek, provide the most complete bedrock exposures near the Watana dam site. These transects demonstrate that the Watana dam site lies within a relatively coherent structural block of folded Kahiltna Basin rocks which have been extensively intruded by mid to early Cenozoic igneous units. Data from these transects, and evaluation of existing geologic mapping,

does not define any apparent crustal scale faults within at least 3 mi (5 km) of the Watana dam site.

The most significant crustal fault structure in the area is the northeast-striking fault-bounded basin along Watana Creek that accommodated Tertiary sedimentation. Structural and stratigraphic data suggests that this basin most likely formed tectonically as an extensional graben in a right step-over between two strands of the Talkeetna fault, which was active at the time as a right lateral strike slip fault (essentially, a syntectonic depocenter) (Panel G on Figure 2-3). The dips, apparent section thickness, and extent of the Watana Creek basin sediments suggest vertical displacements of at least a few hundred meters, which would imply possible lateral offsets of at least a few kilometers. The Watana Creek basin contains non-marine sediments and undated volcanic flows that are tentatively correlated by Csejtey et al. (1978) to the Paleocene Chickaloon Formation of the Matanuska Valley. There appears to be a lack of sedimentary detritus from the surrounding more than 50 million year old dioritic and granitic sediments exposed in the surrounding the area, which in aggregate suggest a relatively older age for this period of strike slip faulting associated with the Talkeetna fault. The mid to early Cenozoic age of faulting implied by this data are consistent with existing mapping, which shows that the Talkeetna fault does not appear to offset or significantly displace plutonic rocks distally to the southwest of the Watana dam site (e.g., (Woodward Clyde Consultants (WCC), 1982); (Wilson, Schmoll, Haeussler, Schmidt, Yehle, & Labay, 2009)). It is also consistent with new mapping in the Talkeetna Mountains Quadrangle that shows an absence of continuity for the Talkeetna fault south of the Susitna River (Twelker, et al., 2014).

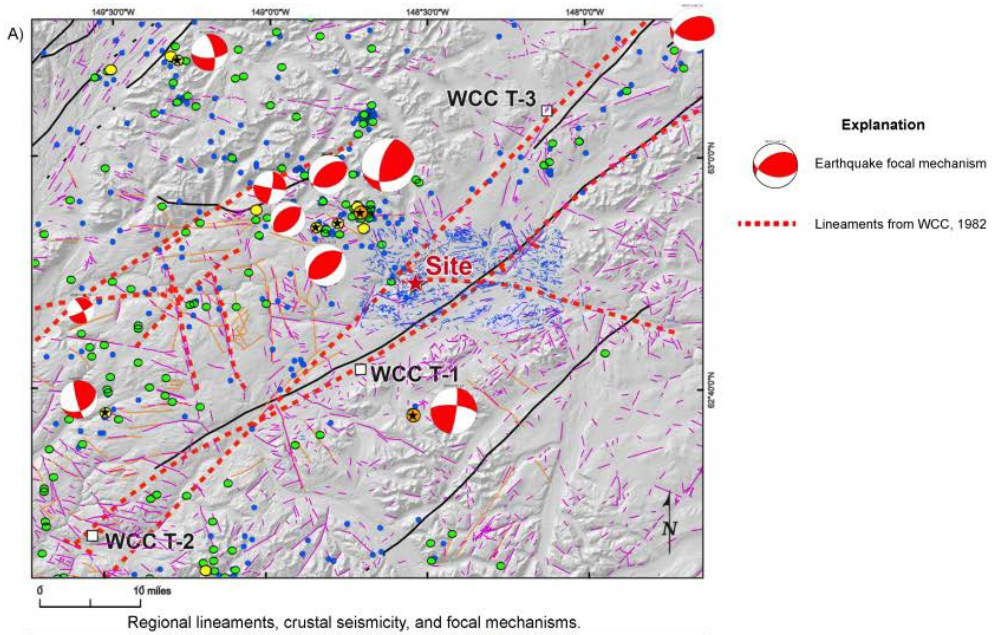


Regional lineaments, crustal seismicity, and focal mechanisms.

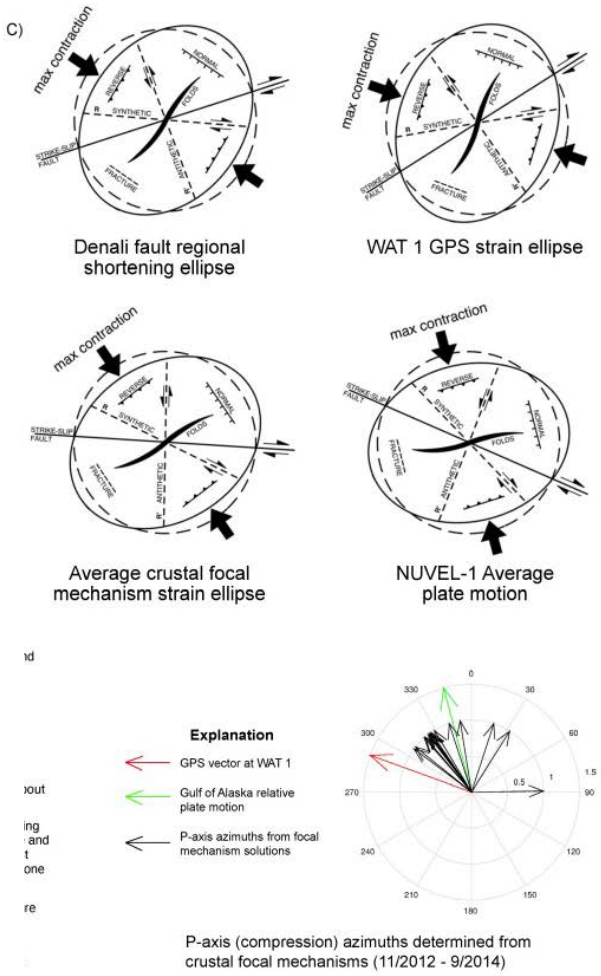


P-axis (compression) azimuths determined from crustal focal mechanisms (11/2012 - 9/2014)

**Figure 5-1. Crustal Stress Orientations and Strain Ellipses**

Published regional mapping does not depict any other faults that would intersect the sub-regional geologic transects or within at least 3 mi (5 km) of the Watana dam site ( (Csejtey, et al., 1978); (Wilson, Schmoll, Haeussler, Schmidt, Yehle, & Labay, 2009)). Some earlier studies suggested the possibility of structural control of the east – west trending sections of the Susitna River near the Watana dam site (e.g. (Gedney & Shapiro, 1975); and Watana lineament of (Woodward Clyde Consultants (WCC), 1982)) based on regional-scale lineament evaluations. However, the recent field mapping evaluations have not revealed evidence for such structures and dam site drilling investigations in 2014, which included two inclined boreholes drilled from opposite banks of the river (DH14-9b and DH14-10) beneath the river channel, through bedrock, encountered no large-scale shears or fault beneath the river nor east-west oriented features.

Previous mapping conducted for Watana dam site has depicted or inferred several nearby potential faults of crustal scale ( (Woodward Clyde Consultants (WCC), 1982); (Acres, 1982b)) as shown on Figure 2-5 and Figure 2-6. These faults are depicted with maximum map lengths of about 0.5 to 3 mi (0.8 to 5 km) and are primarily inferred extensions of shear features found in river valley wall exposures upstream and downstream of the Watana dam site, and extended kilometers northwest to apparently similar features in the nearest bedrock exposures along Susitna River tributaries and Tsusena Creek. Bedrock exposures in the intervening areas are covered by Quaternary deposits, and geomorphic evaluations based on the detailed LiDAR data and ground reconnaissance do not disclose evidence of the fault continuity or offset of the Quaternary units. This fault is approximately 0.5 mi (0.8 km) upstream of the Watana dam site and correlates to Geologic Feature 1 (GF1) of Acres (1982b).

An additional north-northeast trending fault is shown by Acres (1982b) upstream of the dam site near the mouth of Deadman Creek (Figure 2-5 and Figure 2-6); however, no detailed description of the fault was provided. No exposure of this “fault”, or of structures with similar orientations in the Kahiltna Basin rocks near the dam site were observed during mapping for the sub regional transects along the Susitna River in 2014. Moreover, there is no expression in the LiDAR data set of this fault along possible extensions to the northeast, and no indications of this structure in the Susitna River canyon exposures to the southwest or at the dam site. As depicted by Acres (1982b), much of the trace of this fault lies beneath the Susitna River channel or beneath Quaternary glacial deposits. Near the confluence of Deadman Creek and the Susitna River, the mapped location of this “fault” was inferred from widely spaced outcrops at river level observed during 2014 mapping. However, additional outcrops of Kahiltna Basin rocks observed from aerial traverses and evident in the LiDAR data set to the north and east of the confluence suggest the “fault” is more likely the intrusive contact zone between the Tertiary intrusive rocks and the Cretaceous Kahiltna Basin rocks, with an irregular, not planar geometry.

Mapping in 2014 identified two additional minor faults in bank exposures of the Cretaceous rocks along the north bank of the Susitna River at approximately 3.5 mi (~5.5 km) upstream of Deadman Creek. Neither fault can be traced beyond the bank exposures, and there is no indication of these faults is evident along strike in the detailed LiDAR data set. The two faults are located about 165 ft. (50 m) apart from each other and have strike and dip of 303°, 42° S and 300°, 32° S; thus, the faults trend northwest-southeast similar to the structural fabric observed (e.g., geologic features) at the dam site. Bed separation measured on the shallow dipping fault plane was 4 inches (10 cm) on both faults. Net slip estimated based on fault plane slickensides and a dipping bed offset by the fault indicates less than 3 ft. (1 m) of net slip; hence these are considered minor faults. Based on the sub-regional transects, these faults appear to represent a distinctly different style and orientation of faulting compared to that expressed by the geologic features observed at the Watana dam site. Overall, the Cretaceous rocks appear to be a structurally coherent block, not disrupted by major faults and there is no expression of these faults in the overlying Quaternary deposits.

### 5.1.5. Dam Foundation Geologic Features

Based on recent site mapping and re-interpretation of previous mapping (i.e., (Acres, 1982b)), the principal geologic features (GF) that underlie the dam footprint are:

- Geologic Feature GF4
- Geologic Feature GF5
- Other similar but unnamed geologic features
    - An unnamed structure delineated as underlying part of the dam foot print on the north bank of the Susitna River, approximately 220 ft. (67 m) downstream from GF5
    - Another unnamed feature mapped 580 ft. (177 m) downstream of GF5 on the north bank of the Susitna River.

Each of these geologic features was evaluated for their significance as potential fault rupture hazards (Fugro, 2015a).

### 5.1.6. Summary of Dam Foundation Fault Rupture Evaluation

In the evaluation of fault rupture hazards in the dam foundation, the approach used involved separate lines of enquiry that took into consideration various independent types of evidence. The evaluation assessed the weight of evidence in relation to: a) the regional and subregional evidence of Quaternary faulting, b) the presence of significant faulting or shear zones at the dam site, and c) the

qualitative potential for reactivation of geologic structures at the site within the current tectonic framework.

The evaluation found that one of the more compelling findings is the absence of crustal scale surface faults or apparent "blind" structures within several miles (kilometers) of the dam site. From detailed evaluations of new imagery data, evaluations of local and regional scale mapping, and field investigations, no evidence has yet been revealed of potential Quaternary faulting within at least 15 mi (~25 km) of the Watana dam site. Thus, this information strongly suggests that potential sources of primary or secondary, surface fault rupture at the dam site are absent. Further, geomorphic evaluations based on the detailed LiDAR data within about 3 mi (5 km) of the site has not identified any expression or continuity of potential faults or specific geologic features extending from the site area that would be indicative of deformation of Quaternary deposits. Given the absence of potentially active crustal scale seismic sources in the immediate site vicinity, the potential existence of small and minor structural features in the dam foundation bedrock does not indicate an elevated potential for a fault rupture hazard.

From sub-regional transects and evaluation of the existing mapping within about 3 mi (5 km) of the dam site suggest that the Watana dam site lies within a relatively coherent block of relatively gently folded Kahiltna Basin rocks that have been cross cut and locally disrupted by early Tertiary igneous and volcanic rocks. The intrusive process likely resulted in numerous alteration zones, fractures, and shears, but does not appear to be associated with nearby fault structures of significant crustal extent. The few short faults near the dam site depicted by Acres (1982b) are mostly likely similar features, and not post-intrusive, crustal scale faults. The closest major Tertiary structure appears to be the fault-bounded depositional basin along Watana Creek, approximately 8.5 mi (13.5 km) upstream of the Watana dam site.

The orientation of discontinuities and narrow shear features mapped at the site chiefly have northwest strikes and steep, vertical to near-vertical dips ( (U.S. Army Corps of Engineers (USACE), 1979); (Acres, 1982); (Harza-Ebasco, 1984); Fugro, 2015a). Based on review of the 2012 and 2014 drill hole logs, the bedrock encountered is pervasively fractured, with jointing prevalent in each and every boring. The joints are high-angle, and are reported as 70° dip or greater. Based on geologic mapping and oriented discontinuities in rock core in recent drill holes, it appears that thin shear zones present are high-angle features of about 80° dip. This is relatively consistent with the near vertical shears exposed in outcrop.

Regarding specific features that may lie within the dam footprint, existing data show a dominant structural fabric of northwest strikes and high-angle dips. Site mapping and overlapping drill holes beneath the Susitna River appear to exclude structures with orientations parallel to the river channel at the site. Those joints and shear zones that do cross the dam footprint appear to be relatively discontinuous along strike and are challenging to map and correlate from outcrop to outcrop.

Although not directly observed at the surface, geologic mapping within gullies, particularly those on the right abutment (GF4B and GF5), indicate that gullies likely formed initially by the preferential erosion of weak and relatively narrow fracture zones that have been widened and enhanced to their present dimensions by erosion due to stress relief and freeze thaw processes and/or block movement. Thus, the subset of geologic features that are depicted to transect the dam footprint appear to be relatively minor structures, with potentially limited bedrock continuity or persistence, and appear to have dominant orientations that are least favorable to reactivation in the contemporary stress regime.

The following is a summary of the principal findings and lines of evidence in relation to potential surface fault rupture:

1. The contemporary stress regime, as defined by current plate tectonic models, GPS observations, earthquake focal mechanisms and Quaternary faulting, indicates that the Watana dam site area is subject to northwest-southeast oriented sub-horizontal compressive stress associated with the long-term ongoing subduction of the Pacific Plate in south central Alaska. Crustal deformation associated with the plate interactions has been accommodated primarily along the Denali fault, as right-lateral motion, at a relatively constant rate over the past 10 million years. Between the Denali fault and the Castle Mountain fault, geologic evidence suggests that the intervening Talkeetna Block, a region including the Watana dam site, has been relatively stable.

2. Paleomagnetic data from volcanic rocks with ages of 30 to 50 million years indicates an absence of significant internal rotation or deformation within the Talkeetna Block. Similarly, the extent and distribution of Tertiary volcanic rocks across the Talkeetna Block argues against the existence of large-scale vertical or lateral fault displacements within the area.

3. Within the current stress regime of the Talkeetna Block, the primary modes of tectonic deformation appear to involve right-lateral strike slip structures with east-northeast strikes, and with dip slip or compressional shortening along structures with northeast strikes or elongations (roughly perpendicular to the regional direction of crustal shortening). Structures with these orientations would be oriented roughly parallel to the overall structural grain of the pre-existing tectonic terrains and rock units within the Talkeetna Block. Secondary modes of tectonic deformation might involve left-lateral strike-slip motions along north to north-northwest striking faults, or potentially smaller amounts of extensional deformation along structures with northwest strikes. Because regional evidence suggests the dam site region is dominated by compression, extensional features are expected to be relatively less common and would primarily be expected as second or third order structures found locally in association with structural complexities of the primary east-northeast or northeast striking structures.

4. Detailed evaluations of new imagery data, evaluations of local and regional scale mapping, and field investigations have not identified any evidence of potential Quaternary faulting within at least 15 mi (25 km) of the Watana dam site. These data strongly suggest that potential sources of primary or secondary surface fault rupture at the dam site are absent.

5. Evaluation of existing mapping within the dam site area, and data from sub-regional transects along the Susitna River do not support the existence of major crustal faults near the dam site. Mapped shear zones within this area appear to be primarily associated with the mid-early Tertiary intrusive rocks, similar to those at the site.

6. Geomorphic evaluations based on the detailed LiDAR data within the dam site area have not identified any expression or continuity of potential faults or specific geologic features extending from the site area that would be indicative of deformation of Quaternary deposits. This indicates that although shear features may be present in the foundation, there is evidence to support lack of surface displacement along these features in the last 12,000 to 15,000 years (Fugro, 2015a).

7. Recurrent large earthquakes on blind faults, e.g. M ~6.5 or larger, with repeated dip-slip motion over many events, produce and eventually result in recognizable geomorphic features and topographic uplift which persists in the landscape. No such high-relief topography is present at the dam site, which would be a basis on which to postulate the presence of a nearby blind fault or seismic source in the site vicinity.

8. Bedrock beneath the proposed dam, powerhouse, spillway and appurtenance structures consists of fresh to slightly weathered, blocky, strong to very strong diorite that is locally altered and fractured and includes minor shears and shear zones. Fracture zones, shear zones, and alteration zones tend to trend in a northwest-southeast direction, parallel to the predominant joint set (JS1) and to a lesser extent to a more north–south direction associated with a secondary set (JS3). On the south abutment just upstream of the proposed dam, several narrow northwest trending shear zones are cross-cut by a felsic dike and at least one healed fracture cuts across the shear zones. Together with the observations of healed shear and alteration zone, these observations suggest that many of the fracture and shear zones are likely associated with mid-early Tertiary intrusive processes and are not related to the contemporary seismotectonic regime.

9. Inclined drilling beneath the Susitna River, encountered generally fresh to slightly weathered, strong diorite. Although some widely spaced, narrow fracture zones and minor shear zones were intersected in the drill holes, no significant geologic structure was revealed beneath the river. This supports the interpretation that the river at the dam site is not controlled by a major through-going fault or shear zone.

10. Investigations were made of previously identified "geologic features", shear and/or fracture zones greater than 5 ft. (1.5 m) in width, several of which may cross beneath the dam site. It is now considered that the prominence of these features, particularly those that would be encountered in the dam and spillway foundations, has been over-represented in geologic characterization conducted in previous studies. Further, the subset of geologic features that are depicted to transect the dam footprint appear to be relatively minor structures, with potentially limited bedrock continuity or persistence, and appear to have dominant orientations that are least favorable to reactivation in the contemporary stress regime.

In conclusion, therefore, it is considered that the potential for any reactivation of the geologic features that might transect the dam footprint must be considered extremely low given the following:

- The apparent lack of continuity and small scale of structural geologic features at the site (shear zones) upon which surface fault rupture could conceivably take place;
- The dominant northwest-southeast trend is unfavorably oriented with respect to the contemporary tectonic stress regime, as the primary mode of tectonic deformation appear to involve right-lateral strike slip structures with east-northeast strikes, ;
- The absence of nearby crustal scale fault structures and neotectonic or paleoseismic evidence of Quaternary faulting; and
- The absence of Quaternary faults mapped with about 15 mi (25 km) of the dam site.

# 6. SEISMIC SOURCE CHARACTERIZATION

The seismic source characterization was developed as an update to WCC (1980) model. The seismic source model summarized herein addresses deep (subducting plate) and shallow (crustal) seismic sources, as well as background (aerial) seismic sources.

## 6.1. Subduction Zone

The Alaska subduction zone (ASZ) is one of the world's most seismically active subduction zones. Relative plate motion between the Pacific and North American Plates increases from about 2 in/yr (5.4 cm/yr) at its eastern end near the Talkeetna Mountains to about 3 in/yr (7.8 cm/yr) at the west end of the Aleutian arc (Carver & Plafker, 2008) (Figure 2-13). The ASZ is also termed the Alaska-Aleutian Arc. East of longitude 170 degrees West, the Pacific Plate is subducting beneath continental crust, while to the west it subducts beneath oceanic crust that was trapped after initiation of the arc in the middle Eocene. This results in a more shallow-dipping plate interface to the east than to the west.

Earthquakes associated with the ASZ are of two main types: large "megathrust" events due to accumulated frictional strain along the interface of the two plates (most notable being the 1964 M 9.2 earthquake, described in Section 2.4.2), and those occurring within the down going Pacific Plate as it descends into the mantle. These "intraslab" earthquakes, considered capable of reaching magnitudes of M 7.5 and higher, are due to factors such as spreading ridge push, gravitational pull of the plate due to density contrasts between it and the mantle, and metamorphic reactions due to increasing temperature and pressure within the down going plate.

The dam site area lies at the eastern end of the ASZ. At this location the plate interface has an extremely low dip, almost flat (Figure 6-1). The northern boundary of the interface is at a depth of about 22 mi (35 km) and lies about 50 mi (80 km) southeast of the site. To the northwest of this line intraslab earthquakes are produced as the plate dips more steeply as it descends into the mantle. Beneath the site the top of the plate is at a depth of about 31 mi (50 km) (Figure 6-1).

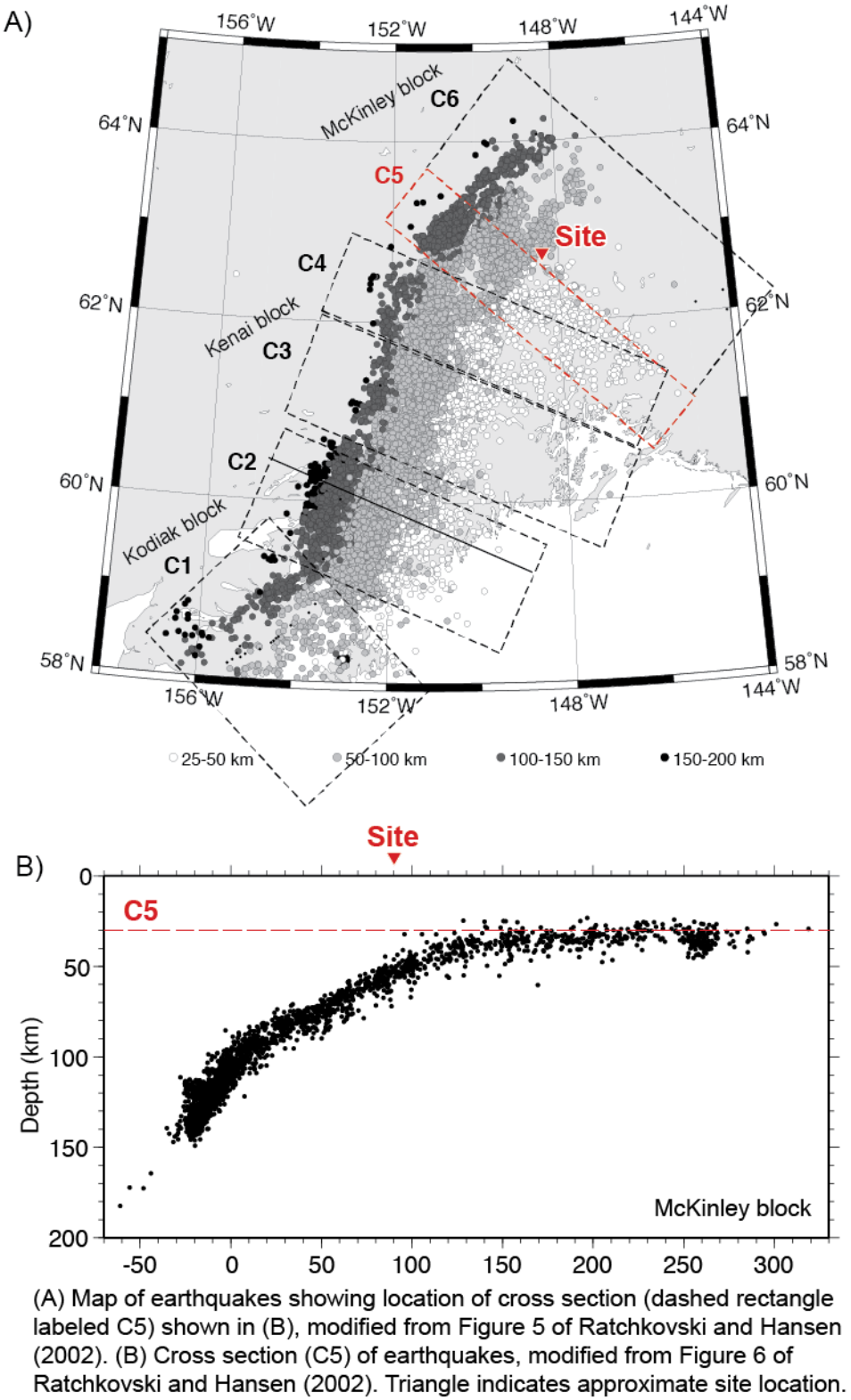


(A) Map of earthquakes showing location of cross section (dashed rectangle labeled C5) shown in (B), modified from Figure 5 of Ratchkovski and Hansen (2002). (B) Cross section (C5) of earthquakes, modified from Figure 6 of Ratchkovski and Hansen (2002). Triangle indicates approximate site location.

**Figure 6-1. Map and Cross Section of Alaska Subduction Zone Earthquakes**

### 6.1.1. Interface

The interface between the North American and Pacific Plates is the source of the largest magnitude earthquakes in the source model. Due to studies of the 1964 M 9.2 earthquake, seismic refraction/reflection surveys (e.g. (Brocher, et al., 1994)), and research results from a regional seismograph network operated by the Alaska Earthquake Information Center (AEC) (Ratchkovski & Hansen, 2002), the geometry of the down going plate within a few hundred km of the site is fairly well known. In this region, Wesson et al. (2007) following cross sections of relocated seismicity shown in Ratchkovski and Hansen (2002), modeled the interface as shown in Figure 6-2. In this figure the up-dip 12 mi (20 km) contour is seen to the southeast. The contour representing the down-dip boundary of the plate interface is seen to the northwest. To the southwest its depth is 25 mi (40 km), reflecting the steeper interface dip to the west, and at longitude 151 degrees West, it begins to shoal from 25 mi (40 km) to 20 mi (33 km) to the end of the interface at the northeast end. This reflects the slightly tilted interface seen in Figure 6-1.

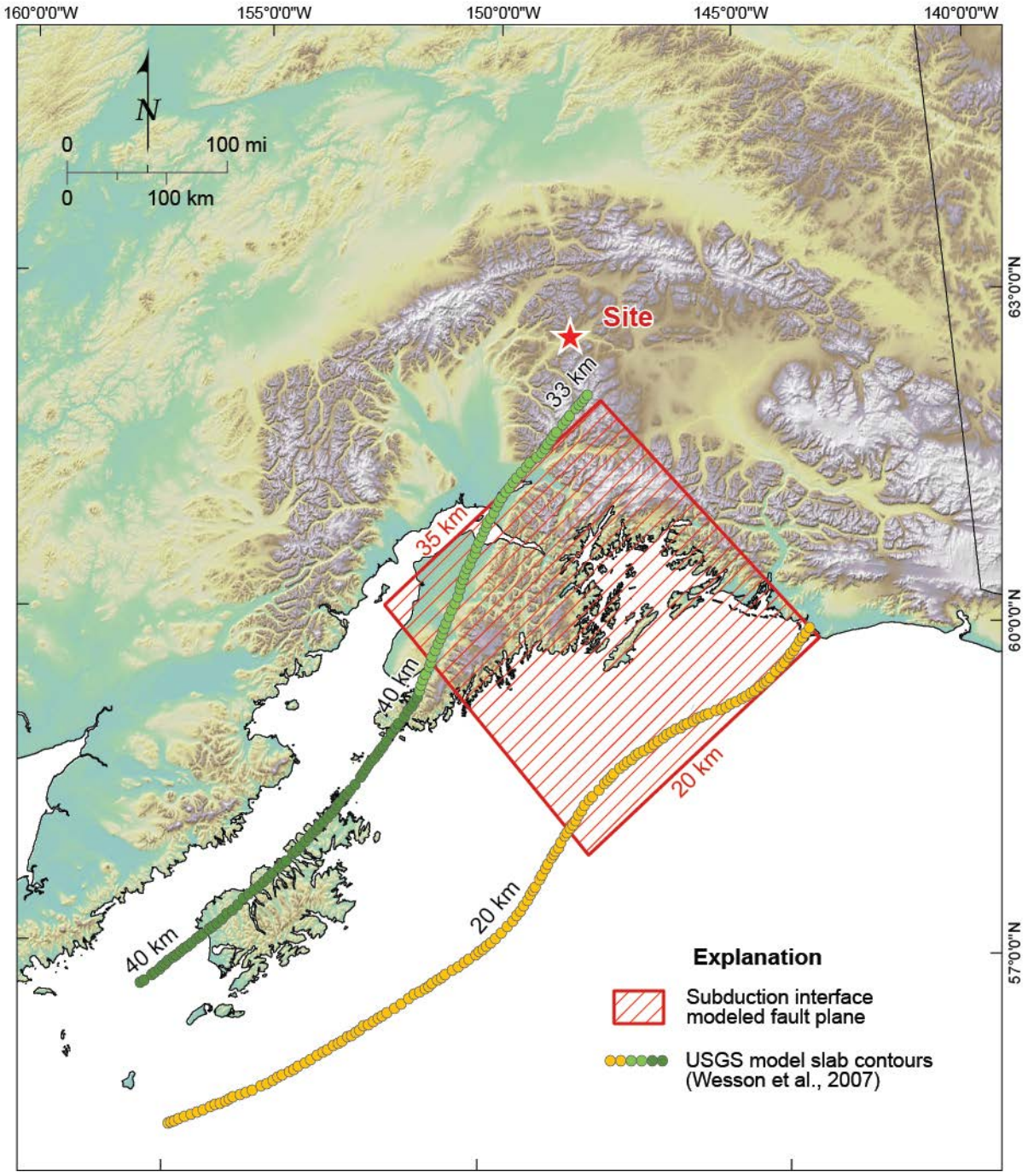


**Figure 6-2. Subduction Interface Model**

### 6.1.2. Intraslab

Intraslab earthquakes occur within the down going Pacific plate, after it breaks contact with the North American Plate in the megathrust zone, and assumes a steeper dip as it descends into the upper mantle. Notable earthquakes of this type include the M 6.5 1965 and M 6.8 2001 Nisqually, Washington earthquakes associated with the Cascadia subduction zone. As seen in Figure 6-1, in the dam site region this megathrust zone consists of two parts: an intermediate zone dipping about 25 degrees between depths of 31 and 50 mi (50 and 80 km), and a deeper zone from 50 to 93 mi (80 to 150 km) that dips more steeply. The physical sources of these earthquakes include ridge push from oceanic spreading ridges, gravitational pull of the slab due to density contrasts between it and the surrounding mantle, and chemical reactions due to increasing pressure and temperature.

## 6.2. Crustal Faults

The following section discusses all faults within 125 mi (200 km) of the dam site with evidence of historical or Quaternary activity, as well as suspicious faults that may or may not be active structures (Figure 1-1, Table 6-1 and Table 6-2). The primary compilation of faults in Alaska, and the initial basis for the seismic source model included is the “Neotectonic Map of Alaska” by Plafker et al. (1994). Quaternary faults identified after the Plafker et al. (1994) map and presented in published literature have also been included in the model. A Quaternary fault and fold database of Alaska has been compiled by the Alaska Division of Geological & Geophysical Surveys (Koehler R. , Farrell, Burns, Combellick, & Weakland, 2011a), however, final publication of the database was subsequent to the source model development (Fugro, 2012). Table 8-1 and Table 8-2, numerates the closest distance from the site area to the faults listed in Table 6-1 and Table 6-2.

**Table 6-1. Fault Characterization**

| Fault Name | Section | Age from Plafker et al. (1994) | Age from Other Sources | Sense of Slip | Dip | Seismogenic Depth (km) | Slip Rate (mm/yr) | Recurrence (years) |
|---|---|---|---|---|---|---|---|---|
| Castle Mountain fault | Eastern Castle Mountain - Caribou fault | Eastern Castle Mountain = Historic; Caribou = Pleistocene | Historic based on 1984 seismicity (Lahr, Page, Stephens, & Fogleman, 1986) | RL - Reverse | 76° N (Lahr, Page, Stephens, & Fogleman, 1986) ; 80°-90° (Fuchs, 1980) | ? | lateral: 0.5 - 0.6 (Fuchs, 1980) thrust:? | N/A |
| | Western Castle Mountain | Holocene | Holocene ( (Haeussler, Best, & Waythomas, 2002); (Willis, Haeussler, Bruhn, & and Willis, 2007) | RL - Reverse | 70°-90° N (Haeussler, Bruhn, & Pratt, 2000) | 20 [based on 1984 EQ Lahr et al., (1986) ] | lateral: 2.8-3.6, [preferred rate of 3.0 - 3.2] (Willis et al., (2007)); 2.9 mm/yr (Wesson et al. (2007)); 0.45-0.63 (Koehler and Reger, (2011)) thrust: 0.07-0.14 | 700 (Haeussler, Best, & Waythomas, 2002) |
| Denali fault | Eastern | Holocene | Holocene (Matmon, et al., 2006) | RL | ? | ? | 8.4 +- 2.2 mm/yr (Matmon, et al., 2006) | 380 (mean ages from (Plafker, Carver, Cluff, & and Metz, 2006)and DFWG summarized in Koehler et al., (2011)) |
| | Central | Holocene/ Suspicious | Historic - 2002 M7.9 (Eberhart-Phillips, et al., 2003). | RL | 75°-90° (Haeussler, et al., 2004). | 12 [from 2002 aftershocks (Ratchkovski, Wiemer, & Hansen, Seismotectonics of the Central Denali Fault, Alaska, and the 2002 Denali Fault Earthquake Sequence, 2004)] | 14.4 +- 2.5 mm/yr (Matmon, et al., 2006), 85 km W = 13.0 +- 2.9 mm/yr 255-283 km W = 9.4 +- 1.6 mm/yr 323 km W = 6.7 +- 1.2 mm/yr (Mériaux, et al., 2009) (distance relative to Totschunda junction) | 400 (mean age from DFWG summarized in Koehler et al., (2011)) |
| | Western | Holocene/ suspicious | N/A | RL | ? | ? | ? | ? |
| Pass Creek - Dutch Creek fault | N/A | Late Pleistocene | Holocene (Haeussler P. , An overview of the neotectonics of interior Alaska—Far-field deformation from the Yakutat Microplate collision, 2008) | Normal | ? | ? | 1.72 mm/yr min slip rate based on scarp height of Willis and Bruhn (2006) | 1340 max (Willis & Bruhn, 2006) |
| Sonona Creek fault | N/A | N/A | Holocene (Williams & Galloway, 1986) | ? | ? | ? | ? | ? |
| East Boulder Creek fault | N/A | Late Pleistocene | Holocene (1994) | ? | ? | ? | ? | ? |
| Matanuska Glacier fault | N/A | N/A | Holocene (Haeussler & Anderson, 1995) | Right normal | ? | ? | ? | ? |
| Susitna Glacier fault | N/A | N/A | Historic 2002 M7.9 (Eberhart-Phillips, et al., 2003) | Reverse | 19-48 (Crone et al., (2004)and Ratchovski et al.,) | ? | ? | ~4000 (Crone, Personius, Craw, Haeussler, & Staft, 2004) |
| Broxson Gulch fault | N/A | Neogene | Cenozoic (Ridgeway et al., (2002)) | Reverse | 5-40 (Stout & Chase, 1980) | ? | ? | ? |
| McCallum-Slate Creek fault | N/A | Late Pleistocene | Early Pliocene (Weber & Turner, 1977) | Reverse ? | ? | ? | ? | ? |
| Bull River fault | N/A | suspicious | N/A | Reverse | ? | ? | ? | ? |
| Foraker fault | N/A | ? | N/A | Reverse | ? | ? | ? | ? |
| Broad Pass fault | N/A | ? | N/A | Reverse | ? | ? | ? | ? |

Notes: See Table 6-2 for Northern foothills fold and thrust belt faults

**Table 6-2. Northern Foothills Fold and Thrust Belt (NFFTB) Fault Data**

| Fault Name | Age from Plafker et al. (1994) | Age from Bemis et al. (2015) | Sense of Slip | Dip (direction) |
|---|---|---|---|---|
| Billy Creek fault | suspicious | Holocene | LL - Reverse (NW up) | >60 (?) |
| Canteen fault | Late Pleistocene | Holocene | LL - Reverse (NW up) | >60 (direction?) |
| Cathedral Rapids fault | N/A | Holocene | Reverse (S up) | 15-60 (S) |
| Ditch Creek fault | N/A | Quaternary | Reverse (SW up) | >60? (SW?) |
| Donnely Dome fault | Late Pleistocene | Holocene | Reverse (S up) | 45-90 (S) |
| Dot "T" Johnson fault | N/A | Holocene | Reverse (S up) | 15-45 (S) |
| East Fork fault | Holocene | Holocene | Reverse (N up) | >60 (S?) |
| Eva Creek fault | N/A | Quaternary | Reverse (N up) | >60 (direction?) |
| Glacier Creek fault | N/A | Quaternary | Reverse (S up) | 30-60 (S) |
| Gold King fault - Section A | N/A | Late Pleistocene | Reverse (S up) | 15-30 (S) |
| Gold King fault - Section B | N/A | Quaternary | Reverse (S up) | 10-30 (N) |
| Granite Mountain fault A | Late Pleistocene | Holocene | LL - Reverse (NE up) | >60 (direction?) |
| Granite Mountain fault B | Late Pleistocene | Quaternary | Reverse (S up) | 30-60 (SW) |
| Healy Creek fault | Late Pleistocene | Late Pleistocene | Reverse (N up) | 60-90 (N) |
| Kansas Creek fault | N/A | Quaternary | RL - Reverse (S up) | >30 (S) |
| Macomb Plateau fault | N/A | Quaternary | Reverse (S up) | 15-60 (S) |
| McGinnis Glacier fault | | Holocene | Reverse (SW up) | >45 (SW?) |
| Molybdenum Ridge Fault | N/A | Holocene | Reverse (S up) | 15-45 (S) |
| Mystic Mountain fault | Neogene | Late Pleistocene | RL - Reverse ( S up) | >30 (S) |
| Nern Foothills thrust | N/A | Late Pleistocene | Reverse (S up) | 15-45 (S) |
| Panoramic fault | N/A | Late Pleistocene | Reverse (NE up) | >60 (?) |
| Park Road fault | N/A | Late Pleistocene | Reverse (N up) | 30-90 (N) |
| Peters Dome Fault | N/A | Quaternary | Reverse (S up) | 15-45 (S) |
| Potts fault | N/A | Quaternary | Reverse (NE up) | >60? (?) |
| Red Mountain fault | N/A | Late Pleistocene | Reverse (S up) | 30-60 (?) |
| Rex fault | N/A | Late Pleistocene | Reverse (S up) | >30 |
| Stampede fault | N/A | Late Pleistocene | Reverse (N up) | 15-30 (N) |
| Trident fault | N/A | Late Pleistocene | Reverse (SE up) | >30 (SE) |
| Trident Glacier fault | N/A | Quaternary | Reverse (S up) | 30-60? (S) |

Notes:
(1) Fault Data from the NFFTB summarized from Bemis et al. (2015)
(2) LL = left lateral, RL = right lateral.

### 6.2.1. Denali Fault

The Denali fault is a right-lateral fault with an arcuate shape striking to the northwest in the east, and an increasingly westerly and southwesterly strike to the west (Figure 2-10). A typical geometry evoked for the fault includes an eastern section located east of the junction with the Totschunda fault, a central section between the Totschunda junction and an asperity in the fault strike near Denali, and a western section west of Denali. The western termination of active faulting is considered in the source model to be at latitude 154.7°W based on Wesson et al. (2007), who propose that slip tapers to 0 mm/yr at this location. Western continuation of the fault beyond this point would not be expected to have significant impact on the site ground motions due to the large distance, ~202 mi (~324 km), to the western end of the Denali fault. The fault sections outlined above serve solely for geographic reference, as there is no evidence that the section boundaries would inhibit seismic rupture.

The largest historical earthquake on the fault is the 2002 M7.9 Denali fault earthquake, which had 211 mi (340 km) of total surface rupture. The earthquake initiating in the west and ruptured a 30 mi (48 km) long section of the previously unrecognized Susitna Glacier thrust fault. Slip propagated primarily eastward rupturing 140 mi (226 km) of the Central Denali fault. At the eastward limit of slip on the Central Denali fault the rupture stepped southeastward rupturing 66 km of the Totschunda fault (Haeussler, et al., 2004).

Subsequent studies of Quaternary slip rates along the fault using cosmogenic exposure dating of offset moraines and other glacial features show a westward reduction in slip rate on the Denali fault (Figure 2-10). Matmon et al. (2006) calculate an 8.4 ± 2.2 mm/yr slip rate for the eastern Denali fault, and a 6.0 ± 1.2 mm/yr on the Totschunda fault. The slip rates of the Totschunda and Eastern Denali faults sum to 14.4 ± 2.5 mm/yr at the eastern part of the Central Denali fault section. The preferred slip rates on the central Denali fault west of the Totschunda fault junction are: 53 mi (85 km) west of the site is 13.0 ± 2.9 mm/yr (Mériaux, et al., 2009), 255-283 km west is 9.4 ± 1.6 mm/yr (Matmon, et al., 2006), 323 km west is 6.7 ± 1.2 mm/yr (Mériaux, et al., 2009), and 390 mi ( 626 km) west is 0 mm/yr (Wesson, Boyd, Mueller, Bufe, Frankel, & Petersen, 2007). The westward reduction in slip rate is widely considered to be the result of the partitioning of slip onto the Northern foothills fold and thrust belt (Figure 2-12) ( (Bemis, Wldon, & Carver, 2015); (Haeussler P. , 2008); (Matmon, et al., 2006); (Mériaux, et al., 2009) ). These slip rates are in line with measurements of strain accumulation via geodetics, 6.5 to 9 mm/yr (Fletcher, 2002), and INSAR, 10 mm/yr (Biggs, Wright, Lu, & Parsons, 2007). The westward reduction in slip rate is also consistent with the westward decrease in displacement during the 2002 earthquake (Haeussler, et al., 2004).

Paleoseismic studies performed by the Denali Fault Working Group after the 2002 earthquake found that the penultimate slip events were of similar magnitude to the 2002 event

(Schwartz & (DFEWG), 2003). Carver et al. (2004) used tree ring counts from damaged trees near the Delta River to propose that the penultimate event was a M7.2 earthquake on July 6, 1912. Results from test pits adjacent to the Delta River by Plafker et al. (2006) suggest two paleo-events at 310 to 460 years before present, and 650 to 780 years before present. Trenching by the Denali Fault Working Group produced the following Denali fault earthquake chronology:

- The 2002 rupture trace had earthquakes between 350 and 600 years before present, and between 715 and 1,080 years before present;
- West of the 2002 earthquake the fault ruptured between 110 and 380 years before present, and between 560 and 670 years before present;
- East of the Totschunda – Denali fault junction the fault experienced three events between 110 and 356 years before present; ≥560 and 690 years before present; and ≤1,020 and 1,230 years before present (summarized in (Koehler, Personius, Schwarz, Haeussler, & Seitz, 2011b)).

Koehler et al. (2011b) trenched a site along the 2002 rupture trace and found that the penultimate event at this location was after 560 to 670 years before present. None of the paleoseismic trenching studies found evidence for the 1912 Delta River earthquake discussed in Carver et al. (2004)and Doser (2004).

### 6.2.2. Castle Mountain Fault

The Castle Mountain fault is an active, oblique strike-slip fault with a western and eastern section (Figure 6-3). The eastern section is combined with the Caribou fault of Plafker et al. (1994) due to their parallel geometry and the designation by Plafker et al. (1994) that both sections have evidence for Quaternary displacement. The eastern section-Caribou fault is primarily recognized in bedrock, has no evidence for Holocene surface rupture, and has historic seismicity to Mb 5.7 (1984 EQ documented in (Lahr, Page, Stephens, & Fogleman, 1986) ). The western section is defined by a 39 mi (62 km) Holocene fault scarp (north side up); and has no known historic seismicity greater than M5 (Flores & Doser, 2005). The fault trace was mapped in detail by Detterman et al. ( (1974) and (1976) ), and also by Haeussler (1998). Detterman et al. (1974) document a near surface fault dip of 75 degrees northward and seismic reflection data shows the fault to be steeply dipping (70 to 90 degrees) at depth (Haeussler, Bruhn, & Pratt, 2000).

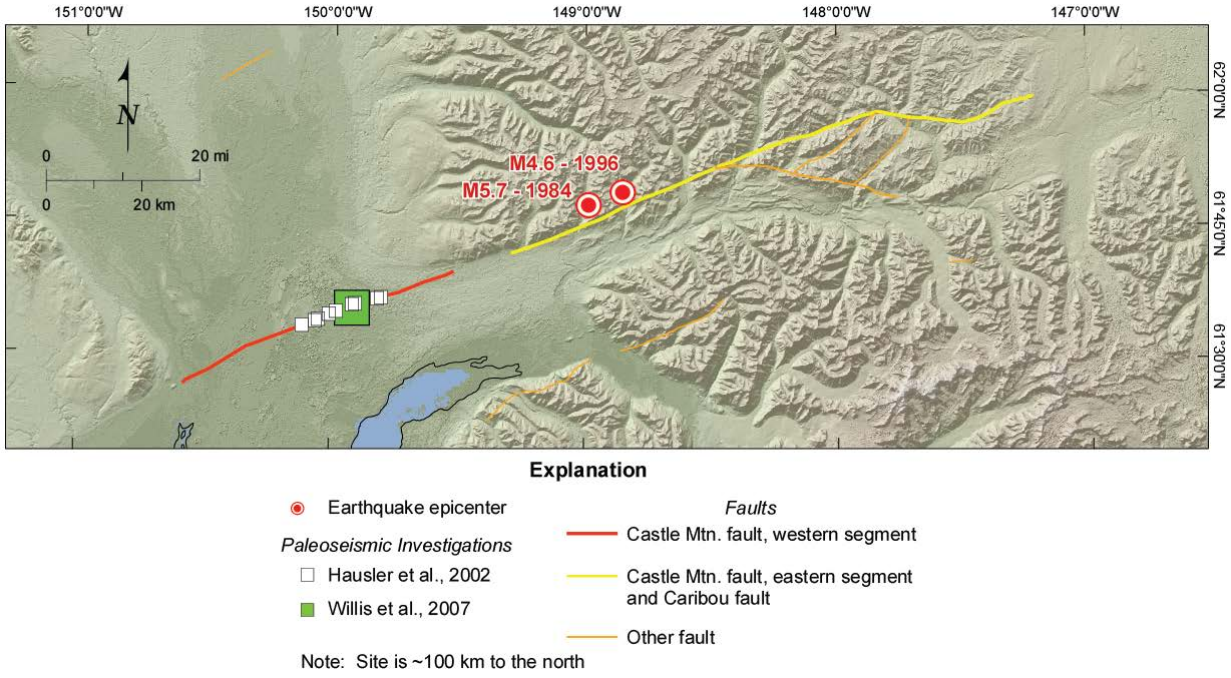


**Figure 6-3: Castle Mountain Fault**

Paleoseismic investigations of the Castle Mountain fault have yielded varying Quaternary slip rates and interpretations of deformational style. Detterman et al. (1974) proposed a maximum age for the most recent event of 1860 ± 250 years based on a radiocarbon ages of a displaced soil horizon exposed in a trench across a 6.9 ft. (2.1 m) high scarp. Detterman et al. (1974) also document 23 ft. (7 m) of horizontal displacement of a linear sand ridge across the fault. Trenching by Haeussler et al. (2002) on the western section identified 4 earthquakes on the fault (including one event on an adjacent fault strand) in the past 2800 years with a recurrence interval of approximately 700 years. The most recent rupture occurred 730-610 years before present. Haeussler et al. (2002) determined a shortening rate of 0.07 to 0.14 mm/yr but no lateral offset was observed in the trenches. Willis et al. (2007) use an offset post-glacial outwash channel on the western section to constrain a lateral slip rate of 2.8 mm/yr to 3.6 mm/yr), with a preferred rate of 3.0 mm/yr to 3.2 mm/yr Koehler and Reger (2011) propose that a lateral slip rate of 0.45 to 0.63 mm/yr may be more appropriate for the western section. Fuchs (1980) proposed a post-Eocene slip rate of 0.5 to 0.6 mm/yr for the eastern section.

### 6.2.3. Pass Creek – Dutch Creek Fault

The Pass Creek – Dutch Creek fault is a northeast-striking, south side down, normal fault bounding the northern edge of the Peters Hills Basin (Haeussler P. , 2008) (Figure 1-1). The Peters Hills basin is a small Neogene basin that may be a piggyback basin in the hanging wall of a "Broad Pass fault" (see discussion on the Southern Denali fault zone below)

(Haeussler P. , 2008). The Pass Creek – Dutch Creek fault forms a 21 ft. (6.5 m) tall scarp that displaces Holocene sediments, and creates a vegetation lineament on the north side of the Skwentna River. The last significant rupture on the fault had > 6.5 ft. (>2 m) of uplift and cut a moraine with a radiocarbon age of 1340 ± 60 years before present (Willis & Bruhn, 2006).

### 6.2.4. Sonona Creek Fault

The Sonona Creek fault is located in the western Copper River basin. The structure is mapped by Williams and Galloway (1986) as a 4 mi (7 km) long, northeast-striking fault with north side down sense of displacement, offsetting Late Pleistocene glaciolacustrine sediments. No information is provided by Williams and Galloway (1986) to indicate further the age, sense or amount of displacement on this fault. Although resolution is low, topographic height of the scarp appears limited, suggesting that at least the vertical slip rate is relatively low. As a singular surface rupture along a potentially active fault, the length of the scarp is relatively short. The presently available aerial imagery (Google Earth) of the fault is permissive of extensions and certainly do not rule out extensions of this fault in either direction.

## 6.3. Zones of Distributed Deformation

Zones of distributed deformation are regions with poorly characterized or suspected active faults; where the Quaternary geologic and fault mapping may be incomplete, and/or the slip-rate and recurrence of individual faults is poorly understood. The site region includes two areas classified as zones of distributed deformation: the Northern foothills fold and thrust belt, and the Southern Denali faults.

### 6.3.1. Northern Foothills Fold and Thrust Belt Zone

The Northern foothills fold and thrust belt (NFFTB) is a zone of Quaternary faults and folds along the north side of the Alaska Range ( (Bemis & Wallace, 2007); (Bemis, Wldon, & Carver, 2015)) (Figure 2-12, Table 6-2). The zone is primarily comprised of variably dipping thrust faults with dominantly north vergent deformation. Bemis and Wallace (2007), propose that much of the NFFTB is underlain by a gently south-dipping basal detachment that may daylight at the Northern foothills thrust along the northern margin of the NFFTB in the vicinity of the Nenana River. The surface trace of the basal detachment is not identified in the western and eastern margins of the NFFTB. The western margin of the NFFTB is marked by the termination of uplifted topography northwest of the Peters Dome fault and the Kantishna Hills anticline. The eastern margin is constrained by the paleoseismic investigation by Carver et al. (2010) which found no evidence for Quaternary deformation east of the Cathedral Rapids fault in the vicinity of Tok, Alaska. Quaternary deformation is presumed across the uplifted region within the NFFTB; however, rates of Quaternary deformation along individual faults are still poorly constrained (Bemis, Wldon, &

Carver, 2015). Mapping of deformation in Pleistocene gravels by Bemis (2010) suggests that the region west of the Nenana River has a maximum shortening rate of 3 mm/yr. Bemis et al. (2015) used offset Nenana gravel along the Granite Mountain fault to suggest horizontal shortening 1-4 mm/yr of in the eastern NFFTB. Meriaux et al. (2009) proposes that the partitioning of slip from the Denali fault onto the NFFTB could produce convergence rates up to about 4 mm/yr in the eastern NFFTB end, and about 12 mm/yr to the west. Due to the apparent variability in slip rates longitudinally across the NFFTB the zone is divided into a western and eastern zone.

## 6.4. Talkeetna Block Structures

The region is characterized by bedrock faults and distributed deformation associated with Cretaceous accretion of the Wrangellia Terrane ( (Csejtey, et al., 1978), (1992); (Ridgway K. D., Trop, Nokleberg, Davidson, & Eastham, 2002) ) and post-accretionary right-lateral bulk shear in the Tertiary, (O'Neill, Schmidt, & Cole, 2005); (Glen, Schmidt, & and Morin, 2007b)). To date, no direct geologic evidence to conclusively evaluate the late Quaternary fault activity in the Talkeetna Block exists, although new mapping is underway by the DGGS (Twelker, et al., 2014). The proximity of the Talkeetna block structures to the Watana dam site area requires a thorough discussion of the previously mapped faults with respect to the seismic hazard characterization (Fugro, 2013; 2015a.

### 6.4.1. Talkeetna Thrust Fault / Talkeetna Suture

A previously mapped through-going structure within the Talkeetna block is the Talkeetna thrust fault along the eastern margin of the Talkeetna suture zone (e.g. Figure 2-1 and Figure 2-2). The Talkeetna thrust is mapped as a northeast-striking, southeast-dipping fault by Csejtey et al. (1978), WCC (1982), and Wilson et al. (1998) (Figure 6-4). The fault juxtaposes Triassic and Permian metavolcanic and metasedimentary Wrangellia terrane rocks on the south against late Jurassic through Cretaceous sedimentary rocks of the Kahiltna Assemblage on the north. The mapped trace of the fault, depicted as concealed and inferred along much of its extent, projects in the northeast toward the younger Broxson Gulch thrust and is mapped as being obscured in the southwest by Tertiary igneous rocks. The approximate fault trace follows a broad topographic lineament striking northeast across the Talkeetna Mountains (Figure 6-4); however, the precise location of the fault (expressed as a lineament) is obscured along much of its length by Tertiary igneous rocks and Quaternary sediments. The investigation by WCC (1982) found indeterminate geologic evidence for conclusively evaluating Quaternary activity along the fault.

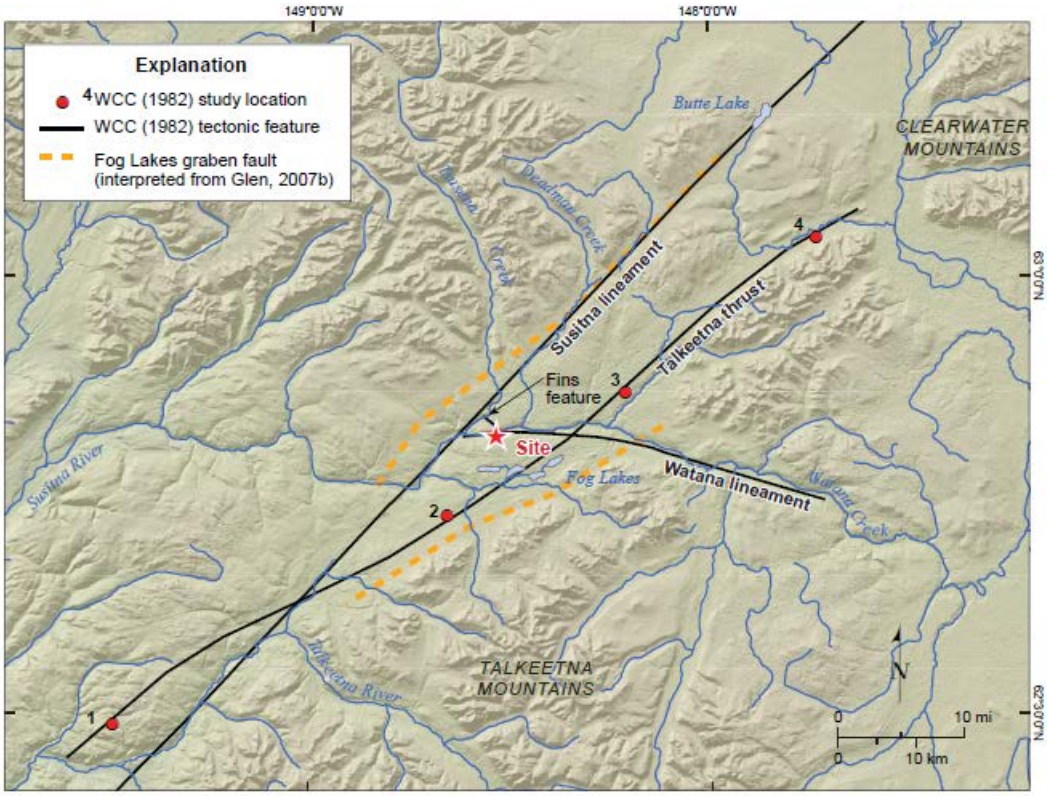


**Figure 6-4. Site Vicinity Tectonic Features**

The Talkeetna fault was recognized as a major tectonic feature near the Watana dam site by Kachadoorian and Moore (1979) and WCC (1982) although no evidence of Quaternary faulting was located during their either investigation. This study reached similar conclusions, based on the initial literature review for seismic source characterization and subsequently based on field investigation, mapping, and lineament mapping using LiDAR-derived DEM's (Fugro, 2015a). The WCC (1982) investigations included paleoseismic trenching at two locations along the suspected map trace of the Talkeetna fault: trench T-1 and trench T-2. Trench T-1 is located directly southwest of the Fog Lakes, and lies about 9 mi (15 km) southwest from the proposed dam site (number 2 on Figure 6-6), although the trench location was not directly atop the map trace. Trench T-2 is located much farther to the southwest, about 40 mi (65 km) from the proposed dam site, and is slightly west of the confluence of the Talkeetna River and Iron Creek (number 1 on Figure 6-4).

Recent geologic mapping by Twelker et al. (2014) as part of the Talkeetna Mountains C-4 quadrangle map updates the T-1 trench site and broader area geology at 1:50,000-scale based on field mapping, analysis of gravity and electromagnetic data, and mineralogic analysis. Key conclusions from their mapping effort are that the Talkeetna fault is not expressed in bedrock geology as a single, continuous fault. Rather, it is now characterized from geophysical-based bedrock interpretation and mapping as a series of complex, high angle, northeast-trending fault

strands, and strands of the Talkeetna fault themselves appear to be cross-cut and truncated by north-northwest trending bedrock faults providing evidence suggesting that the Talkeetna fault is not active in the contemporary stress regime.

### 6.4.2. Susitna Lineament

The Susitna lineament is a pronounced northeast-southwest trending lineament located near the dam site area (Figure 6-6). Gedney and Shapiro (1975) described the feature as a fault based on differential K-Ar cooling data in the Talkeetna Mountains and seismicity. However, subsequent mapping by Csejtey et al. (1978) found no evidence for a major fault in the location of the Susitna lineament. This study concluded similarly (Fugro, 2015a). The lineament is mapped near Butte Lake by Smith et al. (1988) and through the central Talkeetna Mountains near the dam site by Clautice (1990). Fault and lineament mapping by Wilson et al. (2009) shown no northeast trending faults in the vicinity of the Susitna lineament but do show several short lineament segments (5-7.5 mi [8-12 km]) that are adjacent to, and parallel with, the previously mapped lineament trace (Figure 6-4). WCC (1982) interpreted the Susitna lineament to be a bedrock feature not related to faulting, except for possible erosion along a minor shear zone parallel to the fault. This conclusion was based on bedrock and surficial mapping, a magnetometer survey, and paleoseismic trenching along the trace of the lineament.

Glen et al. (2007b) describes the Susitna lineament as a series of 6- to 12-mi (10 to 20 km) long en echelon segments stepping eastward along strike to the north. They report east side down motion on the lineament which exposes Eocene volcanic rocks and Miocene and Oligocene sedimentary rocks in the Fog Lakes and Watana basins. O'Neill et al. ( (2003b) and (2005) ) suggest that the en echelon pattern of the lineament may be the result dextral motion during post-accretion right-lateral bulk shear. Reger et al. (1990) do not depict the Susitna feature as a photo-geologic lineament and the map shows no direct evidence to support faulting or offset of late Pleistocene glacial till deposits or kame-esker deposits (Reger map units Qd3 and Qk, respectively).

### 6.4.3. Shorter Structures Proximal to the Dam Site

In addition to the Talkeetna fault and the Susitna lineament, there are numerous northeast- and northwest-striking bedrock faults and lineaments in the Talkeetna block. Several of these structures, proximal to the Watana dam site area (i.e. the northwest-striking shear zones), were studied in detail by WCC (1982) and this study. The results and are applied in Section 5 of this report, and fully discussed in Fugro (2015a).

The northeast-southwest structural fabric likely originated during Cretaceous accretionary deformation (Csejtey et al., (1978) and (1982); Ridgeway et al., (2002) ). Post-accretionary deformation driven by Tertiary right lateral bulk shear in the Talkeetna block has been

proposed by several studies (O'Neil et al. (2005), Glen et al., (2007a) and (2007b) ). These studies suggest that Tertiary trans-tensional deformation reactivated northeast- southwest oriented structures and produced several grabens and half grabens including the Watana Creek lowland, and Fog Lakes lowland. Based on regional geophysical data, Glen et al. (2007a) propose that the Fog Lakes lowland is structurally bounded on the west by the Susitna lineament, and to the east by a series of range front normal faults (e.g. Talkeetna fault) defining a Fog Lakes graben (Figure 6-4). Whether or not this is true, the seismic source model includes the hypothesized Fog Lakes graben as a model element because of its geographic position with respect to the dam site.

## 6.5. Crustal Seismicity

### 6.5.1. Earthquake Catalog

#### *6.5.1.1. Earthquake Data Source and Magnitudes*

A catalog of earthquakes for the study area was compiled starting with the Alaska Earthquake Center (AEC) earthquake catalog. The catalog contains earthquakes of M 3 and above, down to a depth of 62 miles (100 km), and from 1899 through December 31, 2010. The base AEC catalog was supplemented with the undeclustered (includes aftershock earthquakes) USGS catalog from the 2007 Alaska hazard maps (Wesson, Boyd, Mueller, Bufe, Frankel, & Petersen, 2007). In addition, the earthquake locations, depths, and/or magnitudes were updated using the results of relocation studies by Doser (2004), Doser et al. (2002), Doser et al. (1999), and Ratchkovski et al. (2003). The AEC catalog mb, ML, and MS magnitudes were converted to moment magnitude (Mw) following the relations of Ruppert and Hansen (2010), which apply to earthquakes from 1971 to the present. Earthquakes prior to 1971 were assigned Mw magnitudes according to: (1) the relocation studies noted above, (2) the 2007 USGS Alaska catalog, or (3) following the relation which agrees with the magnitudes used by the USGS. The updated catalog (Figure 6-5) was declustered (remove aftershocks) using the Gardner-Knopoff algorithm (Gardner & Knopoff, 1974). An aftershock exclusion zone was used to identify likely aftershocks of the 2002 Denali earthquake (Figure 6-6). Earthquakes within the exclusion zone, post- dating the 2002 event were removed from the catalog. The 2002 Denali earthquake itself is also removed from the catalog as it is directly associated with the Denali fault, and, therefore, is inappropriate to remain in the catalog database used to derive aerial source zone earthquake recurrence. This event is accounted for in hazard calculations through the characterization of the Denali fault discussed in Section 6.2.1.

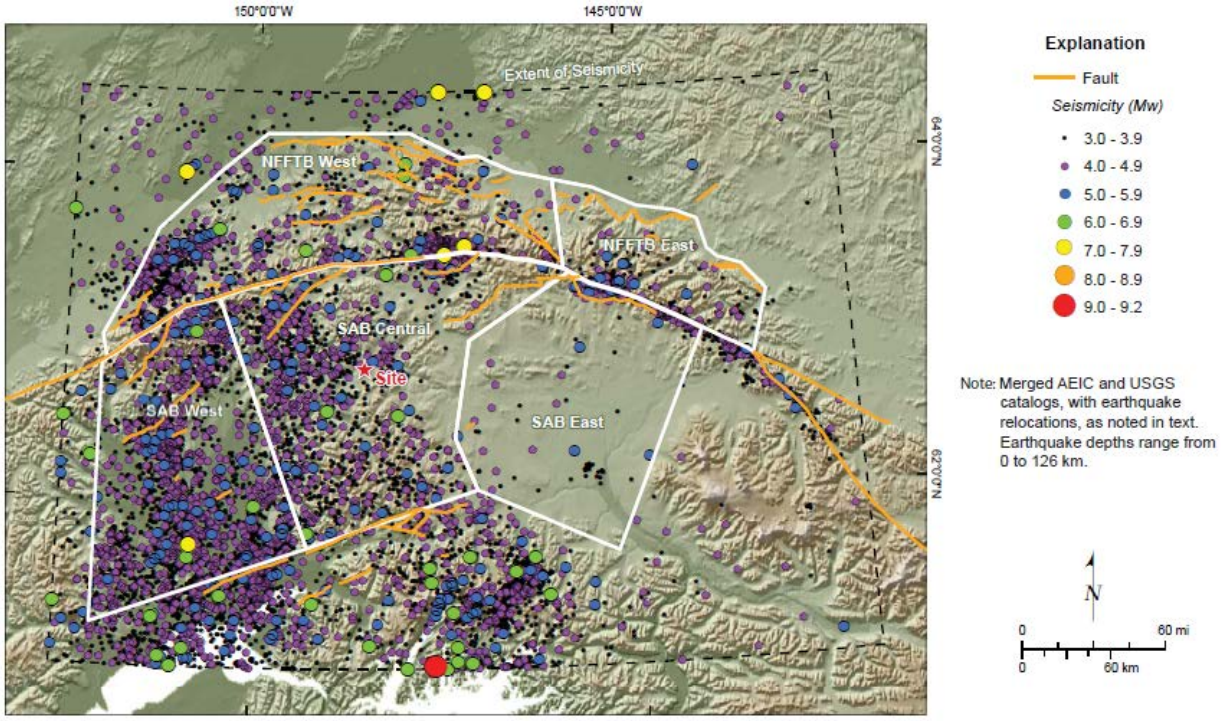


**Figure 6-5. Unfiltered Earthquake Catalog**

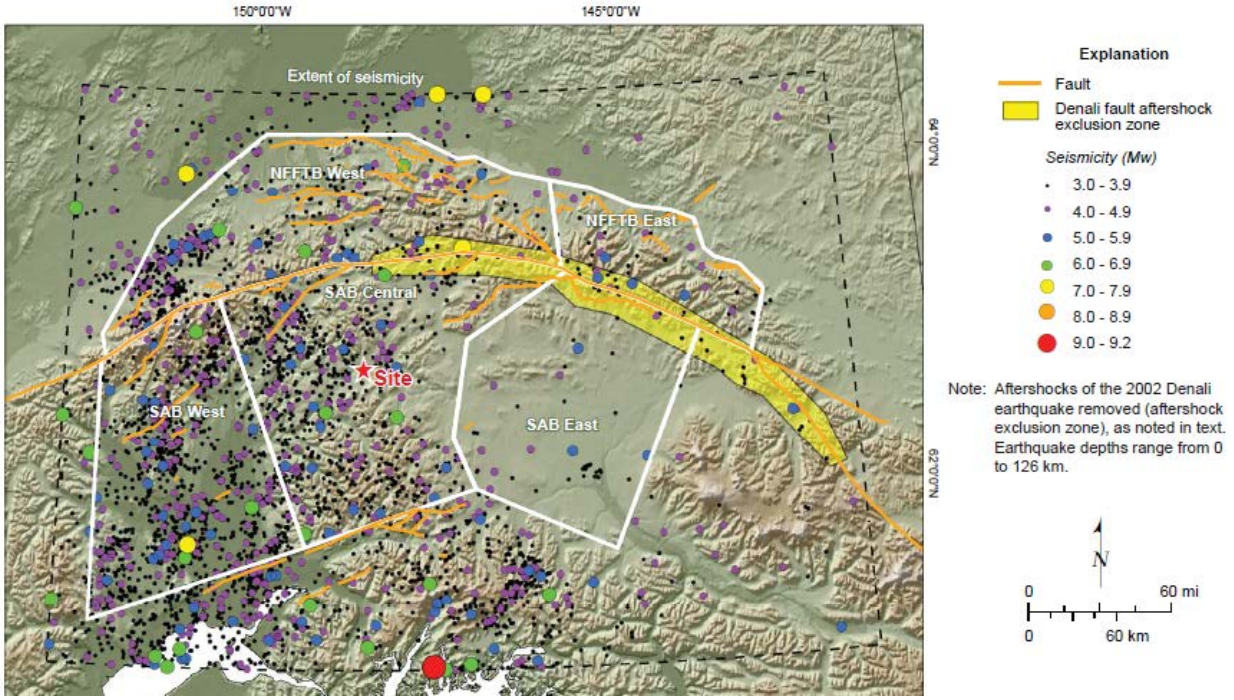


**Figure 6-6. Declustered Earthquake Catalog**

### 6.5.1.2. Earthquake Magnitude Completeness

In order to analyze catalog completeness as a function of magnitude, a "Stepp" plot was constructed which shows the event rate per year as a function of time since the present. This is shown in Figure 6-7 using 5-year bins, and indicates completeness for M 3 since 1970, M 4 and 5 since 1965, and M 6 since 1930. M 7 events are few, thus, completeness for these should rely on population density and reporting. Wesson et al. (2007) estimated completeness for M 4.5 since 1964, M 6 since 1932, and M 6.9 since 1898 for their Alaska catalog. Because the results shown in Figure 6-7 are consistent with Wesson et al. (2007) completeness estimates, the Wesson et al. (2007) completeness estimates are adopted for this study. The M 3 completeness since 1970 is consistent with seismic network information in Ruppert and Hansen (2010). The large bump in rates around 1977 is due to the ML to M conversion formula in Ruppert and Hanson (2010). This formula added 1.13 units to ML values between 1977 and 1989. While this conversion appears to be poorly constrained, it doesn't affect the selection of completeness periods.

The magnitude completeness was for the preliminary PSHA completed in 2012. The completeness analyses have been updated based on the project seismicity network data (Fugro, 2015b).

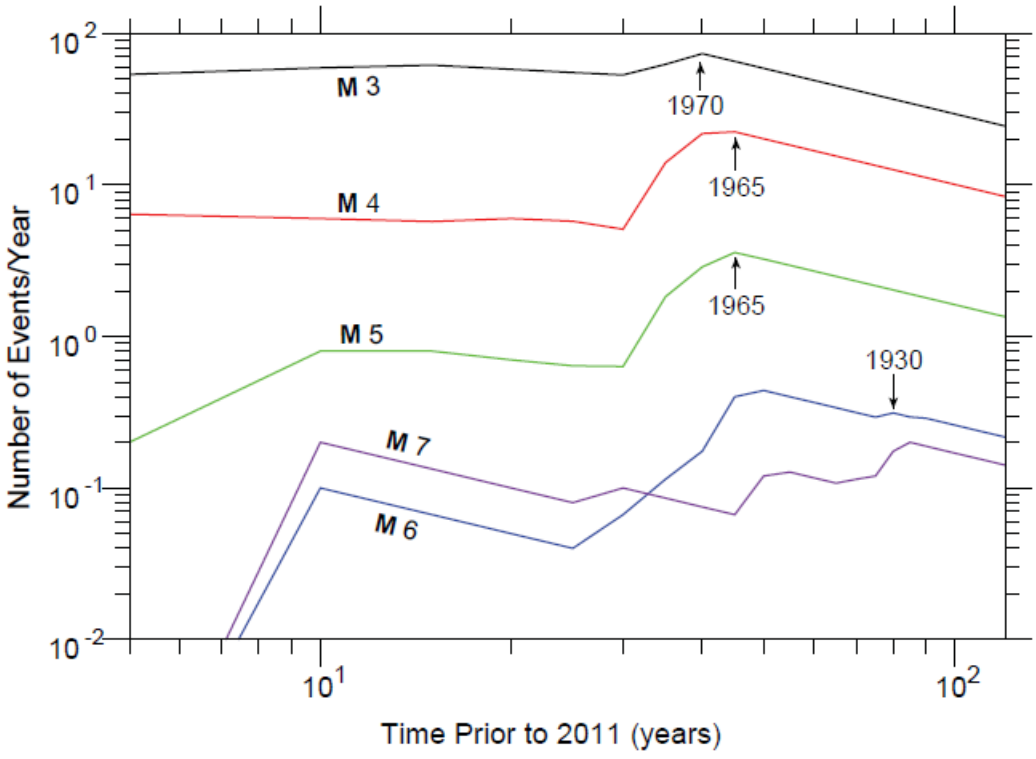


**Figure 6-7. Magnitude vs. Time Prior to 2011**

### 6.5.2. Crustal Source Zones

Crustal thickness in the southern Alaska block (SAB) source zones is estimated to be 16 mi (25 km) in the West and Central zones, and 31 mi (50 km) in the East zone (see Section 3.5 and 3.6; Fugro, 2012). However, the West and Central zones experience earthquakes associated with the subducting slab below 14 mi (23 km) depth (see Fugro, 2012, Figure 27). The maximum depth for earthquakes in the recurrence catalog in the West and Central zones is reduced to 14 mi (23 km) to exclude these apparent slab events, but the source model for these zones allows earthquakes down to 16 mi (25 km), reflecting the uncertainty in crustal thickness. In comparison, WCC (1982) apparently used a seismogenic crustal thickness in their Talkeetna terrane of 12 mi (20 km). The Eastern zone is located off the northwest edge of the subducting slab so events as deep as 31 mi (50 km) are included in the recurrence catalog, and the source model allows for earthquakes down to 31 mi (50 km) as well.

The majority of seismicity in NFFTB zones is located above 12 mi (20 km) depth, and most events below 12 mi (20 km) have high vertical location errors (> 3 mi [5 km]) (see Fugro, 2012, Figure 28), thus seismicity in the recurrence calculations is constrained to a maximum depth of 12 mi (20 km).

## 6.6. Earthquake Recurrence from Seismicity

Earthquake catalogs used for SAB and NFFTB areal source zone recurrence calculations are shown in Figure 6-8. Fewer earthquakes are shown in Figure 6-8 than in Figure 6-6 because of removal of some events after filtering for the completeness periods discussed in Section 6.5.1. The location of the 1912 Denali earthquake, as relocated by Doser (2004), is directly north of the Denali fault. Considering the large location error, the 1912 event conservatively is included in the SAB Central zone recurrence catalog instead of the NFFTB West zone. The truncated exponential recurrence model was used for these areal zone sources, with recurrence parameters computed by the maximum likelihood method. Figure 6-9 presents the maximum likelihood recurrence curves for the SAB Central aerial source zone (background source for dam site). Magnitudes for the PSHA calculations range from 5.0 to 7.0.

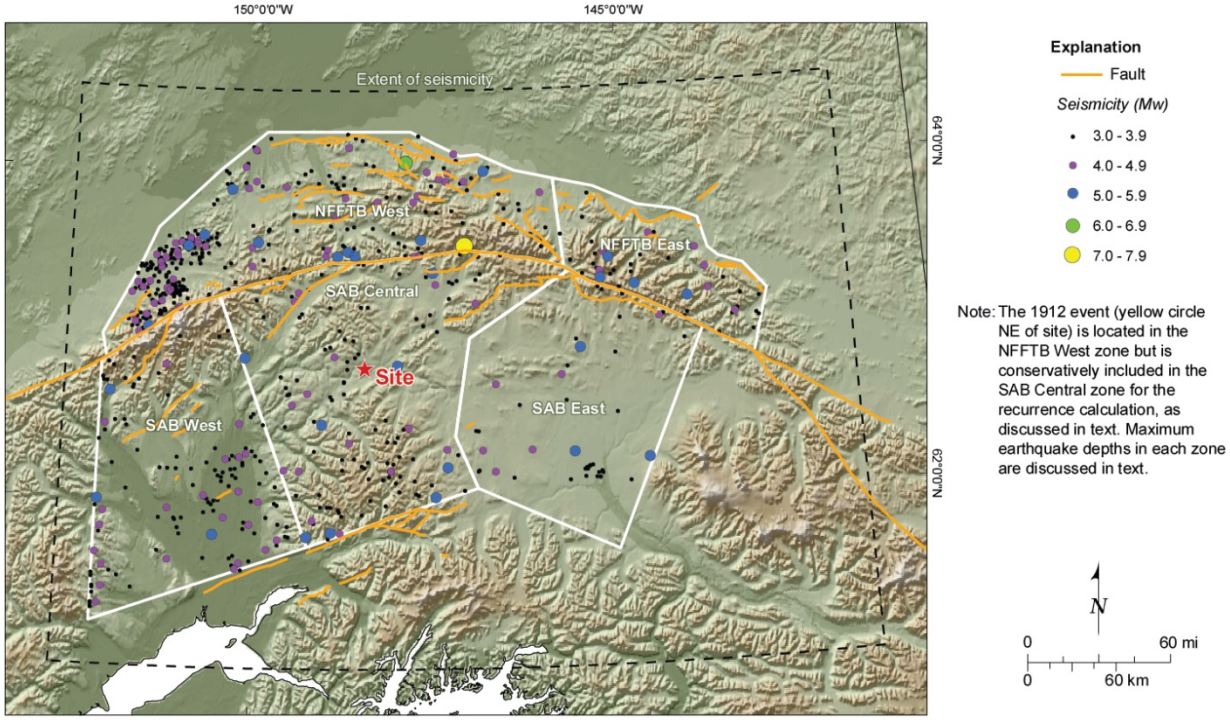


**Figure 6-8. Final Recurrence Catalog**

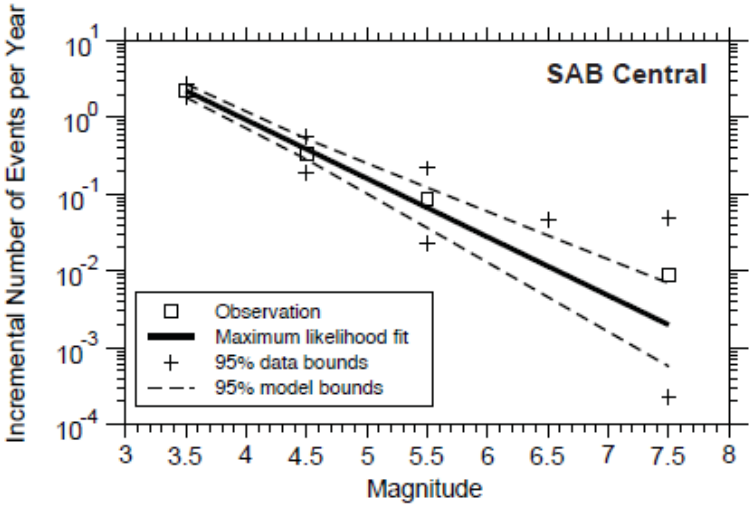


**Figure 6-9. Maximum Likelihood Recurrence Curves for SAB Central Areal Zone**

# 7. GROUND MOTION PREDICTION EQUATIONS

Ground motion prediction equations (GMPEs) transform magnitude, distance, and other ground motion-related parameters into ground motion amplitude distributions for a wide range of vibrational frequencies. Such equations are continually being developed and refined as more strong motion accelerograms become available. For this project, three types of GMPEs were drawn upon: those for crustal sources, those for plate interface sources, and those for intraslab sources. The GMPEs and their weights for the three source categories were selected and are shown in Table 7-1. It is recognized that the GMPEs used to calculate the hazard in Fugro (2012) have since been updated and the revised seismic hazard analysis will use the current GMPEs along with an updated source models.

**Table 7-1. Ground Motion Prediction Equations Used in PSHA**

| Sources | GMPE | Abbreviation | Weight |
|---|---|---|---|
| Megathrust | BC Hydro, 2011[1] | BCH11 | 0.50 |
| | (Zhao, et al., 2006) | ZH06 | 0.25 |
| | (Atkinson & Macias, 2009) | AM09 | 0.25 |
| Intraslab | BC Hydro, 2011[1] | BCH11 | 0.50 |
| | (Zhao, et al., 2006) | ZH06 | 0.25 |
| | (Atkinson & Boore, 2003) | AB03 | 0.25 |
| Crustal | (Abrahamson & Silva, 2008) | AS08 | 0.25 |
| | (Chiou & Youngs, 2008) | CY08 | 0.25 |
| | (Campbell & Bozorgnia, 2008) | CB08 | 0.25 |
| | (Boore & Atkinson, 2008) | BA08 | 0.25 |

Note: (1) as provided by N. Abrahamson, August 2011.

## 7.1. Subduction Zone

For the megathrust and intraslab GMPEs BCH11 is preferred model because it is based on a much larger data set that includes all of the data used by Zhao et al. (2006), and uses the Atkinson and Macias (2009) simulation result to constrain the break in the magnitude scaling at high magnitudes. The Atkinson and Boore (2003) relation uses the "global" version, as opposed to the Cascadia version. The crustal source GMPEs consist of four NGA GMPEs, each weighted equally.

## 7.2. Crustal

The crustal source GMPEs consist of four NGA West1 GMPEs, each weighted equally. The Idriss 2008 NGA West1 relationship was not used in this assessment because the distance range was outside the applicable range for this equation. Any updates to the PSHA should use NGA West2 GMPEs.

### 7.2.1. Shear Wave Velocity

All of the GMPEs in Table 7-1 employ $V_S30$ (average shear-wave velocity in the top 100 ft. (30 m) as a site condition parameter for linear and non-linear site response, either explicitly or as a site category indicator. Based on the initial data review, the hazard was computed using a reference $V_S30$ of 2,625 ft/s (800 m/s), as this is the range that was constrained by the empirical data acquired prior to the seismic hazard computations. Interferometric Multichannel Analysis of Surface Waves (IMASW) was performed at a later date to estimate shear wave velocities (Vs) at seven existing and proposed seismic recording stations operated for the Susitna-Watana Hydroelectric Project (Fugro, 2014a). Existing seismicity station, WAT-1, is located at the dam site. This station had a $V_S30$ value on rock which was calculated to be 3,556 ft/s (1,084 m/s). The adopted value of 2,625 ft/s (800 m/s) which was used in the hazard calculations is considered to be a conservative velocity value that should be updated when the hazard study is revised.

# 8. PROBABILISTIC SEISMIC HAZARD ANALYSIS

## 8.1. Methodology

The basic PSHA methodology employed here follows the precepts of Cornell (1968). The programs used were Fugro Consultants, Inc. codes faultsource_31 version 3.1.228 for fault sources, mrs5.2 version 5.2.228 for areal sources, and agrid1.1 version 1.1.228 for gridded seismicity sources. Earlier versions of these codes were vetted under the PEER PSHA Code Verification Workshop (Wong, Thomas, & Abrahamson, 2004).

## 8.2. Inputs

### 8.2.1. Subduction Zone

#### *8.2.1.1. Intraslab Model*

For the intraslab source the Wesson et al. (2007) model was used, which consists of gridded seismicity for two depth levels, 31 to 50 mi (50-80 km), and 50 to 75 mi (80- 120 km), and a magnitude range of M 5 to M 7.5. Following Wesson et al. (2007), the depth for the 31 to 50 mi (50-80 km) sources was set to 37 mi (60 km), and 56 mi (90 km) for the 50 to 75 mi (80-120 km) points. A correlation distance of 31 mi (50 km) was used by Wesson et al. (2007) to smooth the seismicity. Correlation distance is defined as the standard deviation of the Gaussian smoothing function (Frankel A. D., 1995). The subduction intraslab, as modeled by Wesson et al. (2007), used a truncated exponential recurrence model.

A sensitivity study was performed for the intraslab seismic source (Fugro, 2014b) by comparing different Mmax selections, $V_S30$ values, and slab geometries, however the PSHA with the recommended changes to that source (Fugro 2012) has not been revised. Discussion on the refined intraslab model is included in Fugro (2014b).

#### *8.2.1.2. Interface Model*

For the purposes of this study, the megathrust, or plate interface, geometry was modeled as a single plane (seen as the rectangle in Figure 6-2) dipping 2.6 degrees to the northwest with upper (southeast) and lower (northwest) depth bounds of 12 and 22 mi (20 and 35 km). This geometry also roughly corresponds to the estimated rupture extent of the 1964 event (Figure 2-13). The geometric parameters of this plane, including distances to the site, are listed in Table 8-2.

Following Wesson et al. (2007), the largest megathrust event is modeled as a repeat of the M 9.2 1964 event. A time-independent (Poissonian) annual rate of 1/560 is assigned, based on paleoseismic investigations (Carver & Plafker, 2008). The Poissonian rate of this magnitude

event has been ultimately decreased due to inclusion of time- dependent models (Fugro, 2012, Appendix A).

Also following Wesson et al. (2007), the M 7-8 interface earthquakes are modeled as being exponentially distributed according to rates calculated from the Wesson et al. (2007) earthquake catalog. This catalog resulted from a hierarchical compilation of several catalogs, resolution of magnitudes to the Mw scale, and declustering to remove dependent events. The a and b Gutenberg-Richter recurrence values for this source were taken from Wesson et al. (2007). Earthquakes in this magnitude range were modeled as occurring on the fault plane shown in Figure 6-2. The interface earthquakes in the M 5-7 range are modeled as "gridded, smoothed seismicity." As described in Wesson et al. (2007), this model is created by sorting this seismicity into 0.1 degree bins, and performing Gaussian smoothing with a correlation distance (Frankel, et al., 1996) of 46 mi (75 km) (Fugro, 2012, Figures 16 and 17). The grid sources were placed at a depth of 3 mi (5 km), as in Wesson et al. (2007). Although this depth is not realistic, given that the megathrust lies 12 to 19 miles (20 to 30 km) beneath the site, this depth was retained to maintain consistency with the Wesson et al. (2007) model. In addition to the truncated exponential model, the interface magnitude probability density function included the maximum moment magnitude with a Mmax 9.2 and no uncertainty. It is recommended that the interface be updated to a more realistic model in subsequent studies.

### 8.2.2. Crustal Sources

A number of crustal faults were not included the PSHA source model (Table 8-1). Five crustal faults are included in the PSHA with the source characterization parameters contained in Table 8-2 and Table 8-3. Two of these faults, the Denali and Castle Mountain, have been included in the previous USGS source model (Wesson, Boyd, Mueller, Bufe, Frankel, & Petersen, 2007). The source characterizations for these faults have been updated, and include time-dependent alternatives for the Denali fault, as well. The Pass Creek-Dutch Creek fault was not included in the USGS source model, but previously was identified as a Quaternary fault in Plafker et al. (1994). A conservative slip rate distribution is included for this fault. The Sonona Creek and Fog Lakes graben are potential sources within the Southern Alaska block newly considered in this evaluation because of their potential proximity to the Watana Dam site. Evidence to support full seismic source characterization for both sources was incomplete at the time of the initial PSHA (Fugro, 2012). However, a Crustal Source Characterization has since been completed (Fugro, 2015a). Although, updates included in this summary report are not included in the seismic hazard calculation, there are no published estimates for Quaternary displacement on either of these faults. The structures were included in this preliminary evaluation with a full probability of activity, to test the sensitivity of their inclusion to the hazard estimates for the site. Thus, slip rate distributions for these sources span about two orders of magnitude, and range from 0.004 to 0.01 in/yr (0.01 to 0.3 mm/yr) to test a range of

values that would reflect relative inactivity to an activity rate which is similar to the lower range of slip rates on the Castle Mountain fault.

**Table 8-1. Site Region Faults Excluded from the PSHA Source Model**

| Fault Name | Distance from Site (km) | Distance from Site (miles) |
|---|---|---|
| Faults in the Southern Alaska Block – South of Denali fault | | |
| Broad Pass fault | 63.8 | 39.6 |
| Broxson Gulch fault | 62.6 | 38.9 |
| Bull River fault | 78.2 | 48.6 |
| Cathedral Rapids fault | 244.1 | 151.7 |
| East Boulder Creek fault | 101.6 | 63.1 |
| Foraker fault | 135.5 | 84.2 |
| Matanuska Glacier fault | 136.4 | 84.8 |
| McCallum-Slate Creek fault | 153.9 | 95.6 |
| McGinnis Glacier fault | 147.0 | 91.3 |
| Susitna Glacier fault | 77.8 | 44.1 |
| Faults in the Northern fold and thrust belt – North of Denali fault | | |
| Billy Creek fault | > 70 | > 45 |
| Canteen fault | > 70 | > 45 |
| Ditch Creek fault | > 70 | > 45 |
| Donnely Dome fault | > 70 | > 45 |
| Dot "T" Johnson fault | > 70 | > 45 |
| East Fork fault | > 70 | > 45 |
| Eva Creek fault | > 70 | > 45 |
| Glacier Creek fault | > 70 | > 45 |
| Gold King fault - Section A | > 70 | > 45 |
| Gold King fault - Section B | > 70 | > 45 |
| Granite Mountain fault A | > 70 | > 45 |
| Granite Mountain fault B | > 70 | > 45 |
| Healy Creek fault | > 70 | > 45 |
| Fault Name | Distance from Site (km) | Distance from Site (miles) |
| Kansas Creek fault | > 70 | > 45 |
| Macomb Plateau fault | > 70 | > 45 |
| Molybdenum Ridge fault | > 70 | > 45 |
| Mystic Mountain fault | > 70 | > 45 |
| Northern Foothills thrust | > 70 | > 45 |
| Panoramic fault | > 70 | > 45 |
| Park Road fault | > 70 | > 45 |
| Peters Dome fault | > 70 | > 45 |
| Potts fault | > 70 | > 45 |
| Red Mountain fault | > 70 | > 45 |
| Rex fault | > 70 | > 45 |
| Stampede fault | > 70 | > 45 |
| Trident fault | > 70 | > 45 |
| Trident Glacier fault | > 70 | > 45 |

### 8.2.2.1. Denali Fault

The occurrence of an M 7.9 earthquake on the Denali fault in 2002 (Section 6.2.1) led to a number of scientific investigations that greatly improved the characterization of this fault for seismic hazard studies.

As shown in Figure 8-1, two geometric models are considered for this study: one in which a repeat of the 2002 rupture occurs and the segment to the west ruptures independently; and another model in which the entire fault length ruptures. Each of these scenarios has a maximum magnitude of 7.9, and a maximum moment model is used for each (Table 8-3). The two scenarios are weighted equally.

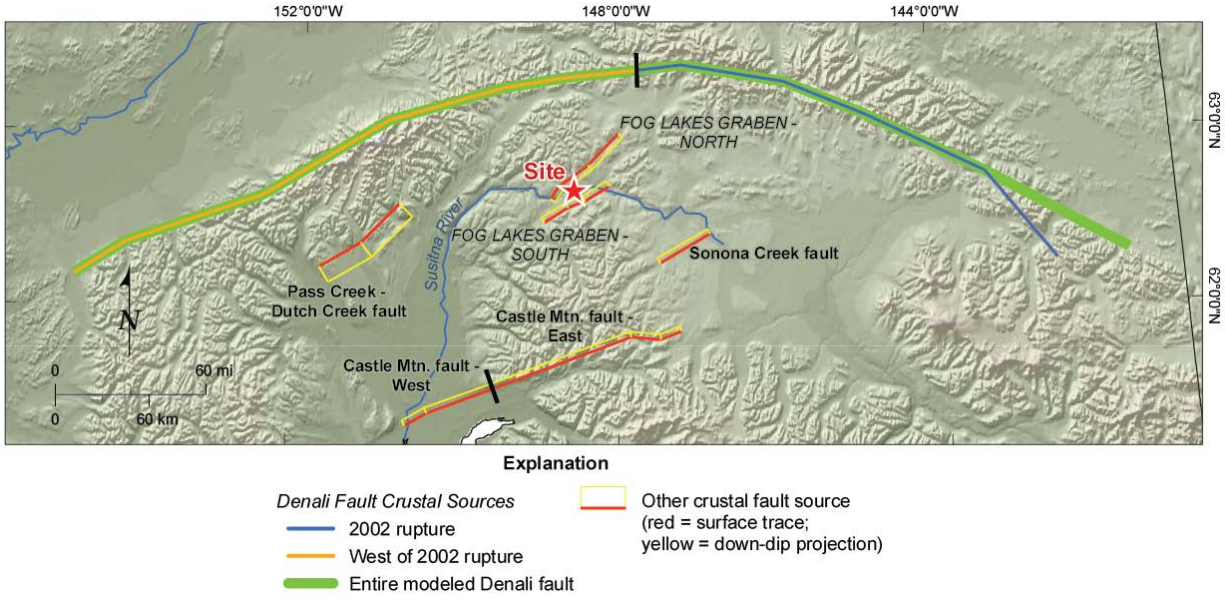


**Figure 8-1. Crustal Fault Model**

Following Wesson et al. (2007), the modeled slip on the Denali fault decreases monotonically from 14.4 mm/yr at the east end to zero at the west end. The estimated slip rate as a function of distance along the fault is shown in Figure 18 (Fugro, 2012). This was accounted for in the PSHA as follows: In modeling ruptures on a fault, a rupture that has less area than the fault itself is assumed to occur at any location with equal probability. Such ruptures are modeled by placing them sequentially along strike and up and down dip with some spacing interval (0.6 mile [1 km] in this study). A rupture will consequently correspond to a portion of the fault along the x-axis in Figure 18 (Fugro, 2012). The slip rate assigned to that rupture will, therefore, be the average slip rate along that portion of the fault. Alternative models of the Denali fault in which the fault extends farther west are not considered, because these models would primarily extend the fault beyond 200 mi (320 km) from the site and the initial

sensitivity evaluations (Fugro, 2012), indicate no significant change in the ground motion results from this type of change to the source model.

Time-dependent occurrence rate models also were employed for the Denali fault. The rationale is that since the 2002 rupture occurred so recently, another such event should be less likely than the average rate in the near future. By similar reasoning, an earthquake on the segment west of the 2002 rupture, which has not occurred for about 600 years, is more likely to occur in the near future than the average. Details and results of the time-dependent analysis are contained in Appendix A (Fugro, 2012).

#### *8.2.2.2. Castle Mountain Fault*

The Castle Mountain fault, described in Section 6.2.2, is modeled as two scenarios: a segmented model where the east and west segments rupture independently, and an unsegmented model where the entire fault length ruptures in one earthquake. The fault geometry and location are shown in Figure 8-1. These scenarios are weighted equally.

To account for the uncertainty of the western segment slip rate (i.e. Haeussler et al., (2002); Koehler and Reger, (2011); Willis et al., (2007)) two slip-rate scenarios are used (Table 8-3 also equally weighted. The higher slip-rate scenario reflects the rates used in prior USGS hazard models (Wesson, Boyd, Mueller, Bufe, Frankel, & Petersen, 2007), while the lower slip-rate scenario reflects more recent investigations (e.g., Koehler and Reger, (2011)).

#### *8.2.2.3. Pass Creek-Dutch Creek Fault, Sonona Fault, and Fog Lake Graben Faults*

The Pass Creek-Dutch Creek, Sonona and Fog Lake graben faults are described in Sections 6.2.3, and 6.2.4, respectively, and shown in map view in Figure 8-1. Their geometric properties are listed in Table 8-2, and maximum magnitudes and slip-rate distributions in Table 8-3. No alternative models were employed for these sources.

#### *8.2.2.4. Crustal Areal Zones*

Five areal source zones were included in the model. Details of the geometric properties and recurrence calculations for them are presented in Section 6.5.2 and Fugro (2012).

**Table 8-2. Geometric Fault Parameters for Susitna Source Model, as Modeled for PSHA**

| Fault | Length (km) | Area[1] ($km^2$) | Depth Range (km) | Dip | Rupture Distance[2] (km) | JB Distance[3] (km) | Farthest Distance (km) |
|---|---|---|---|---|---|---|---|
| ASZ - megathrust interface model | 319.9 | 102,500 | 20.0 to 35.0 | 2.6 | 78.4 | 70.2 | 529.4 |
| Denali - 2002 rupture | 307.5 | 4612 | 0.0 to 15.0 | 90.0 | 86.0 | 86.0 | 312.3 |
| Denali - West segment | 386.4 | 5795 | 0.0 to 15.0 | 90.0 | 71.2 | 71.2 | 324.0 |
| Denali - entire fault | 726.0 | 10,889 | 0.0 to 15.0 | 90.0 | 71.2 | 71.2 | 356.5 |
| Castle Mtn fault | 189.6 | 3856 | 0.0 to 20.0 | 80.0 | 99.8 | 97.8 | 186.1 |
| Castle Mtn West fault high | 61.4 | 1253 | 0.0 to 20.0 | 80.0 | 136.9 | 135.4 | 186.1 |
| Castle Mtn West fault low | 61.4 | 1253 | 0.0 to 20.0 | 80.0 | 136.9 | 135.4 | 186.1 |
| Castle Mtn East fault | 128.2 | 2602 | 0.0 to 20.0 | 80.0 | 99.8 | 97.8 | 138.0 |
| Pass Creek-Dutch Creek fault | 65.6 | 1552 | 0.0 to 20.0 | 60.0 | 106.8 | 104.9 | 170.4 |
| Sonona fault | 36.9 | 749 | 0.0 to 20.0 | 80.0 | 71.5 | 69.2 | 91.6 |
| Fog Lake graben north | 60.9 | 1230 | 0.0 to 20.0 | 80.0 | 6.9 | 3.5 | 49.4 |
| Fog Lake graben south | 47.7 | 969 | 0.0 to 20.0 | 80.0 | 9.5 | 6.1 | 34.3 |

Notes:
(1) Magnitude-area formula for strike-slip faults from UCERF2 (Field et al., 2009), all others from Wells & Coppersmith (1994
(2) Rupture distance is the closest distance to the fault plane. (3) JB (Joyner-Boore) distance is the closest horizontal distance to surface projection of the fault plane.

**Table 8-3. Fault Slip Rate and Magnitude Parameters, as Modeled for PSHA**

| Fault | Slip Rate (mm/yr) | Mean (mm/yr) | Slip Rate Distribution Type | Maximum Magnitude | Magnitude Models |
|---|---|---|---|---|---|
| Denali System | | | | | |
| Unsegmented | 0.0 – 14.4 | N/A | tapered | 7.9 | |
| West of 2002 | 9.8 – 0.0 | N/A | tapered | 7.9 | Maximum Moment (Normal Distribution, sigma=0.2) |
| 2002 rupture segment[1] | 14.4 – 9.8 | N/A | tapered | 7.9 | |
| Eastern segment | Not modeled separately due to distance from site | | | | |
| Southern Alaska Crustal faults | | | | | |
| Sonona Creek | 0.1 – 0.5 | 0.3 | triangle,sym | 7.0 | Maximum Moment (Normal Distribution, sigma=0.2) |
| Pass Creek – Dutch Creek | 0.5 – 1.5 | 1.0 | triangle,sym | 7.0 | |
| Fog Lake graben north | 0.01 – 0.3 (0.1)[2] | 0.14 | triangle,asym[2] | 7.0 | |
| Fog Lake graben south | 0.01 – 0.3 (0.1)[2] | 0.14 | triangle,asym[2] | 7.0 | |
| Castle Mountain fault scenarios | | | | | |
| Segmented Model (weight 0.5) | | | | | |
| Castle Mtn east | 0.5 | 0.5 | none | 7.2 | Maximum Moment (Normal Distribution, sigma=0.2) |
| Castle Mtn west (weight 0.5) | 0.4 – 0.6 | 0.5 | uniform | 7.2 | |
| Castle Mtn west (weight 0.5) | 2.1 – 3.6 | 2.9 | uniform | 7.2 | |
| Unsegmented Model (weight 0.5) | | | | | |
| Castle Mtn combined | 0.4 – 0.6 | 0.5 | triangle,sym | 7.6 | Maximum Moment (Normal Distribution, sigma=0.2) |

Notes:
(1) 2002 rupture segment includes the 72 km of the Totschunda fault ruptured in 2002
(2) Apex value for asymmetric triangular distribution in parentheses.

## 8.3. Results

### 8.3.1. Hazard Curves

A hazard curve consists of a ground motion level (in g) on the x-axis, and the mean annual frequency of exceeding that ground motion on the y-axis. Mean hazard curves were developed for four spectral response periods, peak horizontal acceleration (PHA), and 0.5, 1.0, and 3.0

seconds acceleration response at 5% damping. The PHA plot is shown in Figure 8-2, Figure 8-3, Figure 8-4, and Figure 8-5. The major sources have been grouped together for purposes of presentation.

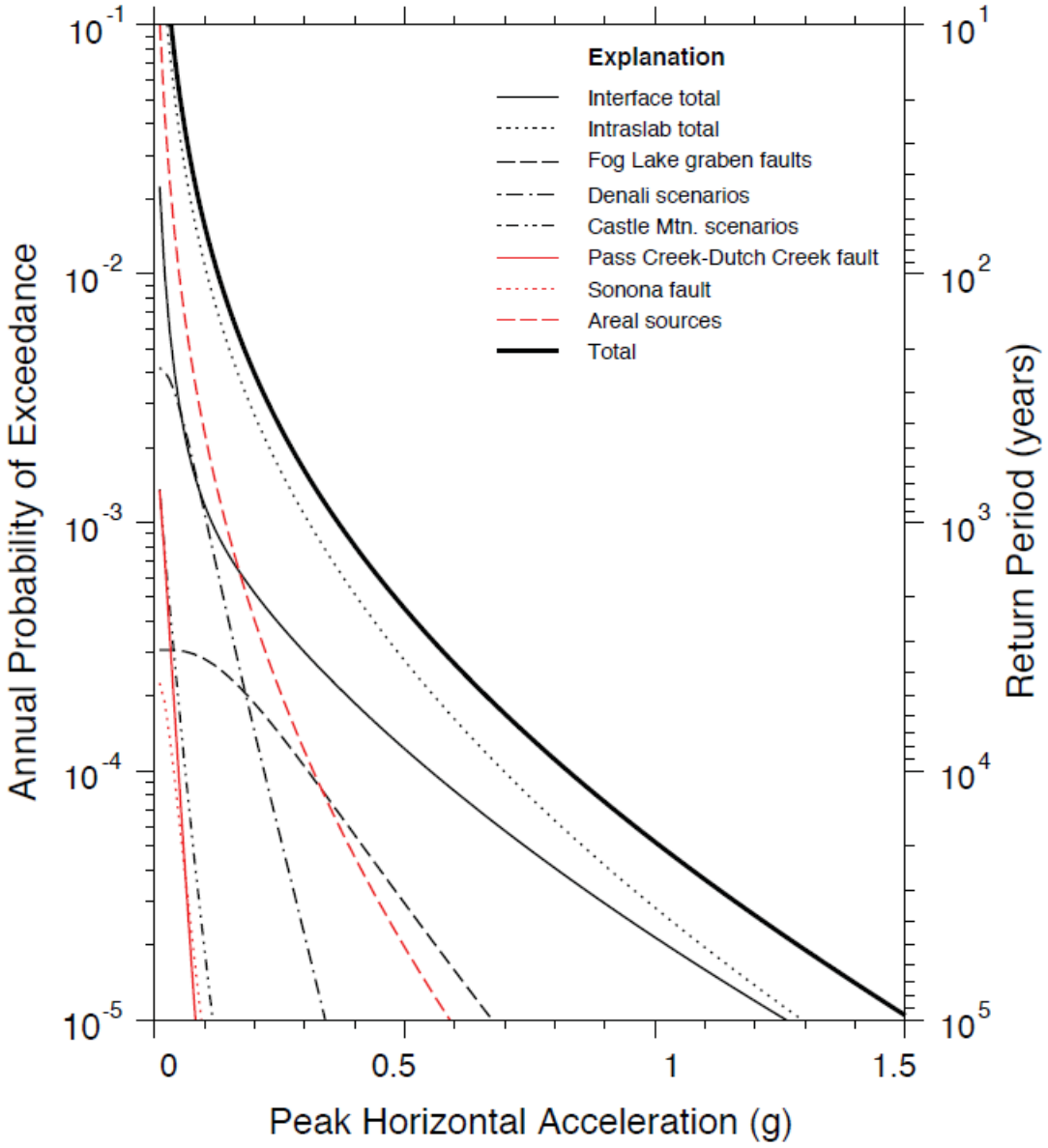


**Figure 8-2. Hazard Curves for Peak Horizontal Acceleration**

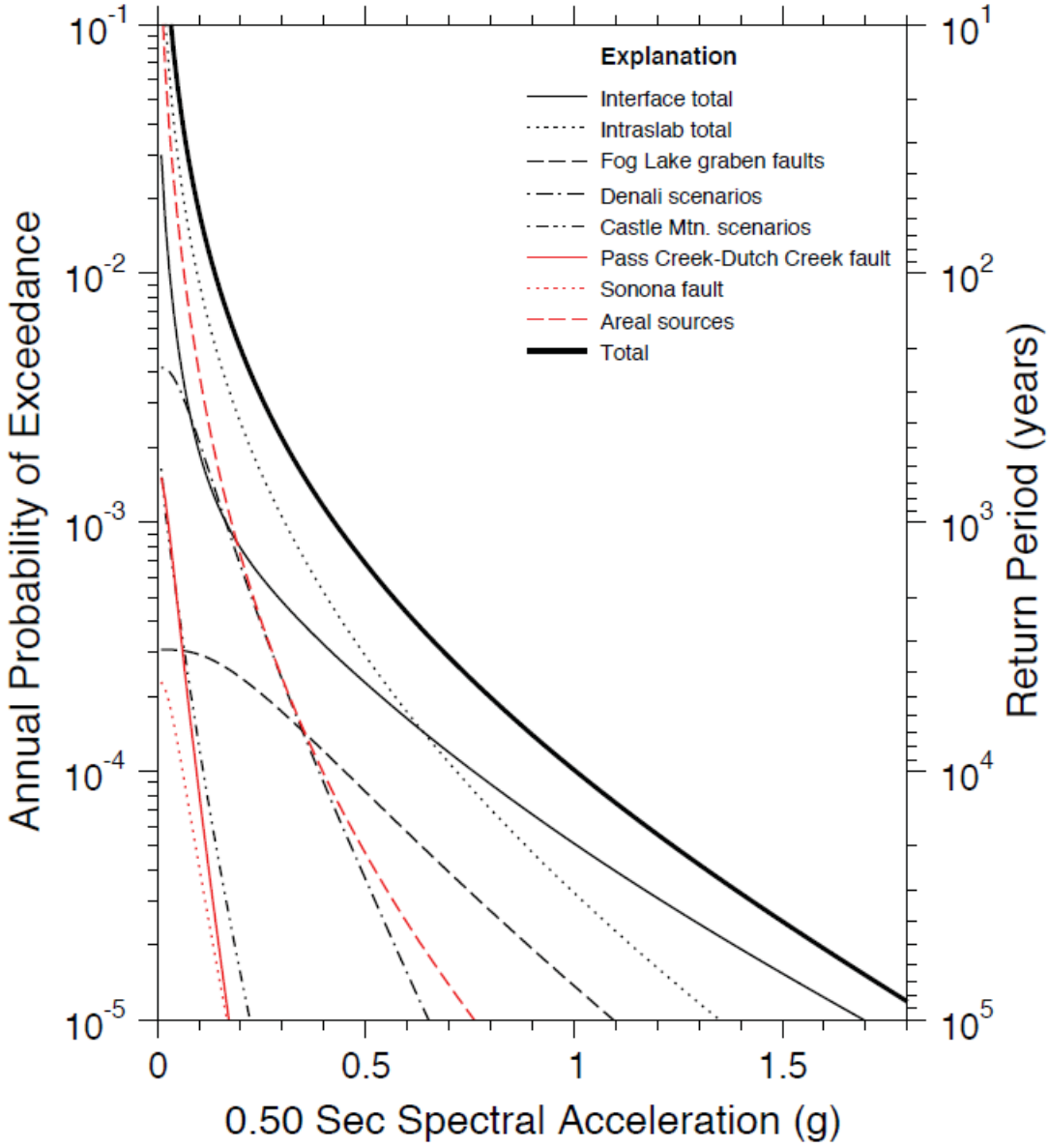


**Figure 8-3. Hazard Curves for 0.5 sec Spectral Acceleration**

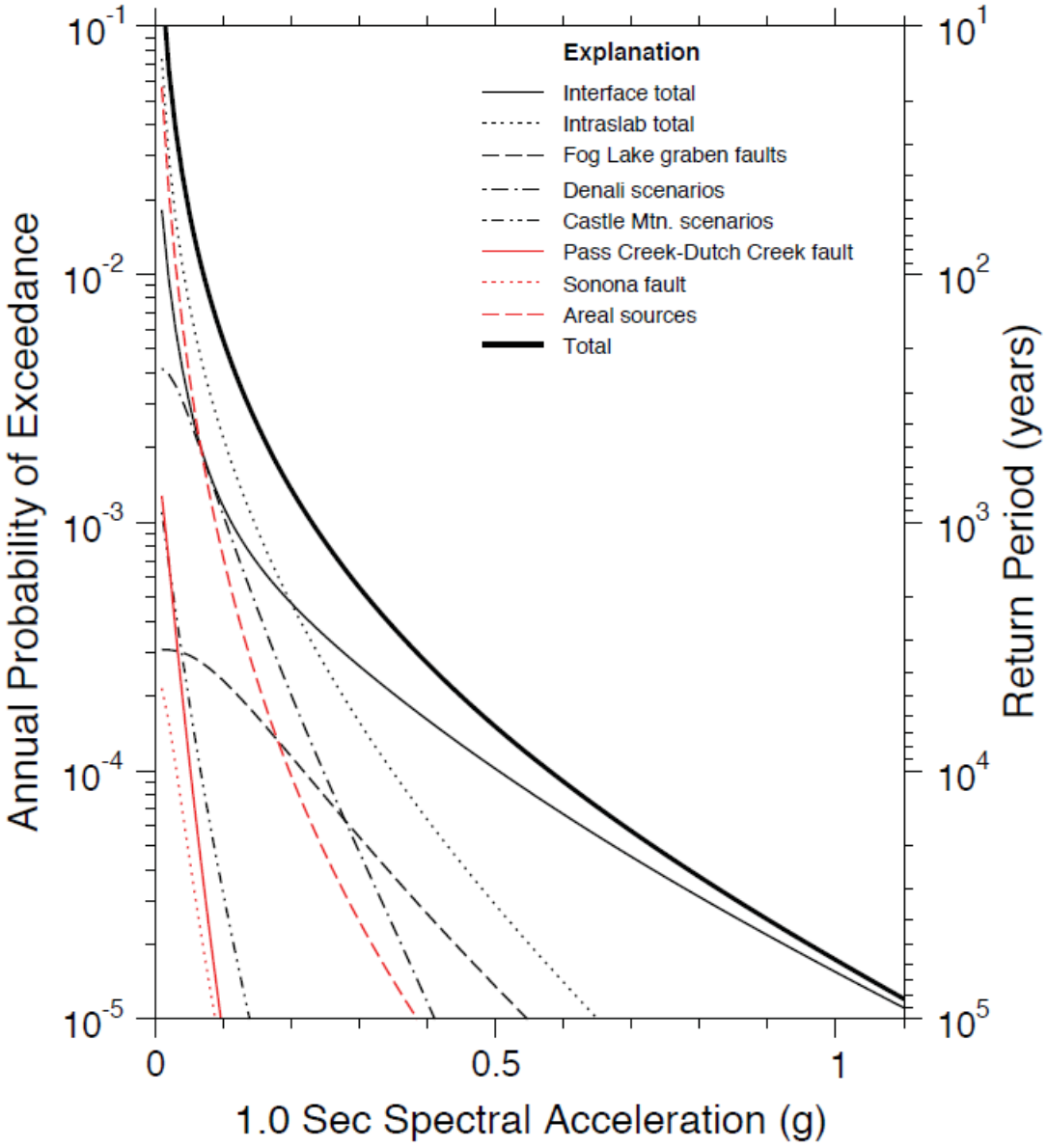


**Figure 8-4. Hazard Curves for 1.0 sec Spectral Acceleration**

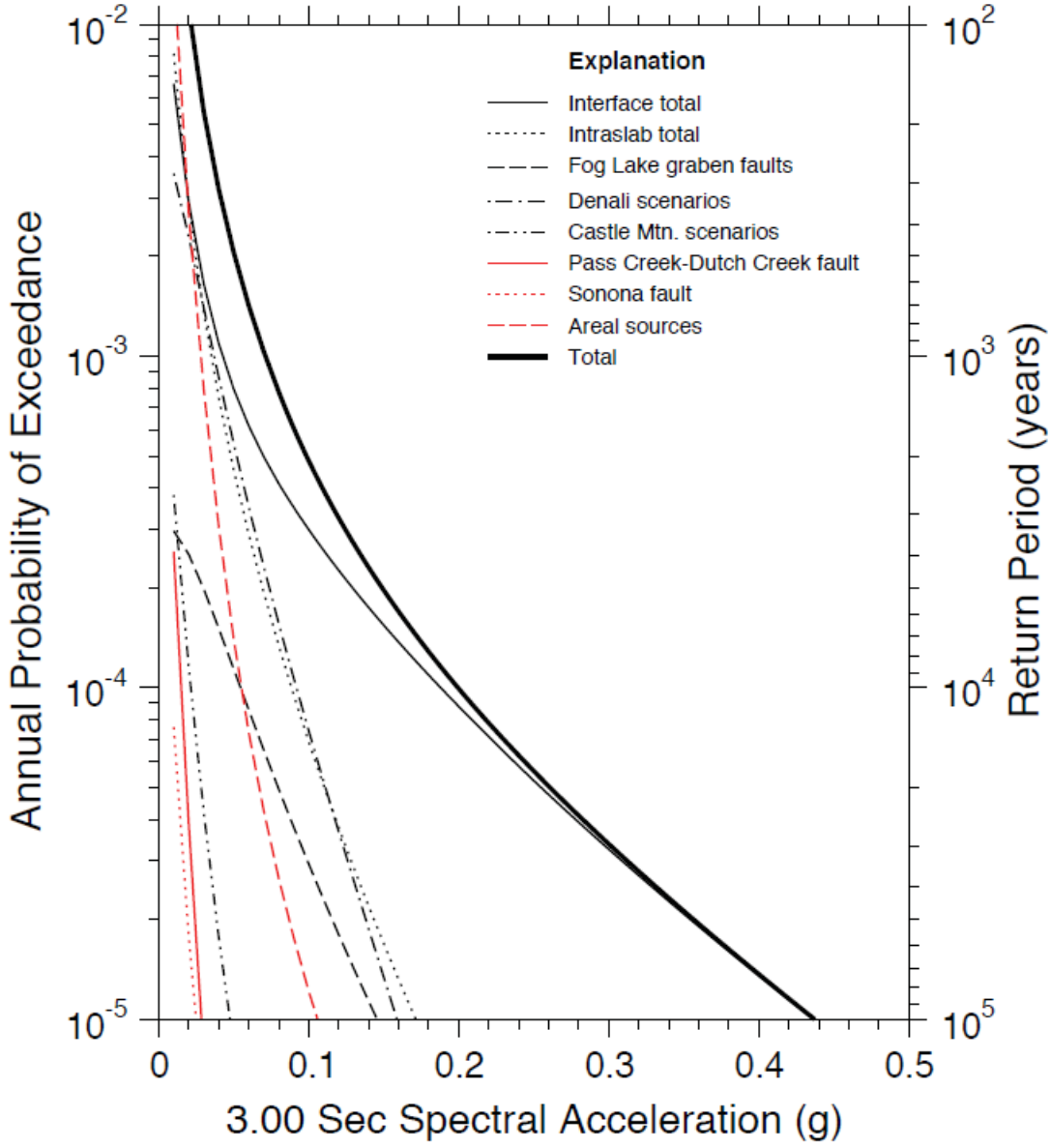


**Figure 8-5. Hazard Curves for 3.00 sec Spectral Acceleration**

### 8.3.2. UHS

A uniform hazard spectrum (UHS) is developed from the suite of total hazard curves, each of which is calculated for a specific spectral period (or its inverse, spectral frequency) at the specified damping level. The spectrum is keyed to a return period, which is the inverse of annual frequency of exceedance. For example, to construct a 10,000-year uniform hazard spectrum, the ground motion level for PHA (0.00 or 0.01 spectral period) at the 0.0001 (1/10,000) y-axis level of that hazard curve is tabulated. The same is done for the hazard for

the other spectral periods. The spectral period is then plotted on the x-axis, and the tabulated ground motion level on the y-axis. These spectra, therefore, indicate the ground motion amplitudes across the entire range of periods for a common hazard level.

Mean uniform hazard spectra for the total hazard were developed for return periods of 100, 250, 1000, 2,500, 5,000, and 10,000 years. These results are shown in Figure 8-6, values are provided in Table 8-4.

**Table 8-4. Uniform Hazard Spectra (g)**

| Period (sec) | 100 yrs | 250 yrs | 1,000 yrs | 2,500 yrs | 5,000 yrs | 10,000 yrs |
|---|---|---|---|---|---|---|
| 0.01 | 0.1270 | 0.1991 | 0.3671 | 0.5222 | 0.6641 | 0.8271 |
| 0.02 | 0.1397 | 0.2184 | 0.3997 | 0.5662 | 0.7179 | 0.8918 |
| 0.03 | 0.1578 | 0.2467 | 0.4506 | 0.6370 | 0.8064 | 1.0004 |
| 0.05 | 0.1855 | 0.2898 | 0.5275 | 0.7437 | 0.9394 | 1.1631 |
| 0.075 | 0.2417 | 0.3784 | 0.6914 | 0.9807 | 1.2461 | 1.5527 |
| 0.10 | 0.2895 | 0.4545 | 0.8344 | 1.1897 | 1.5184 | 1.9008 |
| 0.15 | 0.3007 | 0.4732 | 0.8782 | 1.2609 | 1.6152 | 2.0264 |
| 0.20 | 0.2780 | 0.4383 | 0.8181 | 1.1764 | 1.5067 | 1.8874 |
| 0.25 | 0.2430 | 0.3837 | 0.7175 | 1.0325 | 1.3231 | 1.6586 |
| 0.30 | 0.2140 | 0.3391 | 0.6373 | 0.9200 | 1.1816 | 1.4844 |
| 0.40 | 0.1717 | 0.2746 | 0.5204 | 0.7540 | 0.9703 | 1.2201 |
| 0.50 | 0.1387 | 0.2233 | 0.4255 | 0.6179 | 0.7969 | 1.0038 |
| 0.75 | 0.0938 | 0.1532 | 0.2963 | 0.4351 | 0.5661 | 0.7209 |
| 1.0 | 0.0713 | 0.1179 | 0.2304 | 0.3421 | 0.4496 | 0.5791 |
| 1.5 | 0.0466 | 0.0774 | 0.1529 | 0.2305 | 0.3085 | 0.4054 |
| 2.0 | 0.0345 | 0.0569 | 0.1125 | 0.1709 | 0.2313 | 0.308 |
| 3.0 | 0.0221 | 0.0364 | 0.0713 | 0.1093 | 0.1490 | 0.1995 |

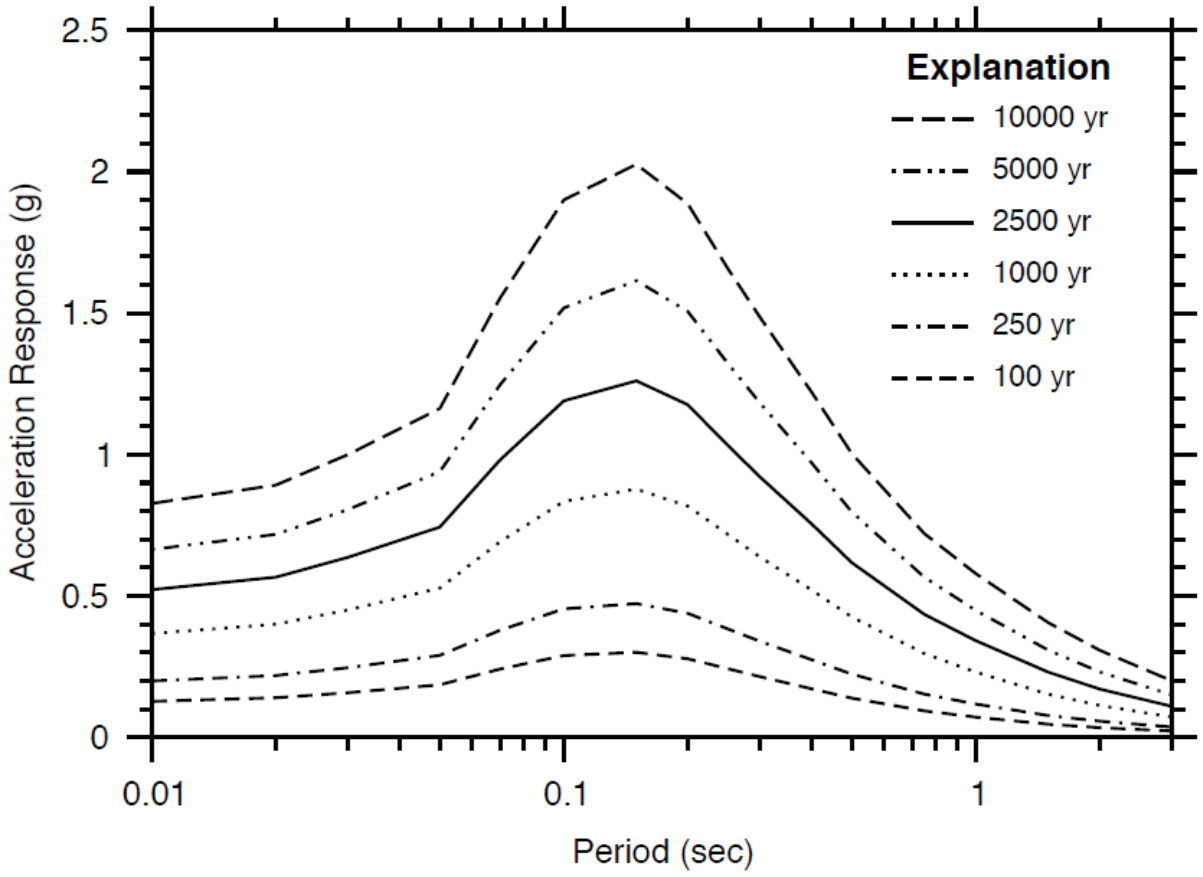


**Figure 8-6. Mean Uniform Hazard Spectra, Total Hazard**

### 8.3.3. Deaggregations

A deaggregation of the ground motion hazard was performed, based on the principles outlined in McGuire (1995) and Bazzurro and Cornell (1999). Bazzurro and Cornell (1999) provide a comparative review of different techniques and their implications. They point out that there is a tradeoff between matching the target spectrum precisely, and identifying the most likely event to produce the target motions. McGuire's (1995) method of collecting contributions that *equal* the target motion for each GMPE was applied here, and the deaggregation therefore is focused on matching the target spectrum.

Source deaggregation plots are shown in Figure 8-7, Figure 8-8, Figure 8-9, and Figure 8-10, one for each of the four spectral response periods (PHA, 0.5 sec, 1.0 sec, 3.0 sec). Only sources contributing 5% or more at any ground motion level are plotted, so the minor sources are not shown. In Figure 8-7, Figure 8-8, Figure 8-9, and Figure 8-10, the 100- and 10,000-year ground motion levels are shown, and in some cases, intermediate return periods. These values can be found in the appropriate cell in Table 8-4.

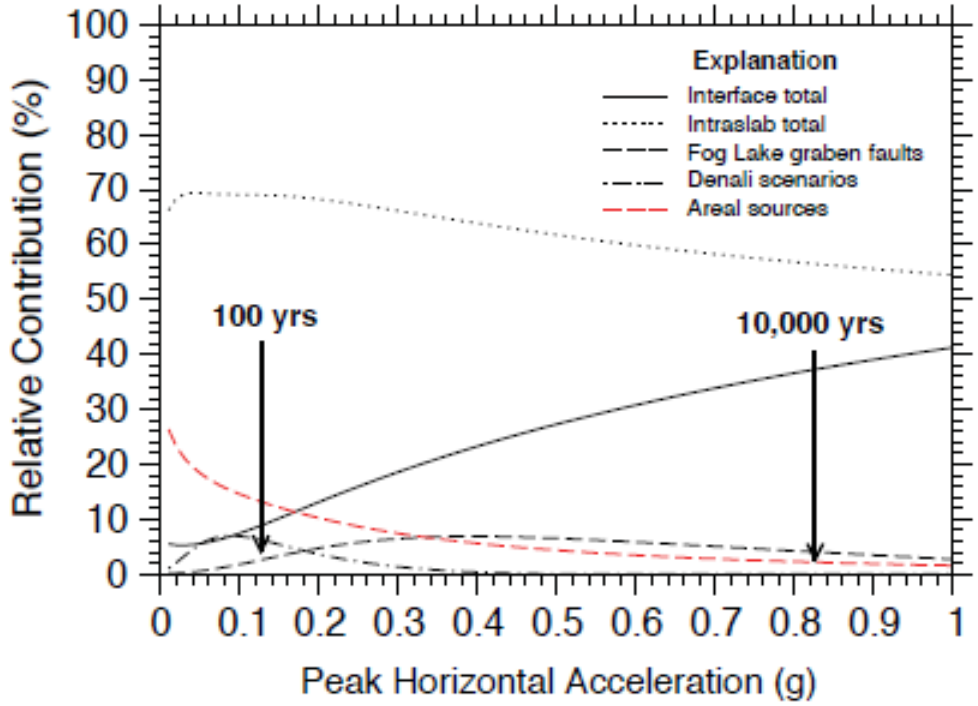


**Figure 8-7. Relative Contributions, Peak Horizontal Acceleration**

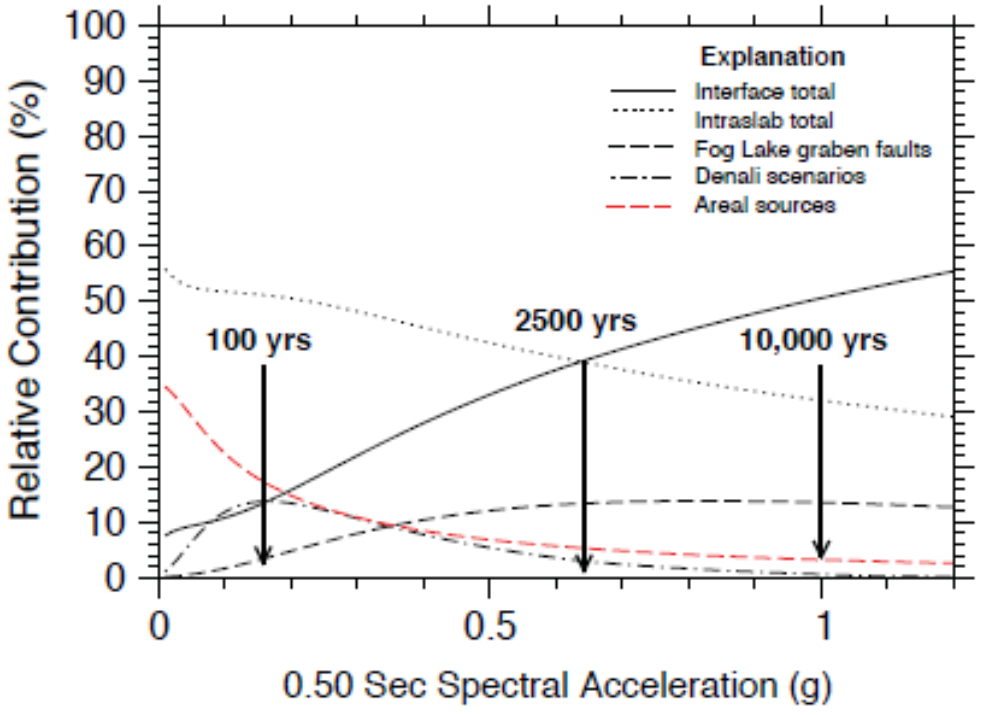


**Figure 8-8. Relative Contributions, 0.5 sec Spectral Acceleration**

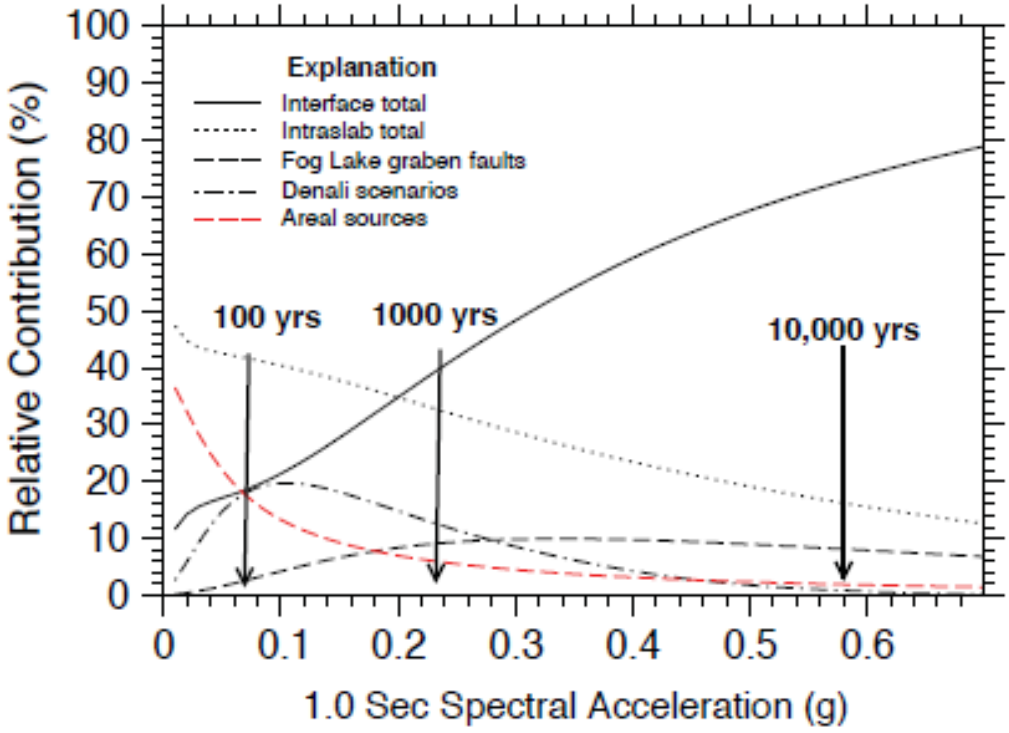


**Figure 8-9. Relative Contributions, 1.0 sec Spectral Acceleration**

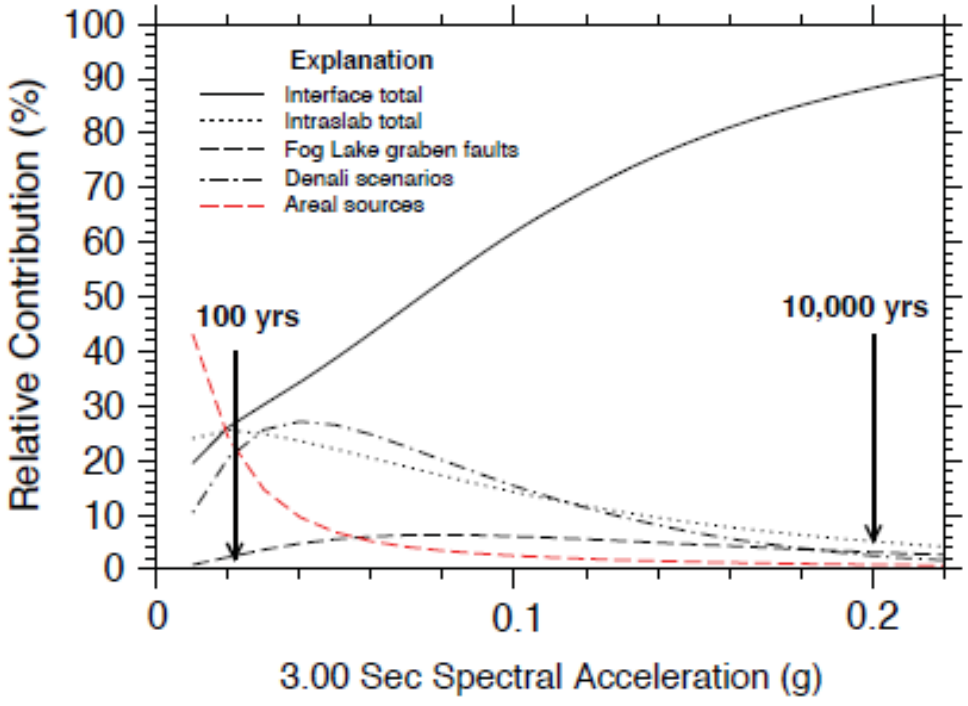


**Figure 8-10. Relative Contributions, 3.00 sec Spectral Acceleration**

The PHA hazard is dominated by the Alaska subduction zone intraslab at all return periods (Figure 8-7). This reflects the high rate of M 5 – 7.5 events produced by this source. The results are mixed for the 0.5 spectral acceleration (SA), with intraslab seismicity dominating at return periods less than 2,500 years, and megathrust seismicity dominating at longer periods (Figure 8-8). A similar result occurs for the 1.0 second SA, but with megathrust activity dominating for the 1,000-year return period and longer (Figure 8-9). For 3.0-second response SA, the Alaska subduction zone sources, Denali fault, and areal sources contribute equally for the 100 year return period, but the Alaska subduction zone megathrust dominates at all longer return periods (Figure 8-10).

Plots showing magnitude, distance, and epsilon contributions to the total hazard were produced for the two major sources (the Alaska subduction zone interface and intraslab), for three return periods (2,500, 5,000, and 10,000 years). Epsilon is the number of standard deviations above or below the median, from which a ground motion amplitude (for a given magnitude and distance) is contributing.

Figure 8-11 shows megathrust results for PHA, 2,500-year return period, and the BC Hydro 2011 GMPE. The plot shows the dominant contribution from the M 9.2 earthquake, with minor contributions from M 7 events. Figure 8-12 shows the same results, but for 1.0-second response and a return period of 10,000 years. For these results, the distance to the megathrust is evident, 48 mi (78 km) or greater. Figure 8-13 shows contributions to the total hazard from the intraslab source, for 0.5-second response, 2,500-year return period, and the Zhao et al. (2006) GMPE. Since the dam site lies above this source, an exponential-appearing decrease with distance is evident. Figure 8-14 shows that the intraslab contributions are coming only from higher magnitude events near the site, at the extreme tails of the ground motion distributions.

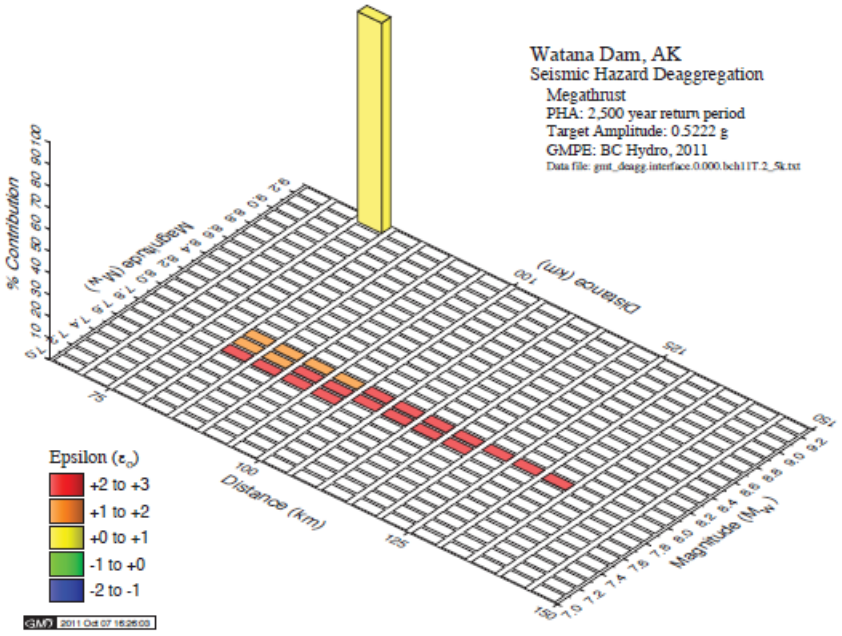


**Figure 8-11. Deaggregation for the Interface, Peak Horizontal Acceleration, 2,500-year Return Period**

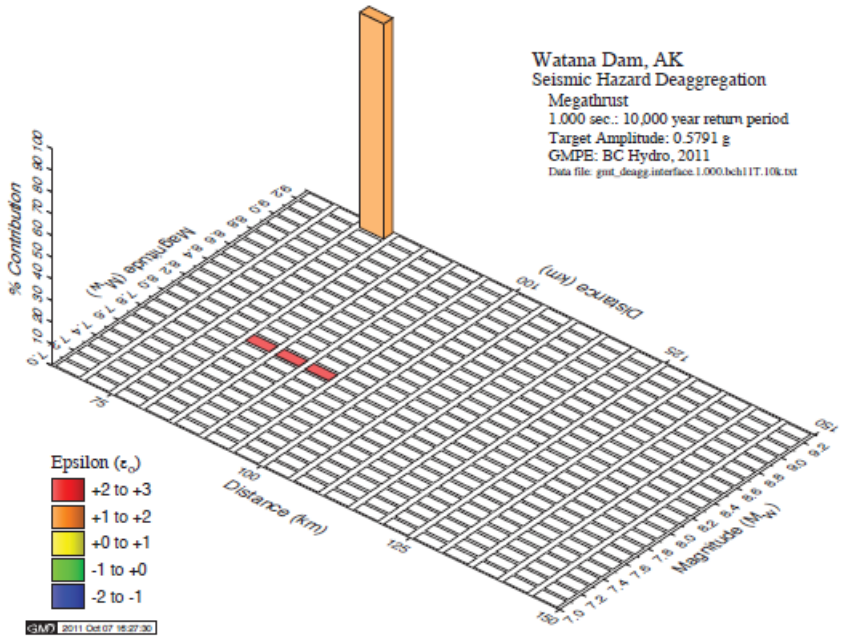


**Figure 8-12. Deaggregation for the Interface,1.0 sec Spectral Acceleration, 10,000-year Return Period**

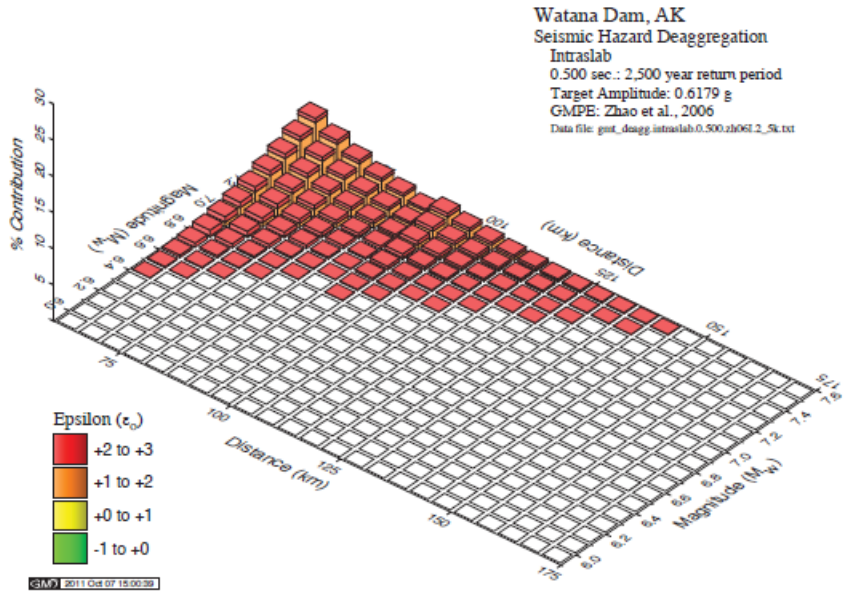


**Figure 8-13. Deaggregation for the Intraslab, 0.5 sec Spectral Acceleration, 2,500-year Return Period**

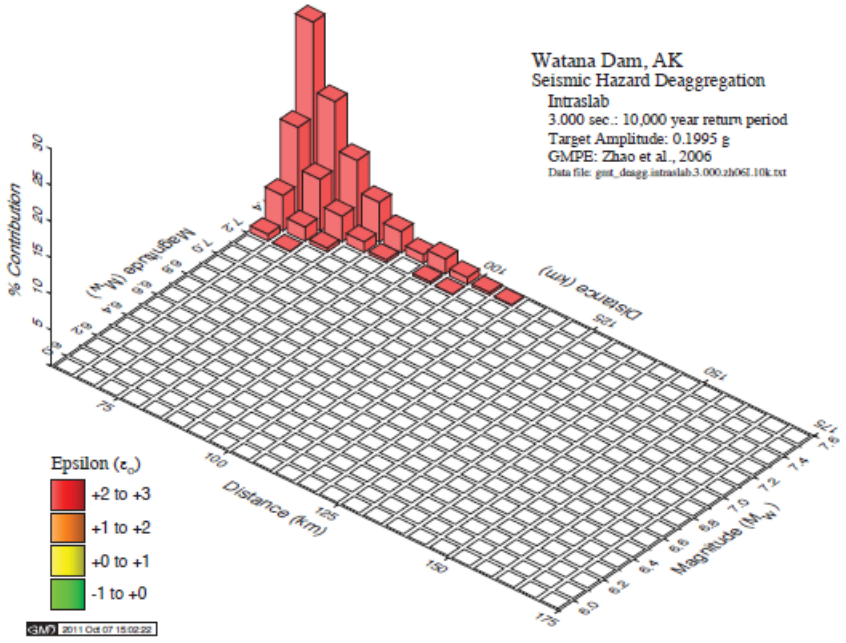


**Figure 8-14. Deaggregation for the Intraslab, 3.0 sec Spectral Acceleration, 10,000-year Return Period**

# 9. DETERMINISTIC SEISMIC HAZARD ANALYSIS

## 9.1. Methodology

The regulatory process for seismic hazard evaluation defined by FERC (Section 1.2) specifies that both probabilistic and deterministic evaluations be conducted. Draft guidance for the deterministic evaluation outlined in Section 5.1 of Idriss and Archuleta (2007) provides the general framework followed here.

The seismic source characterization (Section 4) and the PSHA results (Section 8.3) provide a basis for selecting critical seismic sources for the deterministic evaluation. These critical sources are selected primarily based on consideration of magnitude, distance, and their relative contributions of each source in the PSHA analyses. Other seismic sources in the region may have smaller magnitudes at similar or comparable distances to this group of sources, and are therefore not included in the deterministic evaluation.

## 9.2. Inputs

Four critical fault sources are identified: (1) subduction interface, (2) intraslab, (3) Denali fault, and, (4) Fog Lake graben (Table 9-1). For these fault sources, the same maximum magnitudes used in the both the probabilistic and deterministic evaluations. Distances are measured from the site to the closest approach of the fault source as modeled in the PSHA model, except for the intraslab source. The intraslab source distance is estimated from cross sections which show seismicity associated with the down-going slab beneath southern Alaska and the site (Figure 6-1). Recurrence estimates associated with the largest events on the fault sources likely vary by more than an order of magnitude. Recurrence for the deterministic magnitudes on the Denali fault, subduction interface and intraslab sources are most likely less than 1,000 years. Slip rates on these sources are high (greater than 0.004 in/yr (0.1 mm/yr)). Recurrence for an M 7 on the Fog Lake graben source is unknown, but potentially greater than 10,000 years. Slip rates on this source are also unknown, but are included in the seismic source model as a range from 0.01 to 0.5 mm/yr. As a conservative approach and sensitivity test in the preliminary PSHA, a probability of activity of 1.0 is used for this source, but lack of data and evaluation of the Fog Lake graben source indicate that the present probability of activity should be considerably less than 1.0.

Diffuse seismicity occurring throughout the region is not associated with specific faults, but modeled in the PSHA as background source zones with a maximum magnitude of M7.3. The site area location is near the center of the Southern Alaskan block (SAB) central zone and a deterministic evaluation for this seismic source zone is derived from the 10,000-yr return period deaggregation results from the PSHA (Table 9-2). These results indicate that different

magnitude and distance pairs result for each spectral period. Thus, a separate deterministic magnitude – distance pair could be selected for each of the four spectral periods of interest.

**Table 9-1. Deterministic Hazard Input Parameters**

| Source | Magnitude (Mw) | Rupture Distance (km) | JB Distance (km) | Epsilon | Depth (km)[1] | Ground Motion Prediction Equations [weight] |
|---|---|---|---|---|---|---|
| Megathrust | 9.2 | 78 | n/a | n/a | 35 | ZH06 [0.25]<br>AM09 [0.25]<br>BCH11 [0.50] |
| Denali fault | 7.9 | 71 | 71 | n/a | 0 – 15 | BA08 [0.25]<br>CY08 [0.25]<br>CB08 [0.25]<br>AS08 [0.25] |
| Intraslab | 7.5 | 50 | n/a | n/a | 45 | ZH06 [0.25]<br>AB03 [0.25]<br>BCH11 [0.50] |
| Fog Lake graben | 7.0 | 7.0 | 3.5 | n/a | 0 – 20 | BA08 [0.25]<br>CY08 [0.25]<br>CB08 [0.25]<br>AS08 [0.25] |
| Castle Mtn. fault | 7.6 | 100 | 98 | n/a | 0 – 20 | BA08 [0.25]<br>CY08 [0.25]<br>CB08 [0.25]<br>AS08 [0.25] |

Notes: Depth range indicates top and bottom of faults, individual depths indicate the rupture depth

**Table 9-2. Crustal Seismicity (10,000 yr) Period-Dependent Deaggregation Results Summary**

| Period (sec) | Return Period | Mbar | Dbar | Epsbar | Mod_MD | Mod_MDE |
|---|---|---|---|---|---|---|
| 0.0 | 10k | 6.14 | 17.00 | 1.20 | 5.38 - 10.0 | 5.63 - 12.5 - 1.20 |
| 0.5 | 10k | 6.44 | 21.70 | 1.23 | 6.25 - 11.3 | 6.50 - 18.8 - 0.90 |
| 1.0 | 10k | 6.61 | 23.98 | 1.29 | 6.48 - 11.3 | 6.65 - 17.5 - 0.90 |
| 3.0 | 10k | 6.84 | 24.10 | 1.48 | 6.95 - 11.3 | 7.13 - 18.8 - 0.90 |

Note: These inputs are the average of Next Generation ground motion prediction equations Abrahamson and Silva (2008), Boore and Atkinson (2008), Campbell and Borzorgnia (2008), and Chiou and Youngs (2008).

## 9.3. Results

Deterministic ground motion estimates were developed for five critical seismic sources based on maximum magnitude estimates, site to source distances, and the weighted GMPE's used for each source in the initial PSHA analyses. The deterministic sources are the subduction

interface, subduction intraslab, Denali fault, Castle Mountain fault, Fog Lake graben faults, and a 10,000-year return period earthquake for the background source derived from deaggregation of the PSHA results.

The deterministic ground motion evaluation uses multiple GMPEs appropriate for each type of seismic source with weights shown in Table 9-1. The same weighting of GMPE's is used in the deterministic evaluation as was used in the PSHA.

# 10. COMPARISON OF PROBABILISTIC AND DETERMINISTIC RESULTS

The FERC guidelines ( (FERC, 2011); (Idriss & Archuleta, 2007) ) recommend comparison of the deterministic results to the total UHS from the probabilistic evaluation. The weighted deterministic results, both median and 84th percentile, are shown as individually for each critical source in comparison to the total UHS from the probabilistic evaluation (Figure 10-1 to Figure 10-6). The guidelines recommend use of 84th percentile values for the highly active sources, but use of median values for sources with low average slip rates (Section 5.1 in Idriss and Archuleta (2007)).

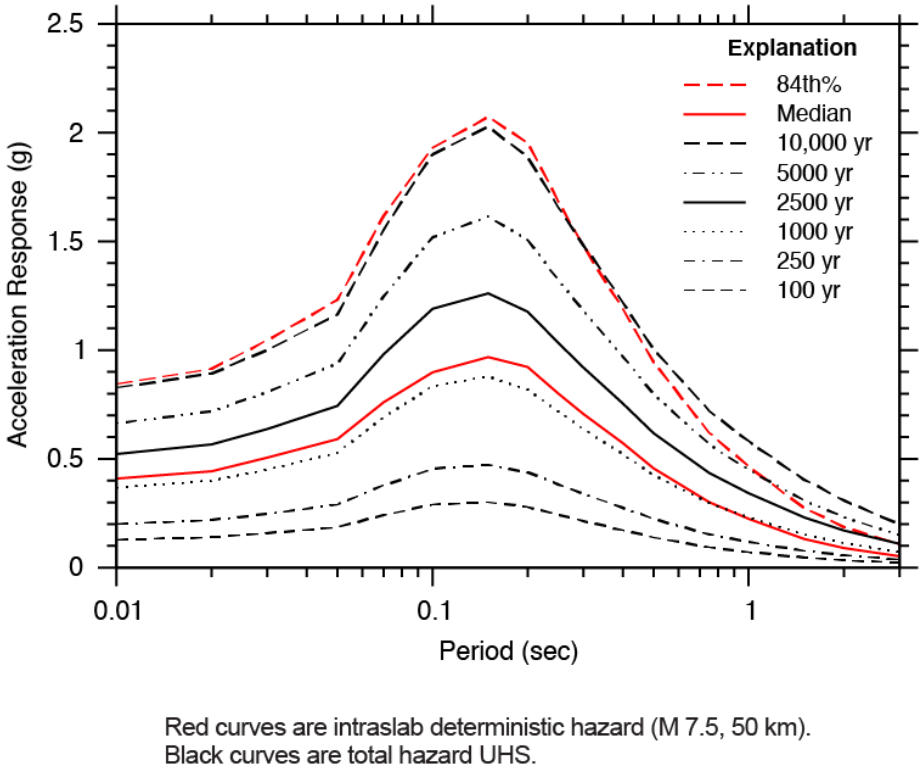


**Figure 10-1. Intraslab Deterministic Hazard Compared to the Total Hazard UHS**

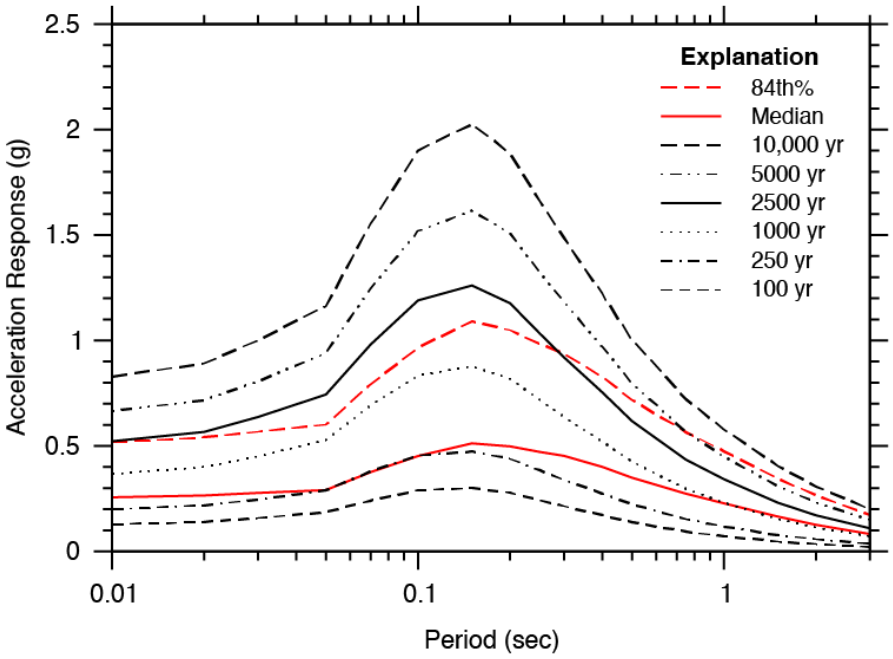


Red curves are megathrust deterministic hazard (M9.2, 78 km).
Black curves are total hazard UHS.

**Figure 10-2. Megathrust Deterministic Hazard Compared to the Total Hazard UHS**

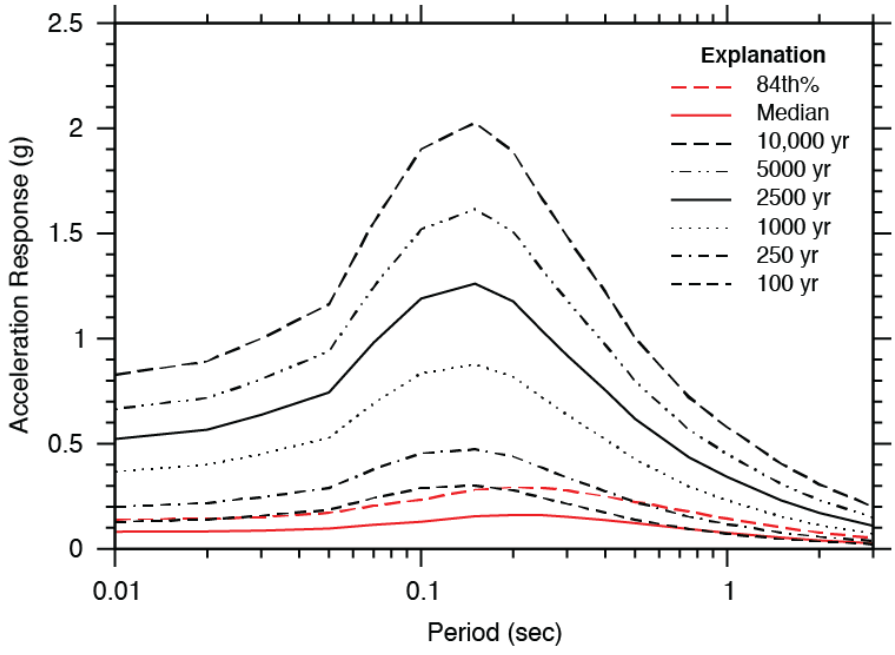


Red curves are Denali fault deterministic hazard (M7.9, 72 km).
Black curves are total hazard UHS.

**Figure 10-3. Denali Fault Deterministic Hazard Compared to the Total Hazard UHS**

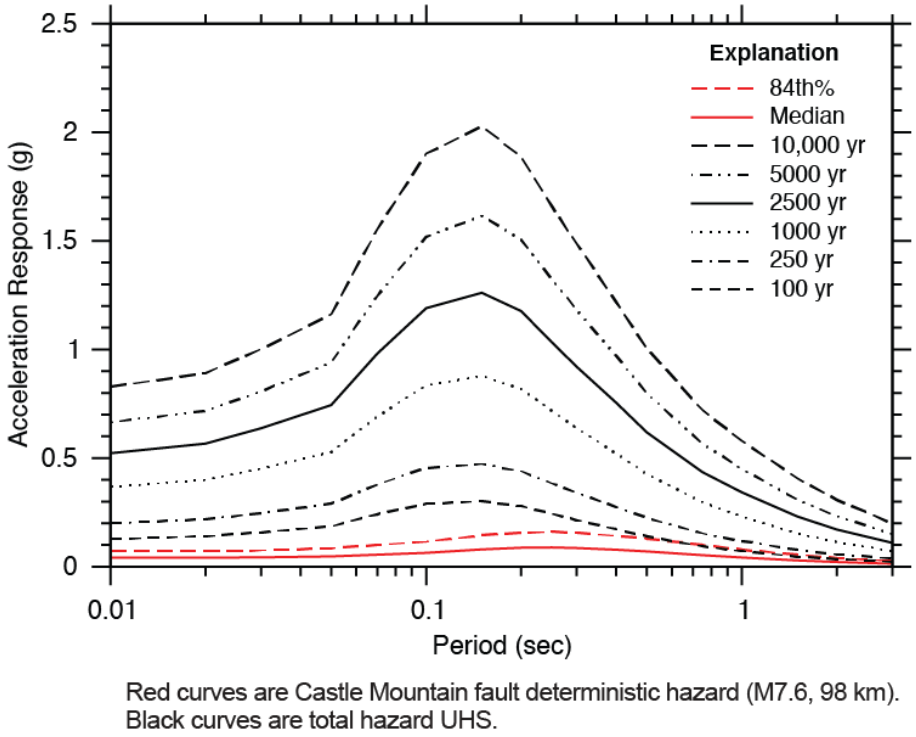


Red curves are Castle Mountain fault deterministic hazard (M7.6, 98 km).
Black curves are total hazard UHS.

**Figure 10-4. Castle Mountain Fault Deterministic Hazard Compared to the Total Hazard UHS**

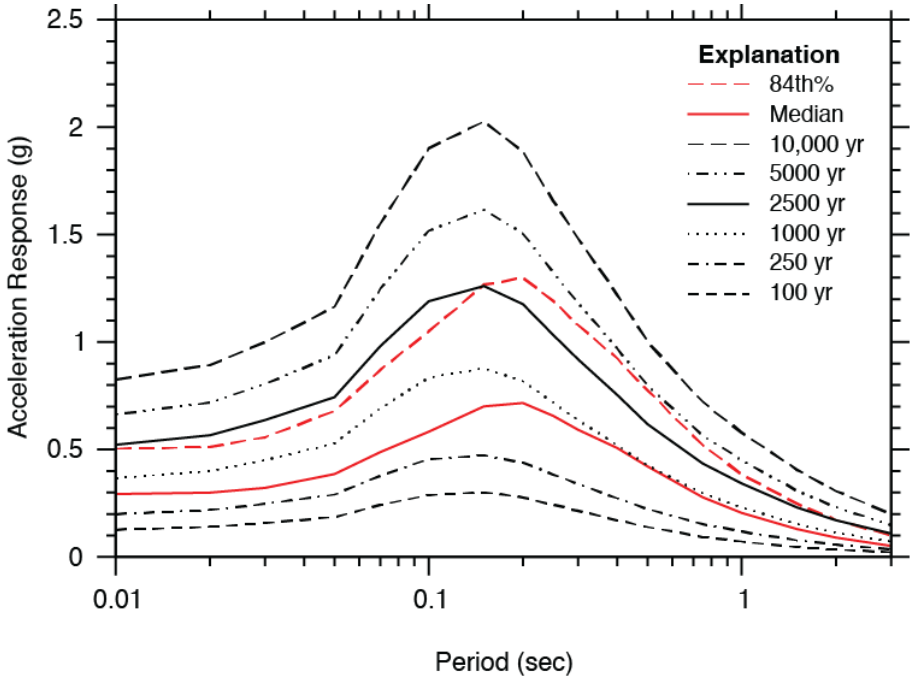


Red curves are Fog Lake graben deterministic hazard (M7.0, 7 km).
Black curves are total hazard UHS.

**Figure 10-5. Fog Lake Graben Deterministic Hazard Compared to the Total Hazard UHS**

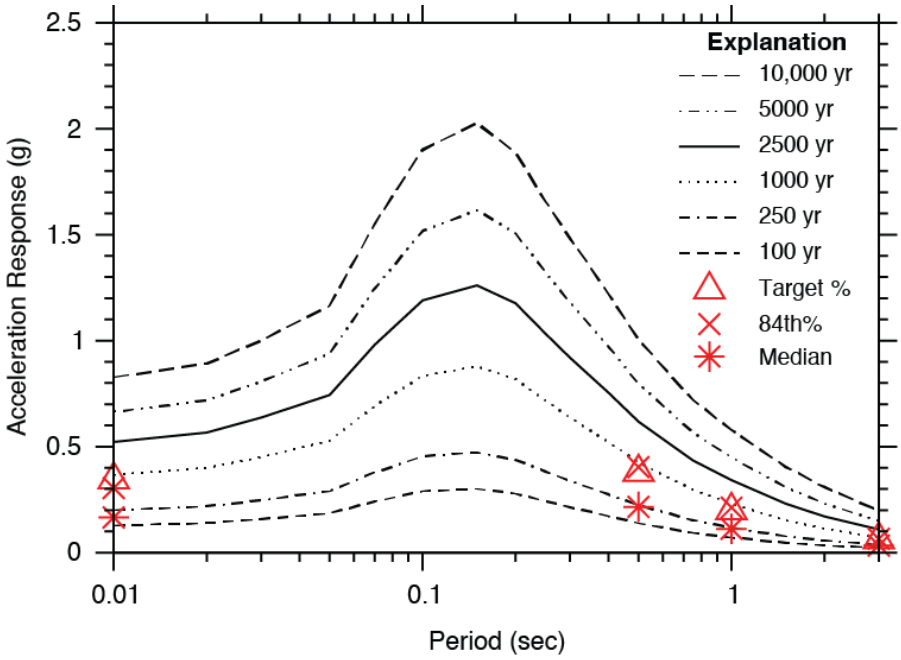


Red symbols are Southern Alaska Block Central areal source deterministic hazard (see Table 9-2 for magnitudes, distances and epsilon values). Black lines are total hazard UHS.

**Figure 10-6. Southern Alaska Block Central Period-Dependent Deterministic Hazard Compared to the Total Hazard UHS**

The deterministic evaluation indicates that the largest values of ground motions at the site are associated with the subduction interface and intraslab sources due to their large magnitude, relatively short distance, and GMPE's used for these sources. For the intraslab source, the deterministic results are generally similar to the 10,000-yr UHS, except at periods greater than 0.5 sec (Figure 10-1). At periods of about 3 sec, the intraslab source contribution corresponds to the 2,500-yr UHS. In contrast, for the subduction interface source, the deterministic results are near the 2,500-yr UHS for periods less than 0.2 sec, but are near the 10,000-yr UHS for periods greater than 2 sec (Figure 10-2).

The median and 84$^{th}$ percentile results for the crustal sources indicate that these sources are relatively less significant compared to the subduction zone sources. The Denali fault source 84th percentile results correspond to the 100-yr UHS for periods up to about 0.2 sec and are below 1,000-yr UHS at periods up to 3 sec (Figure 10-3). The Castle Mountain fault 84$^{th}$ percentile results are lower than the Denali fault, and are below the 100-yr UHS for periods up to about 1 sec and below 250-yr UHS for periods up to 3 seconds (Figure 10-4).

For most periods, the Fog Lake graben source 84$^{th}$ percentile falls at the 2,500-yr UHS (Figure 10-5). Deterministic contributions from the seismicity in the SAB central source zone,

including 84th percentile estimates, also plot between the 250-yr and 1,000-yr UHS hazard (Figure 10-6).

# 11. SEISMIC DESIGN CRITERIA

For Watana Dam, maximum credible earthquake (MCE) ground motions were estimated following FERC guidelines using deterministic seismic hazard analysis (DSHA), while the maximum design earthquake (MDE) was defined based on the 5,000-year return frequency ground motions from a probabilistic seismic hazard analysis (PSHA). The operating basis earthquake (OBE) was selected to be the 500 year return period from the PSHA. Table 11-1 summaries the peak ground acceleration (PGA) resulting from the MCE, MDE and OBE. It should be noted that the MCE is represented by four different response spectra from three different sources: the subduction zone events – interface and intraslab and crustal events. The intraslab is represented by a M7.5 and M8.0. Additional details regarding the PGA and deterministic percentile selected for these events is presented in Table 11-2 and summarized in the remainder of this section.

**Table 11-1. Peak Ground Acceleration Values for the MCE, MDE and OBE**

| CASE | DESIGN EVENT | PGA |
|---|---|---|
| MCE | Deterministic | 0.81g |
| MDE | 5,000-yr Return Period | 0.66g |
| OBE | 500-yr Return Period | 0.27g |

**Table 11-2. Peak Ground Acceleration and Percentile for Deterministic Response Spectra**

| DESIGN EVENT | CASE | Crustal | Interface | Intraslab | |
|---|---|---|---|---|---|
| | | Fog Lake | Alaskan Subduction Zone | | |
| MCE - DSHA | Magnitude | 7.0 | 9.2 | 7.5 | 8.0 |
| | PGA(g) [percentile] | 0.49 [84$^{th}$] | 0.58 [88$^{th}$] | 0.69 [84$^{th}$] | 0.81 [69$^{th}$] |

## 11.1. Response Spectra for the MCE

Based on the Seismic Hazard Characterization and Ground Motion Analyses for the Watana Dam site area, (Fugro, 2012), the seismic hazard at the dam site encompasses contributions from three different sources: the subduction zone events – interface and intraslab (also referred to as the slab), and crustal events. Response Spectra and time histories were developed for each type of event to evaluate the difference in frequency content.

Prior to the completion of the crustal seismic source evaluation, the crustal event was selected to be a M 7.0 event on the Fog Lake graben located at a distance of 4.4 mi (7 km). In the Crustal

Seismic Source Evaluation (Fugro, 2015a) the evaluation of potential crustal seismic sources has not identified any specific features with evidence of late Quaternary faulting within at least 25 mi (40 km) of the Watana dam site; however, this event is a conservative representation of the background crustal event from the PSHA (see Figure 10-5 and Figure 10-6).

Guidance furnished by FERC, Evaluation of Earthquake Ground Motions, was followed and a deterministic spectrum was used (Idriss & Archuleta, 2007). Table 11-3, contains the deterministic parameters for each of the selected events, and Figure 11-1, illustrates the response spectrum. The 2,500, 5,000, and 10,000 year return period uniform hazard spectra are also included on Figure 11-1; this data is from the seismic hazard analysis Report (Fugro, 2012). It should be noted that the $V_S30$ used in the probabilistic seismic hazard assessment is 2,625 ft. (800 m/s).

The 84$^{th}$ percentile or above was used for all of the events, except the M 8.0 event for the slab, where the 69th percentile is used. The interface event was scaled up at the fundamental period of the dam (0.55 seconds) to match the 5,000 year return period, resulting in the 88$^{th}$ percentile, see Figure 11-1.

As an update to the $V_s30$ value in the Seismic Hazard Characterization and Ground Motion Analyses for the Watana dam site area, current field data indicate a $V_S30$ of 3,556 ft. (1,100 m/s) which was used, in Revised Intraslab Model and PSHA Sensitivity Results (Fugro, 2014b) and in the deterministic calculations, from which the time histories were based on. The probabilistic analysis was run for a lower Vs30 value (800m/s) prior to the field data measurements. When the probabilistic analysis is recomputed the new Vs30 value of 3,556 ft. (1,080 m/s) should be used. This change in Vs30 is expected to decrease the uniform hazard spectra (UHS) derived from the PSHA results, as an increase in Vs30 decreases the ground motion.

**Table 11-3. Deterministic Seismic Input Parameters**

| CASE | Crustal | Interface | Intraslab | |
|---|---|---|---|---|
| | Fog Lake | Alaskan Subduction Zone | | |
| Magnitude | 7.0 | 9.2 | 7.5 | 8.0 |
| Hypocentral distance (km) | - | - | 50 | |
| $R_{RUP}$ (km) | 7.0 ($R_{JB}$=3.5) | 78 | - | |
| $V_S30$ (m/s) | 1,080 m/s | | | |
| Type of faulting | Normal | Reverse | Normal | |
| Dip (degrees) | 80 | - | - | |
| Seismogenic Depth (km) | 20 | - | - | |
| Width (km) | 20.3 | - | - | |
| $Z_{1.0}$ (km) | | | | |
| $Z_{2.5}$ (km) | | | | |
| $Z_{TOR}$ (km) | 0.5 | | | |
| Hanging Wall | YES | - | YES | YES |
| PGA(g) [percentile] | 0.49 [84th] | 0.58 [88th] | 0.69 [84th] | 0.81 [69th] |
| Ground Motion Prediction Equation [weight] | BA08 [0.25]<br>CY08 [0.25]<br>CB08 [0.25]<br>AS08 [0.25] | BCH11 [0.5]<br>ZH06 [0.25]<br>AM09 [0.25] | BCH11 [0.5]<br>ZH06 [0.25]<br>AB03 [0.25] | |

Note:
km – kilometer(s)
Source: Deterministic Seismic Hazard Analysis; (Fugro, 2012)
Acronyms: BA08= Boore and Atkinson 2008; CY08=Chiou and Youngs 2008; CB08=Campbell and Borzorgnia 2008; AS08=Abrahamson and Silva 2008; BCH11=BC Hydro 2012; ZH06= Zhao 2006; AM09=Atkinson and Macias 2009, AB03=Atkinson and Boore 2003

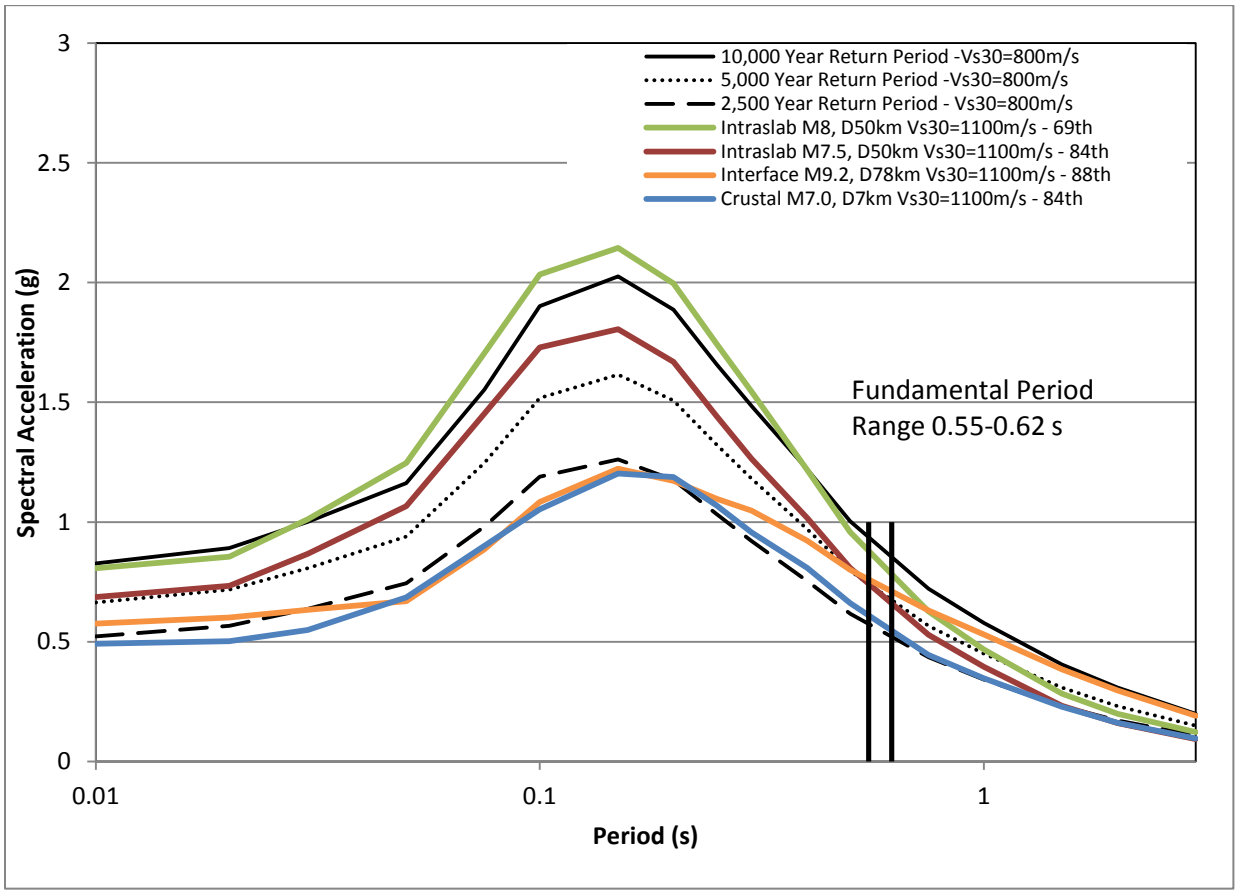


**Figure 11-1. Design Response Spectra**

A vertical response spectrum was developed by computing a vertical to horizontal ratio following the guidance of Gülerce and Abrahamson (2011). The applicability to subduction zone events was based on the work performed by Gregor et al. (2012). The magnitude and distance pair used for the deterministic analysis was used as the input parameters to develop the vertical to horizontal ratios. The ratios correspond to median values and are presented in Table 11-4. The vertical and horizontal response spectra are shown in Table 11-5 through Table 11-7 for each event type together with plots shown in Figure 11-2 through Figure 11-4.

**Table 11-4. Median Vertical / Horizontal Ratios**

| Period (s) | Slab M8.0 | Slab M7.5 | Interface | Crustal |
|---|---|---|---|---|
| 0.010 | 0.658 | 0.652 | 0.579 | 0.728 |
| 0.020 | 0.659 | 0.652 | 0.579 | 0.728 |
| 0.030 | 0.715 | 0.708 | 0.600 | 0.791 |
| 0.050 | 0.719 | 0.710 | 0.582 | 0.902 |
| 0.075 | 0.695 | 0.684 | 0.642 | 0.921 |
| 0.100 | 0.670 | 0.657 | 0.638 | 0.798 |
| 0.150 | 0.652 | 0.640 | 0.634 | 0.660 |
| 0.200 | 0.656 | 0.647 | 0.648 | 0.597 |
| 0.250 | 0.668 | 0.661 | 0.656 | 0.586 |
| 0.300 | 0.683 | 0.678 | 0.669 | 0.590 |
| 0.400 | 0.713 | 0.713 | 0.696 | 0.597 |
| 0.500 | 0.729 | 0.732 | 0.709 | 0.596 |
| 0.750 | 0.838 | 0.842 | 0.802 | 0.655 |
| 1.000 | 0.825 | 0.829 | 0.776 | 0.634 |
| 1.500 | 0.820 | 0.824 | 0.794 | 0.648 |
| 2.000 | 0.791 | 0.795 | 0.782 | 0.639 |
| 3.000 | 0.773 | 0.777 | 0.787 | 0.643 |
| 4.000 | 0.805 | 0.808 | 0.836 | 0.683 |
| 5.000 | 0.816 | 0.820 | 0.848 | 0.693 |
| 7.500 | 0.816 | 0.820 | 0.848 | 0.693 |
| 10.00 | 0.816 | 0.820 | 0.848 | 0.693 |

**Table 11-5. Horizontal and Vertical Design Response Spectra for Intraslab Events**

| Period | M8.0 69th Percentile | | M7.5 84th Percentile | |
|---|---|---|---|---|
| T (s) | Horizontal Acceleration (g) | Vertical Acceleration (g) | Horizontal Acceleration (g) | Vertical Acceleration (g) |
| 0.01 | 0.8075 | 0.531 | 0.6870 | 0.4479 |
| 0.02 | 0.8553 | 0.564 | 0.7337 | 0.4784 |
| 0.03 | 1.0121 | 0.724 | 0.8675 | 0.6142 |
| 0.05 | 1.2464 | 0.896 | 1.0668 | 0.7574 |
| 0.075 | 1.7055 | 1.185 | 1.4522 | 0.9933 |
| 0.1 | 2.0342 | 1.363 | 1.7286 | 1.1357 |
| 0.15 | 2.1449 | 1.398 | 1.8046 | 1.1549 |
| 0.2 | 1.9965 | 1.310 | 1.6686 | 1.0796 |
| 0.25 | 1.7432 | 1.164 | 1.4413 | 0.9527 |
| 0.3 | 1.5443 | 1.055 | 1.2646 | 0.8574 |
| 0.4 | 1.2174 | 0.868 | 1.0162 | 0.7246 |
| 0.5 | 0.9581 | 0.698 | 0.8078 | 0.5913 |
| 0.75 | 0.6262 | 0.525 | 0.5289 | 0.4453 |
| 1 | 0.4679 | 0.386 | 0.3960 | 0.3283 |
| 1.5 | 0.2835 | 0.232 | 0.2326 | 0.1917 |
| 2 | 0.1986 | 0.157 | 0.1603 | 0.1274 |
| 3 | 0.1226 | 0.095 | 0.0935 | 0.0726 |

Note: Deterministic Inputs shown in Table 11-3.

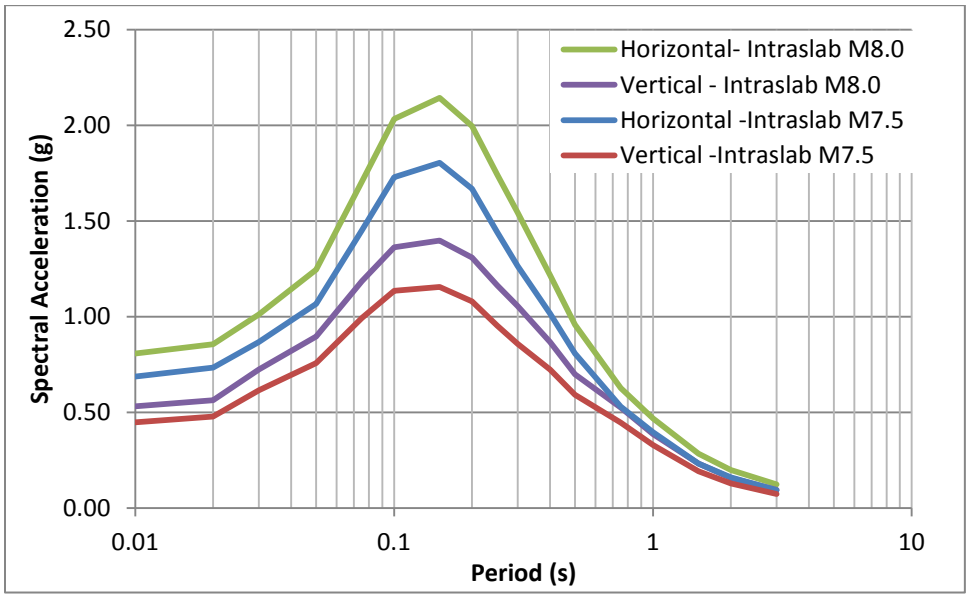


**Figure 11-2. Intraslab M8.0 – 69th Percentile Design Response Spectra and Intraslab M7.5 – 84th Percentile Design Response Spectra**

**Table 11-6. Horizontal and Vertical Design response Spectra for Interface Events**

| Period | M9.2 88h Percentile | |
|---|---|---|
| T (s) | Horizontal Acceleration (g) | Vertical Acceleration (g) |
| 0.01 | 0.5754 | 0.3332 |
| 0.02 | 0.6011 | 0.3481 |
| 0.03 | 0.6328 | 0.3797 |
| 0.05 | 0.6697 | 0.3898 |
| 0.08 | 0.8857 | 0.5686 |
| 0.10 | 1.0832 | 0.6911 |
| 0.15 | 1.2221 | 0.7748 |
| 0.20 | 1.1724 | 0.7597 |
| 0.25 | 1.0975 | 0.7199 |
| 30.30 | 1.0472 | 0.7005 |
| 0.40 | 0.9222 | 0.6419 |
| 0.50 | 0.8005 | 0.5675 |
| 0.75 | 0.6308 | 0.5059 |
| 1.00 | 0.5298 | 0.4111 |
| 1.50 | 0.3848 | 0.3056 |
| 2.00 | 0.2964 | 0.2318 |
| 3.00 | 0.1914 | 0.1506 |

Note: Deterministic Inputs shown in Table 11-3.

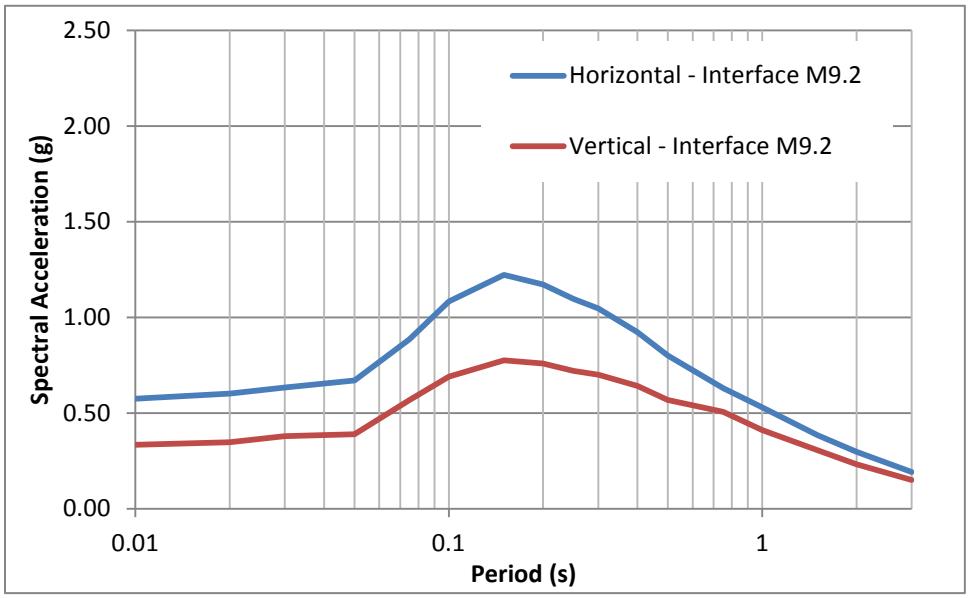


**Figure 11-3. Interface M9.3 – 88th Percentile Design Response Spectra**

**Table 11-7. Horizontal and Vertical Design Response Spectra for Crustal Events**

| Period | M7.0 84h Percentile | |
|---|---|---|
| T (s) | Horizontal Acceleration (g) | Vertical Acceleration (g) |
| 0.01 | 0.4910 | 0.3574 |
| 0.02 | 0.5022 | 0.3656 |
| 0.03 | 0.5487 | 0.4340 |
| 0.05 | 0.6859 | 0.6187 |
| 0.08 | 0.9005 | 0.8294 |
| 0.10 | 1.0523 | 0.8397 |
| 0.15 | 1.2028 | 0.7938 |
| 0.20 | 1.1882 | 0.7094 |
| 0.25 | 1.0686 | 0.6262 |
| 0.30 | 0.9567 | 0.5645 |
| 0.40 | 0.8077 | 0.4822 |
| 0.50 | 0.6615 | 0.3943 |
| 0.75 | 0.4455 | 0.2918 |
| 1.00 | 0.3476 | 0.2204 |
| 1.50 | 0.2289 | 0.1483 |

| Period | M7.0 84h Percentile | |
|---|---|---|
| T (s) | Horizontal Acceleration (g) | Vertical Acceleration (g) |
| 2.00 | 0.1611 | 0.1029 |
| 3.00 | 0.0965 | 0.0620 |

Note: Deterministic Inputs shown in Table 11-3.

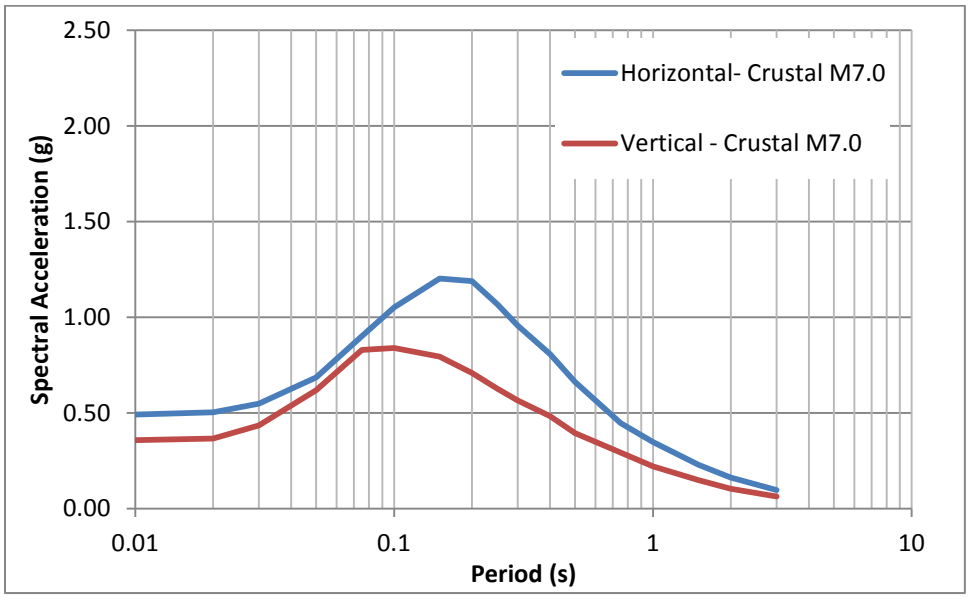


**Figure 11-4. Crustal M7.0 – 84th Percentile Design Response Spectra**

## 11.2. Response Spectra for the OBE

According to the published guidelines ( (ICOLD), (FEMA), Alaska Dam Safety, and (U.S. Army Corps of Engineers (USACE))) the normal choice of operating basis earthquake (OBE) would be the earthquake that can reasonably be expected to occur within the service life of the project, that is, with a 50 percent probability of exceedance during the service life. (This corresponds to a return period of 144 years for a project with a service life of 100 years.) For the Susitna-Watana Project, such an event would equate to a PGA of the order of 0.16g, which could be regarded as unacceptably low by the general public who are not conversant with civil and structural design guidelines. Table 11-8 shows the PGAs for selected return periods.

**Table 11-8. PGAs for Selected Return Periods**

| Return Period, years | PGA |
|---|---|
| 100 | 0.13g |
| 150 | 0.16g |
| 500 | 0.27g |
| 1000 | 0.37g |

MWH recommends that the OBE be selected as the 500 year event, equating to a PGA of 0.27g. The dam structure will be evaluated under this event and from a structural perspective all facilities will be able to continue to operate without interruption or significant repair. The horizontal response spectrum for the OBE is presented in Table 11-9.

**Table 11-9. OBE Horizontal Response Spectrum**

| Period (s) | 500-yr Return Period |
|---|---|
| 0.010 | 0.273 |
| 0.020 | 0.299 |
| 0.030 | 0.337 |
| 0.050 | 0.396 |
| 0.075 | 0.518 |
| 0.100 | 0.623 |
| 0.150 | 0.651 |
| 0.200 | 0.605 |
| 0.250 | 0.551 |
| 0.300 | 0.490 |
| 0.400 | 0.382 |
| 0.500 | 0.311 |
| 0.750 | 0.212 |
| 1.000 | 0.167 |
| 1.500 | 0.110 |
| 2.000 | 0.080 |
| 3.000 | 0.051 |

# 12. SELECTION OF TIME HISTORIES

Pre-selection of time histories was completed by searching COSMOS, PEER, K-NET (Japanese Earthquake Database), and a database run by the University of Chile and the Chile Ministry of the Interior and Public Safety for ground motions that had magnitude, distance and record properties similar to the controlling events.

Ideally, the selected time histories should have the same source, style-of-faulting, magnitude, distance, site conditions and directivity condition as the event for which the evaluation is being performed. However, in practice, it is not always possible to find a perfect match.

The criteria used to select the events are discussed below.

### 12.1.1. Intraslab

The catalog search for slab events included motions recorded during the El Salvador 2001 M7.6 event (14 recordings), Japan 2003 M7.1 event (412 of recorded motions), Chile 2005 M7.9 event (10 recordings) and available records for the Japan 2011 M7.0 event (504 recordings).

The number of slab ground motions considered was then narrowed down to those events that had a recording distance from 50 to 115 kilometers (km) and included all three components. The design distance was 50 km and it was initially chosen to select those events that fell between +/- 50 km, however this limited the database to a total of 28 events. By increasing the maximum distance to 115 km and additional 24 events were able to be included. The closest event distance was 72 km away, so the distance range was revised to 72-115 km. Chile M7.9 events were not able to be used because no records fell within 115 km; the closest distance was recorded to be 135 km. This narrowed down the database to 52 events, 21 from the 2003 M7.1 Japan event, 20 from the 2011 M7.0 Japan event and 11 from the El Salvador event. Those 52 events were then visually compared to the design response spectra and those with similar spectral shapes were spectrally matched. By putting together a catalog of those strong motion events that occurred on the slab, it is believed that the ground motion parameters (e.g., duration and equivalent number of cycles) should be representative of the target slab scenario. Currently, there is a very limited amount of earthquake events, and strong motions, available that can be comparable to the large slab scenario (i.e. M8.0), which leads to high scaling factors. If the selection of time histories includes the record properties of the scaled ground motions, then the time histories could be scaled by large factors without affecting the average response (Watson-Lamprey & Abrahamson, 2005).

### 12.1.2. Interface

The catalog search for interface events included motions recorded during Japan 2011 M9.0 event (1400 of recorded motions) and available records for the Chile 2010 M8.8 event (55 recordings). The design distance is 92 km and it was chosen to select those events that fell between +/- 50 km (42-142 km). This narrowed down the database to 148 events; 138 from the 2011 M9.0 Japan event and 10 from the 2010 M8.8 Chile event. Those 148 events were then visually compared to the design response spectra and those with similar spectral shapes were spectrally matched. By putting together a catalog of those strong motion events greater than M8.8 that occurred on the interface, it is believed that the ground motion parameters (e.g., duration and equivalent number of cycles) should be representative of the target slab scenario.

### 12.1.3. Crustal

The search for the crustal time history was performed using the PEER NGA West 1 Database (Pacific Earthquake Engineering Research (PEER), 2007) for those events having a magnitude ranging between 6.5 and 7.5 at distances of 0 to 15 km, contained all three components and a $V_S30$ greater than or equal to 400 m/s. After using the search criteria the time histories were then narrowed down to those motions that had similar spectral shape.

### 12.1.4. Selected Events

Once the ground motions with similar spectral shape were compiled select recorded strong motions were synthetically modified to match the target spectra. The record parameters for the seed events are presented for the slab, interface and crustal events in Table 12-1 through Table 12-4.

**Table 12-1. Record Parameters for Selected Slab Time Histories – M8.0 -69th Percentile (PGA=0.81)**

| Event Title | Station | | Arias Intensity (m/s) | Predominant Period (sec) | Predominant Freq. (Hz) | Significant Duration (s) | | No. Cycles |
|---|---|---|---|---|---|---|---|---|
| | | | | | | 5–95% | 5–75% | |
| Japan (M7.1) 05/26/2003 Rrup=107km | MYG009EW | Seed | 0.19 | 1.53 | 0.65 | 33.8 | 12.8 | 83 |
| | | Spectrally Matched | 16.05 | 0.22 | 4.46 | 33.5 | 12.6 | 79 |
| | MYG009NS | Seed | 0.18 | 0.22 | 4.53 | 39.7 | 13.7 | 91 |
| | | Spectrally Matched | 16.06 | 0.23 | 4.34 | 36.6 | 14.6 | 87 |
| | MYG009UD | Seed | 0.08 | 0.71 | 1.40 | 36.0 | 16.1 | 135 |
| | | Spectrally Matched | 8.12 | 0.21 | 4.72 | 36.1 | 16.6 | 118 |
| El Salvador (M7.6) 01/13/2001 Rrup=112km | MONTEW | Seed | 1.12 | 0.57 | 1.77 | 17.3 | 10.4 | 44 |
| | | Spectrally Matched | 9.10 | 0.57 | 1.77 | 20.6 | 11.2 | 39 |
| | MONTNS | Seed | 1.14 | 0.25 | 3.95 | 18.2 | 11.2 | 33 |
| | | Spectrally Matched | 9.41 | 0.25 | 3.95 | 20.0 | 12.9 | 40 |
| | MONTUD | Seed | 0.77 | 0.25 | 3.95 | 19.6 | 14.1 | 79 |
| | | Spectrally Matched | 5.67 | 0.25 | 3.95 | 24.6 | 16.0 | 55 |
| El Salvador (M7.6) 01/13/2001 Rrup=114km | STTEC090 | Seed | 7.71 | 0.29 | 3.43 | 10.8 | 5.5 | 36 |
| | | Spectrally Matched | 6.98 | 0.29 | 3.43 | 11.7 | 6.7 | 27 |
| | STTEC180 | Seed | 6.54 | 0.16 | 6.16 | 14.3 | 6.9 | 52 |
| | | Spectrally Matched | 9.15 | 0.16 | 6.08 | 17.6 | 8.9 | 49 |
| | STTECUP | Seed | 2.80 | 0.31 | 3.19 | 15.8 | 11.3 | 47 |
| | | Spectrally Matched | 3.64 | 0.10 | 9.87 | 15.9 | 11.6 | 47 |

**Table 12-2. Record Parameters for Selected Slab Time Histories – M7.5 -84th Percentile (PGA=0.69)**

| Event Title | Station | | Arias Intensity (m/s) | Predominant Period (sec) | Predominant Freq. (Hz) | Significant Duration (s) | | No. Cycles |
|---|---|---|---|---|---|---|---|---|
| | | | | | | 5–95% | 5–75% | |
| Japan (M7.1) 05/26/2003 Rrup=107km | MYG009EW | Seed | 0.19 | 1.53 | 0.65 | 33.8 | 12.8 | 83 |
| | | Spectrally Matched | 11.50 | 0.37 | 2.71 | 34.1 | 12.8 | 72 |
| | MYG009NS | Seed | 0.18 | 0.22 | 4.53 | 39.7 | 13.7 | 91 |
| | | Spectrally Matched | 11.07 | 0.26 | 3.90 | 36.6 | 14.1 | 92 |
| | MYG009UD | Seed | 0.08 | 0.71 | 1.40 | 36.0 | 16.1 | 135 |
| | | Spectrally Matched | 5.89 | 0.13 | 7.79 | 36.0 | 16.5 | 120 |
| El Salvador (M7.6) 01/13/2001 Rrup=112km | MONTEW | Seed | 1.12 | 0.57 | 1.77 | 17.3 | 10.4 | 44 |
| | | Spectrally Matched | 6.60 | 0.24 | 4.12 | 21.3 | 11.8 | 45 |
| | MONTNS | Seed | 1.14 | 0.25 | 3.95 | 18.2 | 11.2 | 33 |
| | | Spectrally Matched | 6.85 | 0.20 | 4.99 | 20.3 | 12.9 | 32 |
| | MONTUD | Seed | 0.77 | 0.25 | 3.95 | 19.6 | 14.1 | 79 |
| | | Spectrally Matched | 4.06 | 0.25 | 4.04 | 25.6 | 16.1 | 60 |
| El Salvador (M7.6) 01/13/2001 Rrup=114km | STTEC090 | Seed | 7.71 | 0.29 | 3.43 | 10.8 | 5.5 | 36 |
| | | Spectrally Matched | 4.76 | 0.20 | 4.94 | 12.6 | 6.9 | 27 |
| | STTEC180 | Seed | 6.54 | 0.16 | 6.16 | 14.3 | 6.9 | 52 |
| | | Spectrally Matched | 6.79 | 0.15 | 6.79 | 17.8 | 9.4 | 46 |
| | STTECUP | Seed | 2.80 | 0.31 | 3.19 | 15.8 | 11.3 | 47 |
| | | Spectrally Matched | 2.54 | 0.10 | 9.87 | 16.8 | 11.8 | 44 |

**Table 12-3. Record Parameters for Selected Interface Time Histories – M9.2 -88th Percentile (PGA=0.58)**

| Event Title | Station | | Arias Intensity (m/s) | Predominant Period (sec) | Predominant Freq. (Hz) | Significant Duration (s) | | No. Cycles |
|---|---|---|---|---|---|---|---|---|
| | | | | | | 5–95% | 5–75% | |
| Chile (M8.8) 02/27/2010 Rrup=85km | CURIEW | Seed | 10.55 | 1.45 | 0.69 | 49.3 | 37.0 | 102 |
| | | Spectrally Matched | 13.06 | 0.23 | 4.35 | 51.1 | 37.3 | 76 |
| | CURINS | Seed | 2.85 | 0.73 | 1.37 | 53.1 | 40.1 | 277 |
| | | Spectrally Matched | 17.11 | 0.55 | 1.83 | 57.3 | 43.0 | 175 |
| | CURIUD | Seed | 10.88 | 0.42 | 2.40 | 50.7 | 38.2 | 134 |
| | | Spectrally Matched | 6.06 | 0.42 | 2.40 | 51.8 | 38.9 | 128 |
| Japan (M9.0) 03/11/2011 Rrup=105km | ATK023EW | Seed | 0.39 | 1.09 | 0.92 | 93.8 | 57.0 | 87 |
| | | Spectrally Matched | 15.2 | 1.09 | 0.92 | 100.3 | 59.8 | 83 |
| | ATK023NS | Seed | 0.49 | 0.78 | 1.28 | 94.3 | 56.8 | 129 |
| | | Spectrally Matched | 19.09 | 0.54 | 1.84 | 102.2 | 61.8 | 106 |
| | ATK023UD | Seed | 0.23 | 0.43 | 2.35 | 95.2 | 61.3 | 130 |
| | | Spectrally Matched | 7.47 | 0.43 | 2.35 | 95.1 | 61.6 | 139 |
| Japan (M9.0) 03/11/2011 Rrup=130km | CHB012EW | Seed | 2.03 | 0.27 | 3.66 | 62.6 | 35.6 | 58 |
| | | Spectrally Matched | 10.27 | 1.35 | 0.74 | 72.8 | 45.8 | 46 |
| | CHB012NS | Seed | 2.63 | 0.34 | 2.94 | 57.7 | 33.0 | 86 |
| | | Spectrally Matched | 12.05 | 0.30 | 3.38 | 73.1 | 43.5 | 47 |
| | CHB012UD | Seed | 0.62 | 4.88 | 0.21 | 66.0 | 36.3 | 84 |
| | | Spectrally Matched | 4.68 | 4.88 | 0.21 | 69.2 | 40.3 | 89 |

Note:
ATK023 - Japanese Interface Earthquake Record – March 2011
CHB012 - Japanese Interface Earthquake Record – March 2011

**Table 12-4. Record Parameters for Selected Crustal Time Histories – M7.0 -84th Percentile (PGA=0.49)**

| Event Title | Station | | Arias Intensity (m/s) | Predominant Period (sec) | Predominant Freq. (Hz) | Significant Duration (s) | | No. Cycles |
|---|---|---|---|---|---|---|---|---|
| | | | | | | 5–95% | 5–75% | |
| California Loma Prieta (M6.93) 10/18/89 Rrup=9.2km | GIL067 | Seed | 0.90 | 0.37 | 2.68 | 5.0 | 1.6 | 20 |
| | | Spectrally Matched | 1.36 | 0.22 | 4.56 | 5.8 | 2.0 | 30 |
| | GIL337 | Seed | 0.70 | 0.37 | 2.71 | 4.8 | 1.3 | 18 |
| | | Spectrally Matched | 1.34 | 0.45 | 2.23 | 5.5 | 1.8 | 23 |
| | GILUP | Seed | 0.17 | 0.44 | 2.28 | 7.5 | 2.8 | 22 |
| | | Spectrally Matched | 0.71 | 0.30 | 3.38 | 7.1 | 3.3 | 27 |
| Iran Dayhook (M7.1) 09/16/1978 Rrup=13.9km | AUL000 | Seed | 0.06 | 0.59 | 1.69 | 19.0 | 12.7 | 36 |
| | | Spectrally Matched | 3.67 | 0.48 | 2.10 | 19.6 | 13.9 | 35 |
| | AUL270 | Seed | 0.07 | 0.36 | 2.80 | 19.2 | 13.1 | 34 |
| | | Spectrally Matched | 3.47 | 0.32 | 3.15 | 19.9 | 13.6 | 27 |
| | AUL-UP | Seed | 0.02 | 0.44 | 2.28 | 19.3 | 13.1 | 30 |
| | | Spectrally Matched | 1.65 | 0.45 | 2.22 | 19.0 | 13.6 | 30 |
| Italy Irpinia (M6.9) 11/23/1980 Rrup=9.5km | DAYLN | Seed | 1.42 | 0.39 | 2.56 | 12.3 | 6.7 | 35 |
| | | Spectrally Matched | 2.56 | 0.95 | 1.05 | 13.6 | 7.5 | 32 |
| | DAYTR | Seed | 1.36 | 0.43 | 2.31 | 12.4 | 6.9 | 15 |
| | | Spectrally Matched | 2.05 | 0.77 | 1.30 | 11.9 | 6.4 | 24 |
| | DAYUP | Seed | 0.65 | 0.18 | 5.54 | 14.8 | 8.3 | 68 |
| | | Spectrally Matched | 1.93 | 0.18 | 5.55 | 15.2 | 8.9 | 56 |

#### 12.1.4.1. Spectral Matching Approach

Time histories were developed using spectral matching techniques. The spectral matching approach uses a time domain approach (RSPMatch, (Abrahamson N. , 2012)) with the goal of modifying a given time history to be spectrum compatible with a given target spectrum but without any significant modification to the non-stationary characteristic of the original time history.

Spectral matching adjusts the time series in the time domain by adding wavelets to the initial time series. A formal optimization procedure for this type of time domain spectral matching was first proposed by Kaul (1978) and was extended to simultaneously match spectra at multiple damping values by Lilhanand and Tseng (1987); (1988). While this procedure is more complicated than the frequency domain approach, it has good convergence properties and in most cases preserves the non-stationary character of the reference time history.

Several passes were performed using the RSPMatch program until the fit to both the spectral shape and displacement time history were acceptable.

#### 12.1.4.2. Results – Selected Ground Motions

The time histories selected for the intraslab, crustal and interface events are presented in Table 12-1 through Table 12-4. The record properties for the seed and output time history are also summarized in the tables.

The Arias intensity for the crustal events was calculated using empirical correlations developed from the NGA West 1 dataset (N. Abrahamson, personal communication 2014). Equally weighting the five ground motion prediction equations resulted in a median Arias intensity of 0.65 m/s and an 84th percentile Arias intensity of 1.48 m/s. The Arias Intensity for the horizontal components of the spectrally matched crustal time histories range from approximately 1.34 to 3.67 m/s.

The Brookhaven Model (Silva, Abrahamson, Toro, & Costantino, 1996) was used to estimate the significant duration between 5 and 75 percent for each of the four response spectra. The rupture distance was used as input to the Brookhaven Model for the crustal and interface events, and the hypocentral distance was used for the intraslab event (N. Gregor, personal communication, August 29, 2014). The Brookhaven Model was originally developed for crustal events, but has been shown to work adequately for the interface and is the best model available for the intraslab (N. Abrahamson, personal communication 2014). The results are summarized in Table 12-5.

**Table 12-5. Estimate of Significant Duration using the Brookhaven Model**

| Event | Horizontal Duration (5-75%), seconds | | Vertical Duration (5-75%), seconds | |
|---|---|---|---|---|
| | 16th percentile | 84th percentile | 16th percentile | 84th percentile |
| Intraslab $M_w$ 7.5 | 6.7 | 20.9 | 7.8 | 20.4 |
| Intraslab $M_w$ 8.0 | 9.6 | 29.8 | 9.7 | 25.3 |
| Crustal $M_w$ 7.0 | 3.4 | 10.6 | 3.7 | 9.6 |
| Interface $M_w$ 9.2 | 25.6 | 79.3 | 19.7 | 53.3 |

Overall, the durations of both the seed and spectrally matched time histories generally fall within the 16th to 84th percentile predicted by the Brookhaven Model. The exceptions are the vertical interface motion recorded at station AKT023 and both horizontal motions for the M8 intraslab event recorded at station STTEC. The spectrally matched vertical motion at station AKT023 had a higher significant duration of 61.6 seconds (5-75 percent) compared to the 84th percentile from the Brookhaven Model of 53.3 seconds. The spectrally matched horizontals from station GIL crustal motion were 1.4 seconds which are slightly lower than the 16th percentile predicted value of 3.4 seconds. The spectrally matched horizontals from station STTEC intraslab motion were 6.7 seconds and 8.9 seconds which are slightly lower than the 16th percentile predicted value of 9.6 seconds. Both the GIL and STTEC events will need to be revised in subsequent studies.

In Appendix B6 to the Engineering Feasibility Report (MWH, 2014) contains the earthquake records plots. In Figure 1 through Figure 5 show plots of acceleration, velocity, normalized displacement, response spectra, Husid plots, and Fourier amplitude spectra for each time history component before and after spectral matching. Each motion has two horizontal components and one vertical component.

Acceleration, velocity, and normalized displacement are plotted in Appendix B6, Figure 1 in blue (labeled SEED) for the first horizontal component (MWH, 2014). The spectrally matched acceleration, velocity, and normalized displacement time histories are shown in red. The plots of acceleration, velocity, and normalized displacement are overlaid so that they can easily be compared. The purpose of these plots is to confirm that the spectrally matched time history remains similar to the original input motion and that extraneous wavelets are not being added to the motion. Appendix B6, Figure 2 is a plot of the acceleration, velocity, and displacement for the SEED motion and Appendix B6, Figure 3 is the same for the spectrally matched motion.

Appendix B6, Figure 4 illustrates the match to the horizontal design spectrum (black line labeled TARGET), with the recorded motion shown in blue and the spectrally matched motion shown in red. The overall goal of spectral matching is to achieve a fit as close as possible to the design response spectrum. It is important to note that the fit to the lower periods (0.01s to ~0.02s) for

some events has more variability about the target spectrum; this result is limited by the sampling rate of 100-200 samples per second and has little impact on the structure, as most dams are impacted by periods greater than 0.1 seconds.

The Arias normalized intensity (also called a Husid plot) for the initial and spectrally matched acceleration time history is plotted at the top in Appendix B6, Figure 5; the bottom plot in Appendix B6, Figure 5 is the Fourier amplitude spectra. Again, the blue line is the seed or initial motion and the red line is the spectrally matched motion. These plots show that the Arias intensity is not significantly different from the original input motion. The Fourier amplitude spectra plot illustrates that the frequency content was not significantly modified in the frequency range of 0.1 to 10 Hz (period range of 0.1 to 10 seconds).

The same presentation order is followed for each component and motion – acceleration, velocity, and normalized displacement; SEED acceleration, velocity, and displacement; spectrally Matched acceleration, velocity, and displacement; response spectra; and Husid plot (top), Fourier amplitude spectra (bottom).

Twelve sets of three component spectrum compatible time histories were developed: three sets were developed for the intraslab event M8.0-69$^{th}$ percentile, three sets were developed for the intraslab event M7.5-84$^{th}$ percentile, three sets for the M9.2-Interface-84$^{th}$ percentile, and three sets for the crustal M7.0-84$^{th}$ percentile.

#### *12.1.4.3. Time Histories Used in the Analysis*

For the feasibility analysis, one spectrally matched time history was selected from each of the design events (two intraslab, one interface and one crustal). Two events were selected from the intraslab to represent the different magnitude levels, 7.5 or 8.0; as this part of the seismic hazard assessment is still in progress.

In total, four sets of time histories containing three records each have been developed for the slab, interface and crustal events using spectral matching techniques. All of the ground motions are based on the deterministic analyses using a $V_S30$ of 1,100 m/s. The intraslab event utilized two different earthquake records, one was from the El Salvador $M_w$7.6 and the other was from the Japan $M_w$7.0.

For the MCE, the following time histories shown in Table 12-6 have been used:

**Table 12-6. Selected Time Histories for Feasibility Analysis– Intraslab and Crustal**

| | | | |
|---|---|---|---|
| El Salvador (M 7.6) | STTEC | $M_w$ 7.5 – 84$^{th}$ percentile | Intraslab |
| Japan 2011 (M 7.0) | MYG 009 | $M_w$ 8.0 – 69$^{th}$ percentile | Intraslab |
| Loma Prieta, California (M 6.93) | GIL | $M_w$ 7.0 – 84$^{th}$ percentile | Crustal |

Based on comments received from the Board of Consultants to increase the design response spectra, the following response spectra for the interface event in Table 12-7 was also used for the analysis:

**Table 12-7. Selected Time Histories for Feasibility Analysis – Interface**

| | | | |
|---|---|---|---|
| Chile 2010 | CURI | $M_w$ 9.2 – 88$^{th}$ percentile | Interface |

### *12.1.4.3.1. OBE Time History*

For the purposes of the feasibility level design only one event was run for the OBE case. The crustal motion, GIL, was scaled by 0.61 to match the 500 year return period from the Probabilistic Seismic Hazard Analysis. The geometric mean of the horizontal components from the Crustal GIL motion was also computed. Figure 12-1 plots the 500 year return period (OBE), the geometric mean from the GIL horizontal components with a factor of 0.61 applied and the crustal response spectrum scaled to 500 year return period event for comparison.

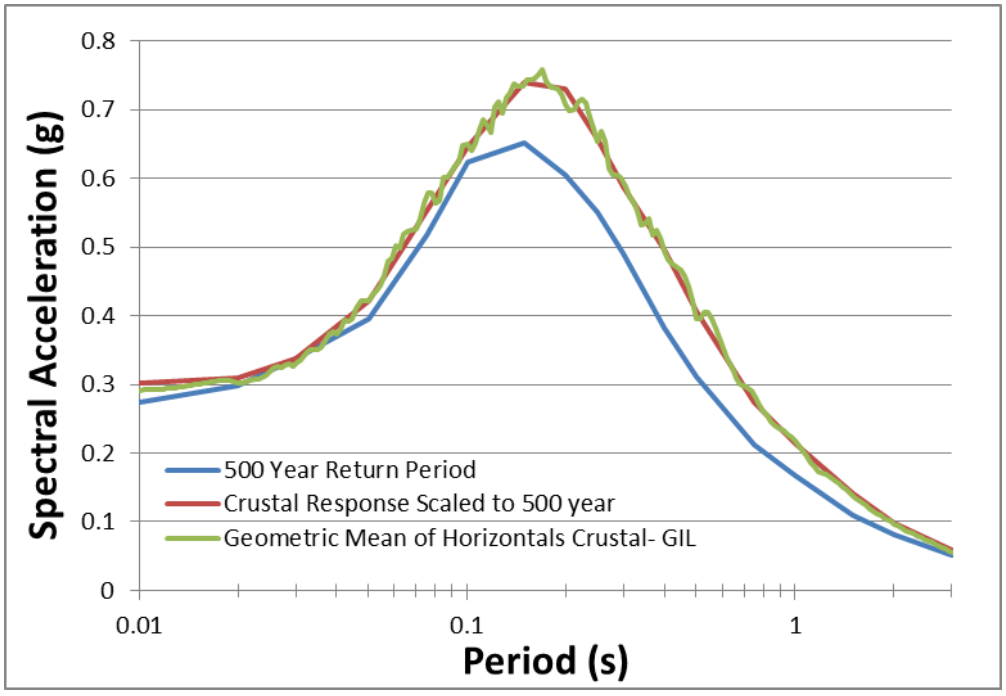


**Figure 12-1. OBE Response Spectra and Scaled Crustal Event**

# 13. ADDITIONAL STUDIES IN PROGRESS

## 13.1. PSHA Sensitivity

A PSHA hazard sensitivity for the intraslab source was computed using the model described in this section (Fugro, 2014a). The ground motion prediction equations (GMPEs) and their weighting were the same as those used in the initial PSHA (Fugro, 2012). A total of 27 results were computed: all combinations of three correlation distances (defined as the width of the spatial smoothing kernel used for the smoothed seismicity) three slab positions, and three Mmaxes. Hazard curves for peak horizontal acceleration (PHA) and 1.0 second spectral acceleration response (5% damping) were computed. These are portrayed for the purpose of comparing the three sets of input parameters to each other, in addition to determining the overall difference in hazard from the initial (2012) results (Fugro, 2012). No weighting of the alternative values were included in this analysis.

In addition, new IMASW site response studies were conducted in the summer of 2013 (Fugro, 2014a), which resulted in a higher $V_S30$ estimate for the site (1080 m/s) than the 800 m/s value used in the initial assessment (Fugro, 2012). The PSHA hazard sensitivity to this higher $V_S30$ value was also evaluated.

## 13.2. PSHA Sensitivity Calculations Conclusions

This study resulted in a more physically realistic geometric model of the downgoing Pacific plate in the vicinity of the site for use in PSHA and ground motion analyses, based on planes fitted to well-located seismicity. These analyses confirm earlier suggestions (e.g. (Ratchkovski & Hansen, 2002) ) that the subducting plate beneath southern and central Alaska consists of several segments or sections with distinctly differing dips and orientations. For each of the geometrically distinct slab sections defined by seismicity, best fit planes with 1σ and 2σ bounding limits were defined to characterize the upper slab surface. For the intraslab section most proximal to the dam site, 1σ and 2σ limits of slab seismicity thickness are 9.0 and 12.3 km, respectively, with dip calculations of 21 and 25 degrees. The +2σ uncertainty for the best fit plane has a closest approach to the dam site of 51 km, and depth beneath the site is 59 km. The best fit plane has a closest approach of 57 km and depth beneath the site of 63 km.

Slab thickness in central Alaska from tomographic studies (Zhao, Christensen, & Pulpan, 1995) is estimated to be 45-55 km, and their slab location indicates that the zone of relatively small-magnitude seismicity shown in this report is occurring near the top of the slab. Using Puget Sound historic Mw 6 slab earthquakes as an analogue, future large intraslab earthquakes beneath the site are likely to stop at the top of the slab, but extend deeper into the slab rather than be

confined to the thin zone of the upper slab based on small magnitude seismicity data that indicates otherwise as shown in this report.

Comparisons to the PSHA results, for this updated intraslab source model show small variations at PHA and 1.0 second spectral acceleration response, indicating that the Wesson et al. (2007) model gives similar results, at least for these response periods, as long as the same Mmax value is used (Fugro, 2012).

The PSHA results indicate negligible sensitivity to the model parameters correlation distance used to develop occurrence rate grids and +/- 2 sigma variations in depth measures from the site to the slab. It is perhaps fortuitous that the Wesson et al. (2007) uniform slab depth of 60 km is very close to the distance from the site to the more refined slab model presented here. The results are also relatively insensitive to a change in $V_S30$ to 1080 m/s (Fugro, 2014b)from the 800 m/s used previously (Fugro, 2012).

Hazard variations due to Mmax choices of 7.8 and 8.1 are significant. Sensitivity of the new intraslab source model to the three Mmax estimates are shown in Figure 13-1 and Figure 13-2. A $V_S30$ of 800 m/s (Fugro, 2012) was used in this comparison. The first observation is that hazard curves are close to the 2012 results, indicating that the Wesson et al. (2007) geometric slab model gives similar results for this site and these response periods, for a Mmax of 7.5. The second observation is that the results are very sensitive to choice of Mmax. For PHA, at a 1/10,000 annual frequency of exceedance (AFE) the ground motion increases from about 0.8 to 1.2 g as Mmax increases from M7.5 to M8.1, an increase of 50% in ground motion. For 1.0 second response the increase is comparable.

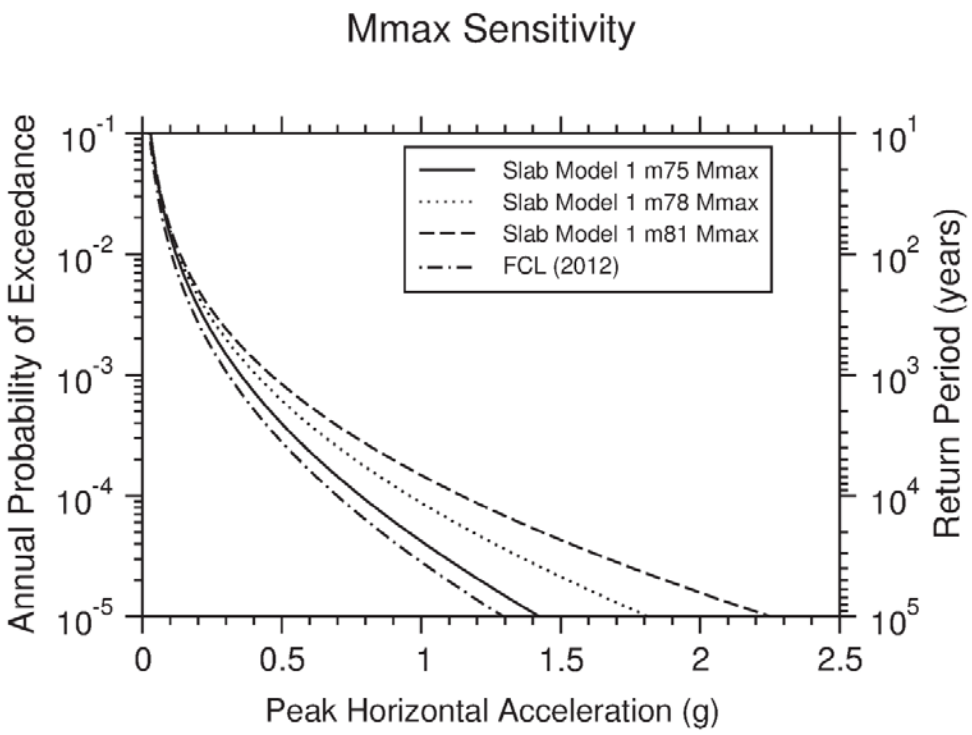


Figure 13-1. Mmax Sensitivity for Peak Ground Acceleration

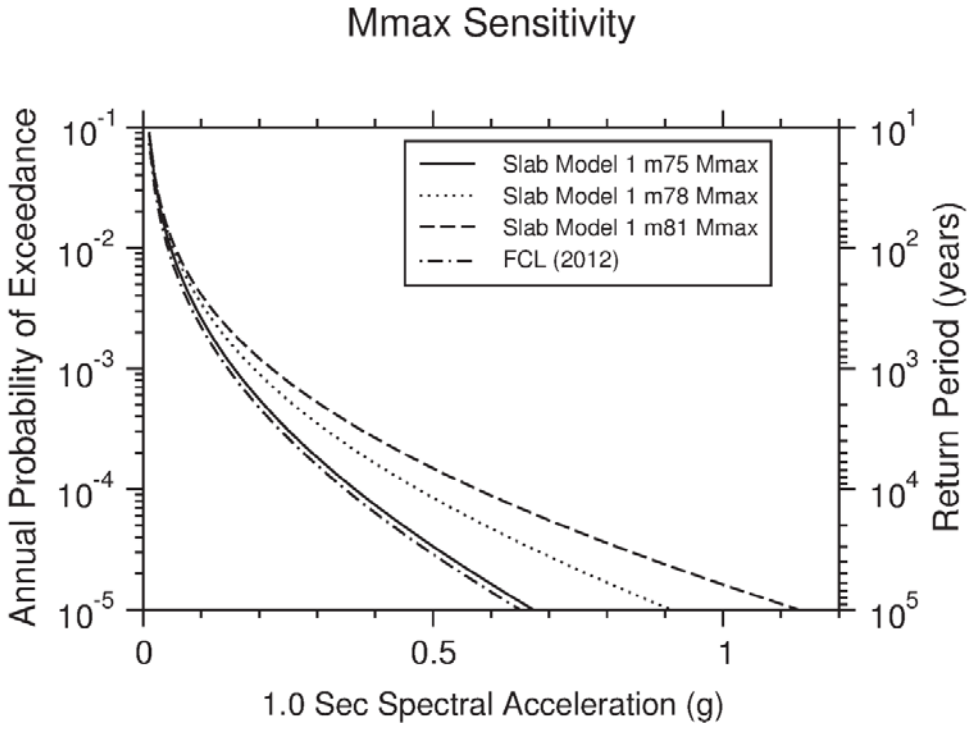


Figure 13-2. Mmax Sensitivity for 1.0 s Spectral Acceleration

In contrast, changes in the slab position, correlation distance, and $V_S30$ do not appreciably alter the PSHA hazard results. Specifically, sensitivity analysis of the PSHA hazard results to the three slab positions for the new model shows that there is essentially no sensitivity to this parameter in the computed PSHA hazard when Mmax was set to 7.5, and correlation distance to 25 km. Similarly, sensitivity of the PSHA hazard results to the three correlation distances for the new model shows that there is negligible sensitivity to this parameter when Mmax was set to 7.5, and slab depth to the mean position. In the case of $V_S30$, sensitivity of the PSHA hazard results showed very little change when an Mmax of 7.5, a correlation distance of 25 km, and the mean slab depths were used with site characterization inputs of $V_S30$ = 800 m/s as compared to use of $V_S30$= 1080 m/s.

For the two response periods, at a 10,000 year return period, ground motion increases of about 25% and 50% are indicated, respectively. However, due to the paucity of ground motion records for magnitudes above 7.5, magnitude scaling of ground motions in the GMPEs above Mw 7.5 is highly uncertain, and warrants further investigation.

# 14. OTHER EARTHQUAKE RELATED HAZARDS

## 14.1. Reservoir Triggered Seismicity

Reservoir-triggered seismicity has been described as earthquake events that are triggered by the filling of a reservoir, or by water-level changes or fluctuations during operation of the reservoir. It is believed that reservoir triggered seismicity (RTS) primarily represents the release of pre-existing tectonic strain, with the reservoir being a perturbing influence ( (Yeats et al, 1997); (US Committee on Large Dams (USCOLD), 1997); (ICOLD, 2011) ). Thus, the reservoir does not cause or induce the seismicity, it merely triggers the release of the accumulated, naturally occurring tectonic strain that already existed.

The potential for reservoir triggered seismicity (RTS) to occur during and after filling of the reservoir has been evaluated. An assessment of the potential for the future occurrence of RTS to occur in the vicinity of the proposed reservoir was made expanding upon the earlier study prepared by Woodward Clyde Consultants in the 1980s (Woodward-Clyde Consultants (WCC), 1980). The preliminary assessment and analysis of RTS is a work in progress as additional background information from the seismic hazard studies (see Section 9.3) and long-term earthquake monitoring data (see Section 2.5) are essential to this study.

The attributes that were considered in evaluating the probability of RTS include reservoir depth; reservoir volume; the tectonic stress state; and the rock type and structure underlying the reservoir. The probabilities that are considered are conditional and represent the total chance for RTS to occur as a result of reservoir filling and operation. Conditional probabilities were also developed for each attribute, as well as for all attributes combined. For the multi-attribute analysis, each attribute is considered independently and also in a discrete-dependent model focusing on depth and volume.

Additionally, a literature review, case study, and numerical analysis was performed of RTS based on other projects with large, deep reservoirs in order to develop an understanding of the potential of RTS at the Susitna-Watana site.

Data from the long-term earthquake monitoring system provides a baseline of the rates and seismological characteristics of local seismic events prior to the impoundment of the reservoir. Seismicity data collected as part of the long-term monitoring system data collection was used to perform seismological analyses to help define local seismotectonic characteristics. Such analyses include development of local velocity models, focal mechanism and regional stress analysis, analysis of spatial patterns, and relationship of seismicity to reservoir operation. The preliminary study will account for possible RTS earthquakes in the development of seismic design parameters.

At reservoirs where RTS has been suspected, the maximum reported earthquake magnitudes for RTS events are primarily less than M 6.0, and typically less than M 4.0, and often below the range felt by the public.

The most significant aspect of the RTS record is that of the verified RTS cases large enough to be potentially damaging. Of recorded instances of RTS, just four events have exceeded M 6.0 and only 13 events were in the range M 5.0 to M 5.9 ( (US Committee on Large Dams (USCOLD), 1997); (Yeats et al, 1997)). The largest reported RTS earthquake was the 1967, magnitude M 6.5, Koyna, India event. The other three events were Hsinfengkiang (China 1962) M 6.1, Kariba (Zambia 1963) M 6.0, and Kremasta (Greece 1966) M 6.3.

For this Project, the reservoir depth, reservoir volume, existing tectonic stress state, rock type underlying the reservoir, and the rate of filling were considered when evaluating the probability of RTS. The Project reservoir will have characteristics that might make it somewhat susceptible to RTS, in that the maximum reservoir depth is greater than 575 ft. (175 meters), and it is within an active tectonic region.

As described above, the Talkeetna Block is bordered by the Denali Fault to the north, and the Castle Mountain Fault to the south, and the Wadati-Benioff Zone (Intraslab) lies at a depth of approximately 50 km below the site based upon the focal depth of recent earthquakes. These distant sources do not lie within the zone potentially influenced by reservoir filling, and thus RTS is unlikely to occur on them.

Studies performed in the 1980s estimated the probability of RTS for the Project to be between 30 percent and 95 percent, with an event up to M 6.0 (Woodward Clyde Consultants (WCC), 1982). Recalculations performed during the present studies indicate that the reservoir has a potential for producing an RTS event up to M 6.5, but the probability of an RTS event is between 16 to 46 percent. Any event would most likely occur within 10 years of initial filling.

RTS has been considered in the derivation of the seismic design parameters for the Project, and will be further updated during detailed design. However, triggered seismicity requires the presence of a causative fault. A seismic hazard assessment requires that all faults be identified; hence, any fault identified during the seismic hazard assessment would likely cover those with the potential for RTS.

For completeness the present studies have also considered the potential effects of RTS on the nearest populated area, the town of Talkeetna, which is about 62 miles (100 km) from the site. Using the RTS event of M 6.5 and GMPE, deterministic methods were used to estimate the peak ground accelerations (PGA). The calculation estimates a PGA in Talkeetna of 0.02g for the

median and 0.04g for the 84th percentile (+1 standard deviation). The inputs to calculate this hypothetical event are shown in Table 14-1.

**Table 14-1. Deterministic Input Parameters**

| CASE | Crustal |
|---|---|
| Magnitude | 6.5 |
| $R_{RUP}$ (km) | 100 ($R_{JB}$=100) |
| $V_S30$ (m/s) | 760 |
| Type of faulting | Strike-slip |
| Dip (degrees) | 90 |
| Seismogenic Depth (km) | 20 |
| Width (km) | 20 |
| PGA(g) [percentile] | 0.02[50th]<br>0.04[84th] |
| Ground Motion Prediction Equation [weight] | BA08 [0.25]<br>CY08 [0.25]<br>CB08 [0.25]<br>AS08 [0.25] |

Acronyms:
BA08= Boore and Atkinson 2008 (Boore & Atkinson, 2008)
CY08=Chiou and Youngs 2008; (Chiou & Youngs, 2008)
CB08=Campbell and Borzorgnia 2008 (Campbell & Bozorgnia, 2008)
AS08=Abrahamson and Silva 2008 (Abrahamson & Silva, 2008)

For comparison, the Shake Map for the 2002 Denali earthquake (Figure 14-1; USGS) was reviewed and indicates the peak ground acceleration in Talkeetna were light and ranged between about 0.09g to 0.18g. Based on the above analysis it is considered that the maximum RTS event would expose the nearest town of Talkeetna to ground shaking substantially less than that experienced during the 2002 Denali event.

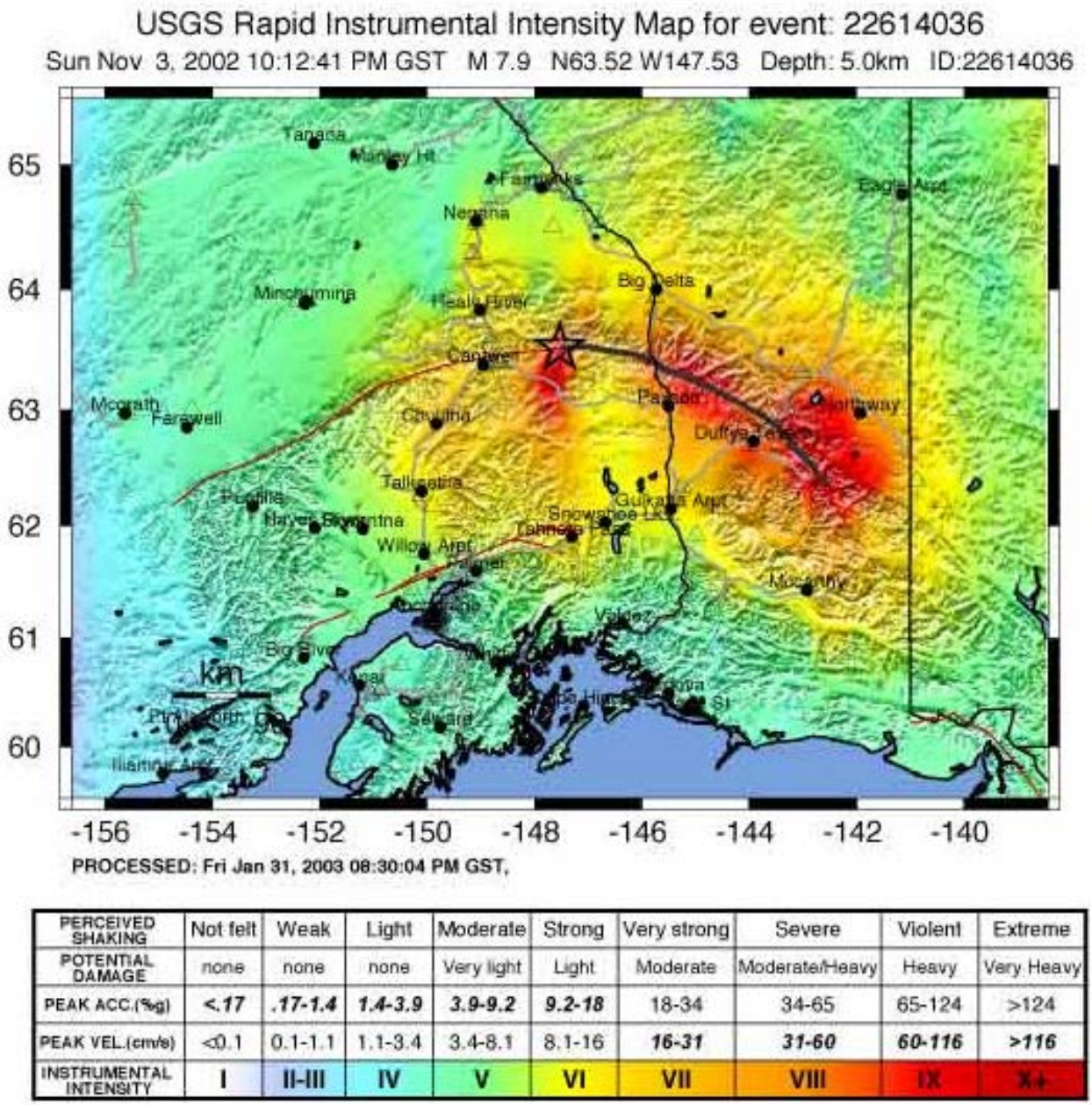


| PERCEIVED SHAKING | Not felt | Weak | Light | Moderate | Strong | Very strong | Severe | Violent | Extreme |
|---|---|---|---|---|---|---|---|---|---|
| POTENTIAL DAMAGE | none | none | none | Very light | Light | Moderate | Moderate/Heavy | Heavy | Very Heavy |
| PEAK ACC.(%g) | *<.17* | *.17-1.4* | *1.4-3.9* | *3.9-9.2* | *9.2-18* | 18-34 | 34-65 | 65-124 | >124 |
| PEAK VEL.(cm/s) | <0.1 | 0.1-1.1 | 1.1-3.4 | 3.4-8.1 | 8.1-16 | *16-31* | *31-60* | *60-116* | *>116* |
| INSTRUMENTAL INTENSITY | I | II-III | IV | V | VI | VII | VIII | IX | X+ |

**Figure 14-1. USGS Shake Map for 2002 Denali Earthquake (USGS)**

### 14.1.1. Summary

The location and magnitude of any future RTS event associated with the Watana Reservoir are highly uncertain. However, empirical data suggest that most RTS events will have relatively small magnitudes and would most likely occur within 10 years of initial reservoir filling. From these types of observations, ICOLD (2011) and Allen (1982) suggest that maximum RTS

magnitudes may be on the order of 6.3 and 6.5, respectively. Others (USGS) have suggested potentially a higher magnitude.

A more quantitative evaluation would require information on the fracture characteristics of reservoir bedrock (density, orientation, length, etc.); more information on the state of stress with respect to the orientation of existing fractures, as informed by local earthquake focal mechanisms; and utilize a Mohr Coulomb approach to evaluating changes in crustal stress associated with reservoir filling.

Additional details regarding RTS can be found in the technical memorandum on Preliminary Reservoir Triggered Seismicity (MWH, 2013a).

## 14.2. Seismic Induced Landslide Potential

The consideration of seismically induced landslide hazard within the reservoir relates to the potential for a large slide to occur and generate an impulse wave with the potential to overtop the dam, and is considered to be very low, as wave generation of such a scale requires both a large volume of material at, above, or within the reservoir, and rapid failure. For this to occur, a very high, steep slope, with a potentially unstable block of large volume would need to exist adjacent to or within the reservoir. High steep slopes above the reservoir are not present downstream of PRM 200, approximately 16 miles upstream of the dam site. Upstream of PRM 200, large active or historical landslides with the potential volume of material required to generate a large wave were not observed. Upstream of approximately PRM 214, or about 30 miles upstream of the dam site, the reservoir will be relatively shallow, narrow, and meandering within the confines of the incised river valley. Waves generated by large slope movements along this reach would displace significantly less water, and likely dissipate much of its energy before reaching the dam. Additionally, most observed slope movements in the area are typically of small volume, and occur as somewhat slower moving flows, which would not generate large impulse waves.

Submerged slopes comprised of fine grained sand and coarse silt materials may be prone to liquefaction during earthquakes. Although these soil materials are not extensive in the reservoir, liquefaction would likely be associated with shallow slides or individual slides of limited aerial extent. In addition, with reservoir impoundment, some sloughing and shallow slides will occur as the slopes adjust to the higher groundwater table, fluctuating reservoir levels, and thawing of permafrost.

There exists a potential failure mechanism whereby a seismically induced landslide blocks the river upstream of the reservoir, interrupting the flow of the river until the landslide debris is overtopped and fails. However, examination of the river basin upstream of the reservoir indicates few locations where significant blocking could occur, and in the event of a major

seismic event, it would be important for any such blockage to be quickly breached to prevent a damaging discharge.

No geomorphic evidence was found to indicate that large-scale, rapid movement landslides or slope failures, either alone or in aggregate, that would cause a significant environmental or operational impact post-impoundment of the reservoir to the Project. Additional details regarding the reservoir slope stability can be found in the technical memorandum on Preliminary Reservoir Slope Stability Assessment (MWH, 2014b)

# 15. CONCLUSIONS AND RECOMMENDATIONS

This report presents the activities undertaken to quantify the seismic hazard at the proposed - Watana Dam site. The results of several studies were used to compile this overall summary report.

***Seismic Hazard***

The preliminary PSHA and seismic source model considers several seismogenic and potentially seismogenic structures. These are: subduction-related sources (plate interface [megathrust], and plate intraslab), the Denali fault, Castle Mountain fault, Pass Creek-Dutch Creek fault, Sonona Creek fault, zones of distributed deformation north and south of the Denali fault, and Talkeetna block structures (Fog Lake graben).

Four critical seismic sources are identified: (1) Subduction interface, (2) Intraslab, (3) Denali fault, and, (4) Fog Lake graben. A deterministic evaluation for the southern Alaskan block (SAB) central zone seismic source zone is derived from the 10,000-yr return period deaggregation results from the PSHA.

In the current study, the deterministic evaluation finds that the intraslab source produces the largest peak ground acceleration (PGA) at the site. The deterministic evaluation indicates that the largest values of ground motions at the site are associated with the subduction interface and intraslab sources, because of their large magnitude, relatively short distance, and GMPEs used for these sources. The deterministic results for the crustal sources (e.g. Denali fault, Fog Lakes graben, Castle Mountain fault, and 10,000-year crustal seismicity) indicate that these sources are relatively less significant, as compared to subduction megathrust and intraslab seismic sources.

The results of detailed evaluations of new imagery data, evaluations of local and regional scale mapping, and field investigations did not identify any specific features with evidence of late Quaternary faulting within at least 40 km (~25 mi) of the Watana dam site. For most of this area, the time and detection limits of the imagery and field investigations imply post-glacial time limits of about 12,000 to 15,000 years, and detection of surface offsets of more than about 1 m extending over several kilometers.

For the area near Watana dam site where detailed LiDAR data was the basis for this evaluation, potential detection limits of surface fault displacements are much lower (about 0.5 m over several hundred meters). This is consistent with the observations that the dam area is structurally coherent with lack of pervasive penetrative deformation. Further, these data strongly suggest that potential sources of primary or secondary, surface fault rupture at the dam site are absent.

Geomorphic evaluations based on the detailed LiDAR data within the dam site area have not identified any expression or continuity of potential faults or specific geologic features extending from the site area that would be indicative of deformation of Quaternary deposits. This indicates that although shear features may be present in the foundation, there is evidence to support a lack of surface displacement along these features in the last 12,000 to 15,000 years. Furthermore, the potential for any reactivation of the geologic features that might transect the dam footprint must be considered extremely low given the following:

- The apparent lack of continuity and small scale of structural geologic features at the site (shear zones) upon which surface fault rupture could conceivably take place;
- The dominant northwest-southeast trend of geologic features is unfavorably oriented with respect to the contemporary tectonic stress regime, as the primary mode of tectonic deformation appear to involve right-lateral strike slip structures with east-northeast strikes;
- The absence of any nearby crustal scale fault structures and any neotectonic or paleoseismic evidence of Quaternary faulting; and,
- The absence of Quaternary faults mapped with about 15 mi of the dam site

Shallow crustal deformation in the nearby region of Watana dam site appears to be characterized by near-horizontal maximum compressive stresses oriented northwest-southeast, based on nearby GPS vectors and earthquake focal mechanisms. Strain ellipse deformation concepts suggest that the likelihood of reactivating northwest-oriented features under existing conditions is low because of their near parallelism with compressive stress. Additional analysis would be needed to evaluate if and how these features might respond to reservoir loading, fully-loaded reservoir conditions, or fluctuating reservoir conditions.

With the installation of the Susitna-Watana Seismic Network, the seismic station density in the region has increased. This has led to greater magnitude detection capabilities, a decrease in magnitude of completeness, and greater location accuracy.

Focal mechanisms produced by the AEC in the Susitna-Watana project area indicate that the crust around the proposed dam site is undergoing north-northwest south-southeast horizontal compression, consistent with the relative Pacific – North America plate motion, with the maximum horizontal stress rotating in a counterclockwise direction from east to west in the network area. This appears to be consistent with what is known about the seismotectonic regime in the project area (Haeussler, Saltus, Karl, & Ruppert, 2008).

The seismicity analyses confirm earlier suggestions (e.g. (Ratchkovski, Wiemer, & Hansen, 2004)) that the subducting plate beneath southern and central Alaska consists of several segments or sections with distinctly differing dips and orientations.

Source deaggregation plots are developed, one for each of the four spectral response periods (PHA, 0.5 sec, 1.0 sec, 3.0 sec). Only sources contributing 5% or more at any ground motion level are plotted on the de-aggregations. The peak horizontal acceleration (PHA) hazard is dominated by the Alaskan subduction zone intraslab source at all return periods.

Sensitivity studies indicate hazard variations due to Mmax choices of 7.8 and 8.1 are significant. For the two response periods, at a 10,000 year return period, ground motion increases of about 25% and 50% are indicated, respectively. However, due to the paucity of ground motion records for magnitudes above 7.5, magnitude scaling of ground motions in the GMPEs above Mw 7.5 is highly uncertain, and warrants further investigation.

Preliminary investigations into historical occurrence of the largest earthquake magnitudes for worldwide subduction zones indicate that an upper bound value for future slab Mmax distributions used in the final PSHA analysis is likely to lie above 7.5.

For final PSHA hazard calculations at the Watana dam site, further evaluation of the ASZ and worldwide subduction zone data will need to be conducted to develop appropriate weighting of uncertain parameters such as Mmax. The present evaluations confirm that the Mmax value of Mw 7.5 used in the preliminary PSHA analyses must likely be considered a minimum estimate for a Mmax distribution. Further evaluations are needed to assess the full range and weights for larger Mmax estimates and to develop a basis for estimation of an appropriate characterization of Mmax for the intraslab source for use in deterministic evaluations.

Ongoing study results such as the seismic network data readings, updates to the GMPEs, and subduction zone intraslab source characterization, will (when completed) provide additional information and should be incorporated into this report. In the interim a deterministic approach was followed and design response spectra were recommended as follows:

***MCE***

- Interface 88$^{th}$ percentile, M9.2 at a rupture distance of 78 km, PGA=0.58g
- Intraslab 84$^{th}$ percentile, M7.5 at a hypocentral distance of 50km, PGA=0.69g
- Intraslab 69$^{th}$ percentile M8.0 at a hypocentral distance of 50km, PGA=0.81g
- Crustal 84$^{th}$ percentile M7.0 at a rupture distance of 3.5km, PGA=0.49g

***OBE***

The development of the OBE followed a probabilistic approach and was assigned a return period of 500 years, which has resulted in a projected PGA of 0.27g.

In addition to the seismic design criteria regarding earthquake events, other earthquake related hazards such as fault rupture in the immediate vicinity of the dam; slope stability at the dam site and within the project boundary; and RTS have been addressed.

Based on the lineament studies and the structural geological mapping – particularly of features that transect the dam foundation - it is considered that the crustal stress pattern and feature characteristics are not conducive to co-seismic movement on existing identified features in the foundation or in the immediate area of the dam.

The potential for a large slide to occur and generate an impulse wave with the likelihood of overtopping the dam is generally considered to be very low. RTS has been considered in the derivation of the seismic design parameters for the Project, and will be further updated. However, reservoir triggered seismicity requires the presence of a causative fault. A seismic hazard assessment requires that all faults be identified; hence, any fault identified during the seismic hazard assessment would likely cover those with the potential for RTS. In addition, the Susitna-Watana micro seismic network will provide a baseline for RTS.

## 15.1. Recommendations to Update Existing Reports and Advance Studies

The seismic hazard analysis (Fugro, 2012) and RTS assessment (MWH, 2013a) should be updated with the results of the crustal seismic source assessment and use of most recent GMPEs. The source characterization for the intraslab should be refined to establish a Mmax and associated weighting, as the seismic hazard results are very sensitive to this parameter. Another factor specific to the intraslab is that the dam site lies above the McKinley Block which may be detached and moving independently placing limits on the available physical volume and in turn limiting the maximum size earthquake it can support. The seismic hazard analysis (Fugro, 2012) should also include these updates to the interface characterization.

Additional field work could improve preliminary studies, such as the crustal seismic source evaluation by expanding the exposures of rock conditions across the foundation footprint. A shear wave velocity study based on the alignment of the dam should be performed to refine the input $V_S30$ parameter used in the ground motion calculations for the seismic hazard analysis.

The ongoing monitoring of the Susitna-Watana network should be continued to help clarify the recurrence relationships, subduction zone geometry, stress field, and the background seismic level to help judge RTS during reservoir filling.

# 16. REFERENCES

Abrahamson, N. 2012. RSP Match 2012.

Abrahamson, N., & Silva, W. 2008. Summary of the Abrahamson & Silva NGA ground-motion relations. *Earthquake Spectra. Vol. 24. No. 1.* p. 67-97.

Acres. 1982a. Susitna Hydroelectric Project: 1980-1981 Geotechnical Report, Volume 1. Prepared for the Alaska Power Authority Volumes 1-3.

Acres. 1982b. 1982 Supplement to the 1980-1981 Geotechnical Report Vol. 2 for Susitna Hydroelectric Project. 288 p.

Acres. (1982c). Susitna Hydroelectric Project Feasibility Report. Prepared for the Alaska Powere Authority. Volumes 1 and 2.

AEC. 2014. *Susitna-Watana Seismic Monitoring Project : January –June 2015 Report. Prepared for the Alaska Energy Authority. September 2015.* 34p.

Alaska Energy Authority (AEA). (2012). Revised Study Plan: Susitna-Watana Hydroelectric Project FERC Project No. 14241. December 2012. *Prepared for the Federal Energy Regulatory Commission by the Alaska Energy Authority, Anchorage, Alaska.*, http://www.susitna-watanahydro.org/study-plan.

Allen, C. (1982). Reservoir-induced seismicity and public policy, California Geology, November. 248-250.

Atkinson, G., & Boore, D. (2003). Empirical ground-motion relations for subduction-zone earthquakes and their application to Cascadia and other regions. *Bulletin of the Seismological Society of America, Vol. 93*, p. 1703-1729.

Atkinson, G., & Macias, M. (2009). Predicted Ground Motions for Great Interface Earthquakes in the Cascadia Subduction Zone. *Bulletin of the Seismological Society of America, Vol. 96*, p. 1552-1578.

Bazzurro, P., & Cornell, C. (1999). Disaggregation of Seismic Hazard. *Bulletin of Seismological Society of America, Vol. 89, No. 2, April*, p. 501-520.

Bemis, S. (2010). Moletrack scarps to mountains: Quaternary tectonics of the central Alaska Range [Ph.D. dissertation]: University of Oregon. 121 p.

Bemis, S. P., & Wallace, W. (2007). Neotectonic framework of the north-central Alaska Range foothills, in Tectonic Growth of a Collisional Continental Margin: Crustal Evolution of Southern Alaska, Geol. Soc. Am. Spec. Pap., vol. 431. (pp. 549-572). Boulder, Colo.: edited by K. D. Ridgway et aI.

Bemis, S., Wldon, R., & Carver, G. (2015). *Slip Partioning Along a Continuously Curved Fault: Quaternary Geologic Controls on Denali Fault System Slip Partitioning, Grown of the Alaska Range, and the Tectonics of South-Central Alaska Lithosphere.*

Biggs, J., Wright, T., Lu, Z., & Parsons, B. (2007). Multi-interferogram method for measuring interseismic deformation—Denali fault. *Alaska: Geophysical Journal International, Vol. 170*, p. 1,165–1,179.

Boore, D. M., & Atkinson, G. M. (2008). round-Motion Prediction Equations for the Average Horizontal Component of PGA, PGV, and 5%-Damped PSA at Spectral Periods between 0.01 s and 10.0 s. *Earthquake Spectra, Vol. 24, no. 1*, p. 99-138.

Brocher, T. M., Fuis, G., Fisher, M., Plafker, G., Moses, M., Taber, J. J., et al. (1994). Mapping the megathrust beneath the northern Gulf of Alaska using wide-angle seismic data. *J. Geophys. Res., 99(B6), 11, 663-11*, 685.

Brocher, T., Filson, J., Fuis, G., Haeussler, P., Holzer, T., Plafker, G., et al. (2014). The 1964 Great Alaska Earthquake and Tsunamis—A Modern Perspective and Enduring Legacies. *U.S.. Geological Survery Fact Sheet 2014-3018, March 2014* , Available from http://pubs.usgs.gov/fs/2014/3018/.

Campbell, K., & Bozorgnia, Y. (2008). NGA ground motion model for the geometric mean component of PGA, PGV, PGD, and 5% damped linear elastic damped response spectra for periods ranging from 0.01 s to 10 s. *Earthquake Spectra, Vol. 24, n. 1*, p. 139-171.

Carver, G., & Plafker, G. (2008). Paleoseismicity and neotectonics of the Aleutian Subduction Zone - An overview, in Freymueller, J.T., Haeussler, P.J., Wesson, R.L., and Ekstrom, Goran, eds. *Active Tectonics and Seismic Potential of Alaska: American Geophysical Union, Geophysical Monograph 179*, p. 83-108.

Carver, G., Bemis, S., Solie, D., Castonguay, S., & and Obermiller, K. (2010). Active and potentially active faults in or near the Alaska Highway corridor, Dot Lake to Tetlin Junction, Alaska: Alaska Division of Geological & Geophysical Surveys Preliminary Interpretive Report. 42p.

Carver, G., Plafker, G., Met, M., Cluff, L., Slemmons, B., Johnson, E., et al. (2004). Surface Rupture on the Denali Fault Interpreted from Tree Damage during the 1912 Delta River Mw 7.2-7.4 Earthquake: Implications for the 2002 Denali Fault Earthquake Slip Distribution. In *Bulletin of the Seismological Society of America 94(6B)* (pp. S58 - S71).

Chiou, B., & Youngs, R. (2008). An NGA model for the average horizontal component of peak ground motion and response spectra. *Earthquake Spectra, Vol. 24, n. 1*, p. 173-215.

Christensen, D., & Beck, S. (1994). The rupture process and tectonic implications of the great 1964 Prince William Sound earthquake. *Pure and Applied Geophysics, Vol. 142*, p. 29-53.

Clautice, K. (1990). Geologic Map of the Valdez Creek Mining District: Alaska Division of Geological & Geophysical Surveys Public Data File. 1 sheet, scale 1:250,000.

Cole, R., Layer, P., Hooks, B. C., & and Turner, J. (2007). Magmatism and deformation in a terrane suture zone south of the Denali fault, northern Talkeetna Mountains, Alaska in Ridgway, K.D., Trop, J.M., Glen, J.M.G., and O'Neill, J.M. eds. *Tectonic Growth of a Collisional Continental Margin: Crustal Evolution of Southern Alaska: Geological Society of America Special Paper 431*, p. 477-506.

Cornell, C. (1968). Engineering seismic risk analysis. *Bulletin of the Seismological Society of America, Vol. 58*, p. 1583-1606.

Crone, A., Personius, S., Craw, P., Haeussler, P., & Staft, L. (2004). The Susitna Glacier thrust fault—Characteristics of surface ruptures on the fault that initiated the 2002 Denali Fault earthquake. *Bulletin of the Seismological Society of America, Vol. 94, no. 6, part B*, 5-22.

Csejtey, B. J., Cox, D., Evarts, R., Stricker, G., & and Foster, H. (1982). The Cenozoic Denali fault system and the Cretaceous accretionary development of southern Alaska. *Journal of Geophysical Research, v. 87 no. B5*, p. 3741–3754.

Csejtey, B., Mullen, M.W., Cox, D., & Stricker, G. (1992). Geology and geochronology of the Healy quadrangle, south-central Alaska. *U.S. Geological Survey Miscellaneous Investigations Series* .

Csejtey, B., Nelson, W., Jones, D., Silberling, N., Dean, R., Morris, M., et al. (1978). Reconnaissance geologic map and geochronology, Talkeetna Mountains quadrangle, northern part of Anchorage quadrangle, and southwest corner of Healy Quadrangle, Alaska. *U.S. Geological Survey Open File Report 78-558-A*, 62 p., 1 plate.

Demets, C., & Dixon, T. (1999). New kinematic models for Pacific-North America motions from 3 Ma to present, 1: Evidence for steady motion and biases in the NUVEL-1A model. *Geophysical Research Letters, Vol. 26*, p. 1921-1924.

Detterman, R. L., Plafker, G., Russell, G. T., & Hudson, T. (1976). Features along part of theTalkeetna segment of the Castle Mountain-Caribou fault system, Alaska. *U.S. Geol. Surv. MF Map 738*, 1 sheet.

Detterman, R., Plafker, G., Hudson, T., Tysdal, R., & Pavoni, N. (1974). Surface geology and Holocene breaks along the Susitna segment of the Castle Mountain fault, Alaska. *U.S. Geological Survey Miscellaneous Field Studies Map MF-618*, 1 sheet, scale 1:63,360.

Doser, D. I. (2004). Seismicity of the Denali-Totschunda fault zone in central Alaska (1912-2008) and its relation to the 2002 Denali fault earthquake sequence. *Bull. Seismol. Soc. Am., 94(6B)*, S132-S144.

Doser, D., Veilleux, A., & Velasquez, M. (1999). Seismicity of the Prince William Sound Region for Thirty-two years following the 1964 Great Alaskan Earthquake. *Pure and Applied Geop., Vol. 154,*, p. 593-632.

Doser, D., W.A., B., & Velasquez, M. (2002). Seismicity of the Kodiak Island region (1964-2001) and its relation to the 1964 great Alaska earthquake. *Bull. Seismol. Soc. Am. Vol. 92, no. 8*, p. 3269-3292.

Eberhart-Phillips, D., Haeussler, P., Freymueller, J., Frankel, A., Rubin, C., Craw, P., et al. (2003). The 2002 Denali fault earthquake, Alaska: A large magnitude, slip-partitioned event. *Science*(300 (5622)), pp. 1113-1118.

FEMA. (2005). *Federal Guidelines for Dam Safety: Earthquake Analyses and Design of Dams.* NDSRB.

FERC. (2011). *Engineering guidelines for the evaluation of hydropower projects*. Retrieved October 6, 2011, from Federal Energy Regulatory Commission: http://www.ferc.gov/industries/hydropower/safety/guidelines/eng-guide/chap13-draft.asp

Fletcher, H. (2002). Crustal deformation in Alaska measured using the Global Positioning System Fairbanks, Alaska, University of Alaska Fairbanks, Ph.D. dissertation. 135 p.

Flores, C. F., & Doser, D. (2005). Shallow seismicity of the Anchorage, Alaska region (1964–1999). *Bull. Seism. Soc. Am. 95*, p. 1865-1879.

Frankel, A. D. (1995). Mapping seismic hazard in the Central and Eastern United States. *Seismological Research Letters, Vol. 66, no. 4*, p.8-21.

Frankel, A., Mueller, C., Barnhard, T., Perkins, D., Leyendecker, E., Dickman, N., et al. (1996). National seismic-hazard maps: documentation June 1996. *U.S. Geological Survey Open-File Report 96-532*.

Freymuller, J. W., Cohen, S., Cross, R., Elliot, J., Larsen, C., Hreinsdottir, S., et al. (2008). Active deformation processes in Alaska, based on 15 years of GPS measurements. *ctive Tectonics and Seismic Potential of Alaska, Geophyscial Monograph Series 170*.

Fuchs, W. (1980). *Tertiary tectonic history of the Castle Mountain–Caribou fault system in the Talkeetna Mountains.* Alaska: Salt Lake City, University of Utah, Department of Geology and Geophysics. Ph.D. dissertation.

Fugro Consultants, Inc. (FCL). (2013). Lineament Mapping and Analysis for the Susitna-Watana Dam Site. *Report to the Alaska Energy Authority, Technical Memorandum No. 8*, Dated March 27, 2013, 61 pages plus figures, plates, and 1 appendix.

Fugro Consultants, Inc. (FCL). (2014a). Watana Seismic Network Station Vs30 Measurements for the Susitna-Watana Dam Site. *Report prepared for Alaska Energy Authority, Technical Memorandum No. 14-12-TM*, Dated March 20, 2014, 51 pages and 1 appendix.

Fugro Consultants, Inc. (FLC). (2012). Seismic Hazard Characterization and Ground Motion Analyses for the Susitna-Watana Dam Site Area. *Report prepared for Alaska Energy Authority, Seismic Studies Technical Memorandum No. 4*, Dated February 24, 2012, 146 pages and 4 Appendices.

Fugro Consultants, Inc., (FCL). (2014b). Revised Intraslab Model and PSHA Sensitivity Results for the Susitna-Watana Dam Site Area. *Report prepared for Alaska Energy Authority, Seismic Studies Technical Memorandum No. 14-11TM*, Dated April 25, 2014, 31 pages.

Fugro Consultants, Inc., (FCL). (2015a). Crustal Seismic Source Evaluation for the Susitna-Watana Dam Site. *Report prepared for Alaska Energy Authority, Report No. 14-33-REP*, Dated May 2015, 141 pages and 3 appendices.

Fugro Consultants, Inc., (FCL). (2015b). Seismic Network 2014 Annual Seismicity Report for the Susitna-Watana Dam Site Area. *Report prepared for Alaska Energy Authority, Report No. 14-32-REP*, Dated March 31, 2015, 55 pages.

Fuis, G., Moore, T., Plafker, G., Brocher, T., Fisher, M., Mooney, W., et al. (2008). Trans-Alaska Crustal Transect and continental evolution involving subduction underplating and synchronous foreland thrusting. *Geology, 36, no. 3*, p. 267-270.

Gardner, J., & Knopoff, L. (1974). Is the sequence of earthquakes in southern California, with aftershocks removed, Poissonian? *Bulletin of the Seismological Society of America Vol. 64*, p. 1363-1367.

Gedney, L., & Shapiro, L. (1975). Structural lineaments, seismicity and geology of the Talkeetna Mountains area, Alaska: Unpublished report prepared for the U.S. Army Corps of Engineers, Alaska Division. 18 pgs.

Glen, J., Schmidt, J., & and Morin, R. (2007b). Gravity and magnetic character of south-central Alaska: Constraints on geologic and tectonic interpretations, and implications for mineral exploration. In K. Ridgway, J. Trop, J. Glen, a. O'Neill, & e. J.M., *Tectonic Growth of a Collisional Continental Margin: Crustal Evolution of Southern Alaska: Geological Society of America Special Paper 431* (pp. 593-622).

Glen, J., Schmidt, J., Pellerin, L., McPhee, D., & O'Neill, J. (2007). Crustal structure of Wrangellia and adjacent terranes inferred from geophysical studies along a transect through the northern Talkeetna Mountains, in Ridgway.

Glen, J., Schmidt, J., Pellerin, L., McPhee, D., & O'Neill, J. (2007a). Crustal structure of Wrangellia and adjacent terranes inferred from geophysical studies along a transect through the northern Talkeetna Mountains. In K. Ridgway, J. Trop, J. Glen, & J. e. O'Neill, *Tectonic Growth of a Collisional Continental Margin: Crustal Evolution of Southern Alaska: Geological Society of America Special Paper 431* (pp. 21-41).

Golder Associates, Inc. (2013). Interim geotechnical data report AEA11-022, Final Draft Report Ver. 0, REP-11-0001-031313. *Prepared for Alaska Energy Authority*, 592 p.

Gregor, N. & et al. (2012). Vertical to Horizontal (V/H) Ratios for Large Megathrust Subduction Zone Earthquakes. *World Conference Earthquake Engineering (WCEE). Lisboa, 2012.*

Gülerce, Z., & Abrahamson, N. (2011). Site-Specific Design Spectra for Vertical Ground Motion. *Earthquake Spectra, Vol. 27, no. 4, November 2011; VC 2011, Earthquake Engineering Research Institute*, p. 1023–1047.

Haeussler, P. (1998). Surficial geologic map along the Castle Mountain fault between Houston and Hatcher Pass Road, Alaska. *U.S. Geological Survey Open-File Report OF-98-480*, scale 1:25,000, 1 sheet.

Haeussler, P. (2008). An overview of the neotectonics of interior Alaska—Far-field deformation from the Yakutat Microplate collision. In J. Freymueller, P. Haeussler, R. Wesson, G. Ekstrom, & eds., *Active tectonics and seismic potential of Alaska: American Geophysical Union, Geophysical Monograph 179* (pp. 83-108).

Haeussler, P. J., Best, T., & Waythomas, C. F. (2002). Paleoseismology at high latitudes: Seismic disturbance of late Quaternary deposits along the Castle Mountain fault near Houston. *Geol. Soc. Am. Bull. 114*, p. 1296-1310, I Plate.

Haeussler, P. J., Bruhn, R., & Pratt, T. (2000). Potential seismic hazards and tectonics of upper Cook Inlet basin, Alaska, based on analysis of Pliocene and younger deformation. *Geol. Soc. Am. Bull., 112*, p. 1414-1429.

Haeussler, P. J., Schwartz, D., Dawson, T., Stenner, H., Lienkaemper, J., Sherrod, B., et al. (2004). Surface rupture and slip distribution of the Denali and Totschunda faults in the 3 November 2002 Ml.9 earthquake, Alaska. *Bull. Seismol. Soc. Am. 96(6B)*, S23-S52.

Haeussler, P., & Anderson, R. (1995). The "Twin Peaks Fault": Not a tectonic or seismogenic structure. In J. Dumoulin, & J. Gray, *Geologic studies in Alaska by the U.S. Geological Survey, 1995: U.S. Geological Survey Professional Paper 1574* (pp. 93-99).

Haeussler, P., Saltus, R., Karl, S., & Ruppert, N. (2008). Evidence for Pliocene to present thrust faulting on the south side of the Alaska Range in the vicinity of the Peters Hills piggyback basin, Eos Trans. *AGU, 89 (53)* , Fall Meet. Suppl., Abstract T44A-08.

Hake, C. A., & Cloud, W. K. (1966). United States Earthquakes 1964, Coast and Geodetic Survey. *U.S. Government Printing Office*, 91 p.

Harza-Ebasco. (1984). Susitna Hydroelectric Project Watana Development Winter 1983 Geotechnical Exploration Program.

ICOLD. (2011). Committe on Seismic Aspects of Dam Design . *Reservoirs and Seismicity - State of Knowledge*.

Idriss, I., & Archuleta, R. (2007). *Evaluation of earthquake ground motions, draft manuscript for FERC Chapter 13, draft 06.5.* Retrieved October 6, 2011, from http://www.ferc.gov/industries/hydropower/safety/guidelines/eng-guide/chap13-draft.pdf

Jicha, B., Scholl, D., Singer, B., Yogodzinski, G., & Kay, S. (2006). Revised age of Aleutian Island Arc formation implies high rate of magma production. *Geology, No. 8*, p661-664.

Kachadoorian, R., & Moore, H. (1979). Preliminary report of the recent geology of the proposed Devils Canyon and Watana dam sites, Susitna River, Alaska: in Southcentral Railbelt Area, Alaska Upper Susitna River Basin Supplemental Feasibility Report. *Alaska District, Corp of Engineers, Dept. of the Army*, Appendix D.

Kalbas, J., Ridgway, K., & and Gehrels, G. (2007). Stratigraphy, depositional systems, and provenance of the Lower Cretaceous Kahiltna assemblage, western Alaska Range: Basin development in response to oblique collision. In K. Ridgeway, J. Trop, J. Glen, & J. O'Neil, *Tectonic Growth of a Collisional Continental Margin: Crustal Evolution of Southern Alaska: Geological Society of America Special Paper 431* (pp. 307-343).

Kaul, M. K. (1978). Spectrum-consistent time-history generation. *ASCE Journal of Engineering Mechanics*, 781-788.

Koehler, R. (2013). *Quaternary Faults and Folds (QFF): Alaska Division of Geological & Geophysical Surveys Digital Data Series 3*. Retrieved from http://maps.dggs.alaska.gov/qff/.

Koehler, R., & Reger, R. (2011). *Reconnaissance Evaluation of the Lake Clark Fault, Tyonek Area, Alaska, Division of Geological & Geophysical Surveys Preliminary Interpretive Report.*

Koehler, R., Farrell, R., Burns, P., & and Combellick, R. (2012). Quaternary faults and folds in Alaska: A digital database. 31 p., 1 sheet, scale 1:3,700,000.

Koehler, R., Farrell, R.-E., Burns, P., Combellick, R., & Weakland, J. (2011a). Digital release of the Alaska Quaternary fault and fold database. *American Geophysical Union annual meeting*.

Koehler, R., Personius, S., Schwarz, D., Haeussler, P., & Seitz, G. (2011b). A Paleoseismic study along the central Denali Fault, Chistochina Glacier area, south-central Alaska. *Alaska Division of Geological & Geophysical Surveys Report of Investigation 2011-1*, 17 p.

Koehler, R., Reger, R., Carver, G., Spangler, E., & Gould, A. (2014). Castle Mountain fault south central Alaska: Observations on slip partitioning from lidar and paleoseismic trenching. *Geological Society of America, Abstracts with Programs, Vol. 46, no. 6*, p. 681.

Lahr, J. C., Page, R. A., Stephens, C. D., & Fogleman, a. K. (1986). Sutton, Alaska, earthquake of 1984: Evidence for activity on the Talkeetna segment of the Castle Mountain fault system. *Bulletin of the Seismological Society of America 76*, 967-983.

Lilhanand, K., & Tseng, W. S. (1987). Generation of synthetic time histories compatiable with multiple-damping response spectra. *SMiRT-9, Lausanne*, K2/10.

Lilhanand, K., & Tseng, W. S. (1988). Development and application of realistic earthquake time histories compatible with multiple damping response spectra. *Ninth World Conference Earthquake Engineering Vol. II* , (pp. 819-824). Tokyo, Japan.

Luco, N., & Bazzurro, P. (2007). Special Issue: Seismic Reliability Analysis of Structures. *Earthquake Engineering & Structural Dynamics Vol. 36, issue 13*, p. 1813-1835.

Matmon, A., Schwartz, D., Haeussler, P., Finkel, R., Lienkaemper, J., Stenner, H., et al. (2006). Denali fault slip rates and Holocene–late Pleistocene kinematics of central Alaska. *Geology, Vol. 34*, p. 645-648.

McGuire, R. K. (1995). Probabilistic Seismic Hazard Analysis and Design Earthquakes: Closing the Loop. *Bulletin of the Seismological Society of America, 85(5),* p. 1275-1284.

Mériaux, A., Sieh, K., Finkel, R., Rubin, C., Taylor, M., Meltzner, A., et al. (2009). Kinematic behavior of southern Alaska constrained by westward decreasing postglacial slip rates on the Denali Fault. *Alaska: Journal of Geophysical Research, Vol. 114*, B03404.

MWH. (2013a9). Preliminary Reservoir Triggered Seismicity. *Report prepared for Alaska Energy Authority, Technical Memorandum No. 10 v3.0*, Dated March 29, 2013, 95 pages.

MWH. (2013b). Preliminary Reservoir Slope Stability Assessment. *Report prepared for Alaska Energy Authority, Technical Memorandum No. 12*, Dated September 18, 2013, 43 pages and 3 attachments.

MWH. (2014). Geotechnical Data Report 2011-2014. *14-34-REP, Ver. 0*, 1314 p.

MWH. (2014b). Preliminary Design Criteria, prepared for Alaska Energy Authority , Technical Memorandum No. 4 v1.0, 76 pages.

MWH. (2014c). Engineering Feasibility Report for the Susitna-Watana Dam. *Report prepared for Alaska Energy Authority*, December 2014.

Nishenko, S. P., & Jacob, K. H. (1990). Seismic Potential of the Queen-Charlotte-Alaska-Aleutian Seismic Zone. *Journal of Geophysical Research-Solid Earth and Planets, Vol. 95, Issue B3*, p. 2511-2532.

Nokleberg, W. J., Jones, D. L., & Silberling, N. J. (1985). Origin and tectonic evolution of the Maclaren and Wrangellia terranes, eastern Alaska Range, Alaska. *Bulletin of the Seismological Society of America, 96*, p 1251-1270.

O'Neill, J., Schmidt, J., Glen, J., & Pellerin, L. (2003b). Mesozoic and Tertiary structural history of the northern Talkeetna Mountains, Paper 230-11. *Geological Society of America Abstracts with Programs, Vol. 35, no. 6*, p. 560.

O'Neill, M., Schmidt, J., & Cole, R. (2005). Cenozoic intraplate tectonics— lithospheric right-lateral bulk shear deformation in the northern Talkeetna Mountains, south-central Alaska. *Geological Society of America Abstracts with Programs, Vol. 37, no. 7,*, p. 79.

Pacific Earthquake Engineering Research (PEER). (2007, May 16). Retrieved from Pacific Engineering Research Center Database: http://peer.berkeley.edu/nga

Plafker, G. (1969). Tectonics of the March 27, 1964, Alaska earthquake. *U.S. Geological Survey Professional Paper 543-I,*, 74 p.

Plafker, G., Carver, G., Cluff, L., & and Metz, M. (2006). Historic and paleo-seismic evidence for non-characteristic earthquakes and the seismic cycle at the Delta River crossing of the Denali fault, Alaska [abs.]. *102nd Annual Meeting of the Cordilleran Section, Geological Society of America, May 8-10, Anchorage, Alaska Vol. 38*, 96 p.

Plafker, G., Gilpin, L., & Lahr, J. (1994). Neotectonic map of Alaska. (a. H. edited by G. Plafker, Ed.) *The Geology of Alaska, The Geology of North America, Vol. G-f, Plate 12,*.

R & M Consultants (R&M). (2009). Task 1- Seismic Setting Review, Susitna Hydroelectric Project. R&M No.1158.21.

Ratchkovski, N. A., Hansen, R., Stanching, J., Cox, T., Fox, O., Rio, L., et al. (2003). Aftershock sequence of the Mw 7.9 Denali fault, Alaska, earthquake of 3 November 2002 from regional seismic network data. *Seism. Res. Lett., 74*, 743-752.

Ratchkovski, N. A., Wiemer, S., & Hansen, R. (2004). Seismotectonics of the Central Denali Fault, Alaska, and the 2002 Denali Fault Earthquake Sequence. *Bulletin of the Seismological Society of America, Vol. 94, No. 6B*, p. S156-S174.

Ratchkovski, N., & Hansen, R. (2002). New evidence for segmentation of the Alaska subduction zone. *Bulletin of the Seismological Society of America, 92*, p. 1754-1765.

Reed, B. L., & Lanphere, M. A. (1974). Offset plutons and history of movement along the McKinley segment of the Denali fault system, Alaska. *Geol. Soc. Am. Bull., 85*, P. 1883-1892.

Reger, R., Bundtzen, T., & Smith, T. (1990). Geologic map of the Healy A-3 quadrangle, Alaska. *Alaska Division of Geological and Geophysical Surveys Public data file 90-1*, scale 1:63,360.

Ridgway, K. D., Trop, J., Nokleberg, W. J., Davidson, C., & Eastham, K. R. (2002). Mesozoic and Cenozoic tectonics of the eastern and central Alaska Range: Progressive basin development and deformation in a suture zone. *Bulletin of the Seismological Society of America, 114*, p. 1480-1504.

Ridgway, K., Trop, J., Glen, J., and O'Neill, J., & eds. (2007). Tectonic Growth of a Collisional Continental Margin: Crustal Evolution of Southern Alaska:. *Geological Society of America Special Paper 431*, 21-41.

Ruppert, N., & Hansen, R. (2010). Temporal and spatial variations of local magnitudes in Alaska and Aleutians and comparison with body-wave and moment magnitudes. *Bulletin of the Seismological Society of America, 100*, p. 1174-1183.

Schwartz, D., & (DFEWG), t. D. (2003). Paleo-earthquakes on the Denali–Totschunda fault system—Preliminary observations of slip and timing. *American Geophysical Union, fall meeting*.

Silva, W., Abrahamson, N., Toro, G., & Costantino, C. (1996). *Description and Validation of the Stochastic Ground Motion Model.* El Cerrito: Pacific Engineering and Analysis.

Smith, T., Albanese, M., & Kline, G. (1988). Geologic map of the Healy A-2 quadrangle. *Alaska Division of Geological and Geophysical Surveys Professional Report 95*, Scale 1:63,360.

Stout, J., & Chase, C. (1980). Plate kinematics of the Denali fault system. *Canadian Journal of Earth Sciences, Vol. 17*, p. 1527-1537.

Stover, C., & Coffman, J. (1993). Seismicity of the United States, 1568-1989 (Revised). *U.S. Geological Survey Professional Paper 1527*, p. 415.

Trop, J., & Ridgway, K. (2007). Mesozoic and Cenozic growth of southern Alaska: A sedimentary basin perspective. In K. T. Ridgway, *Tectonic Growth of a Collisional*

*Continental Margin: Crustal Evolution of Southern Alaska: Geological Society of America Special Paper 431* (pp. 55-94).

Twelker, E., Wypych, A., Sicard, K., Newberry, R., Freeman, L., Reioux, D., et al. (2014). Preliminary results from 2014 geologic mapping in the Talkeetna Mountains (presentation): Alaska Miners Association Annual Convention, Anchorage, Alaska, November 3-9, 2014. *Alaska Division of Geological & Geophysical Surveys file po2014_007.pdf*.

U.S. Army Corps of Engineers (USACE). (1979). *Preliminary report of the recent geology of the proposed Devils Canyon and Watana dam sites, Susitna River, Alaska: in Southcentral Railbelt Area, Alaska Upper Susitna River Basin Supplemental Feasibility Report.* Alaska District, Corp of Engineers, Dept. of the Army.

US Committee on Large Dams (USCOLD). (1997). *Reservoir Triggered Seismicity.*

USGS. (2003). Retrieved from http://earthquake.usgs.gov/earthquakes/eqinthenews/2002/uslbbl/images/AK_mmi_new.jpg

Watson-Lamprey, J., & Abrahamson, N. (2005). Selection of ground motion time series and limits on scaling. *Soil Dynamics and Earthquake Engineering 26 (2006)* , 477-482.

Weber, F. R., & Turner, D. L. (1977). A late Tertiary thrust fault in the central Alaska Range. *US. Geol. Surv. Circ., 751-B*, B66-B67.

Wesson, R., Boyd, O., Mueller, C., Bufe, C., Frankel, A., & Petersen, M. (2007). Revision of time-Independent probabilistic seismic hazard maps for Alaska: U.S. Geological Survey Open-File Report 2007-1043.

Williams, J., & Galloway, J. (1986). Map of western Copper River basin, Alaska, showing lake sediments and shorelines, glacial moraines, and location of stratigraphic sections and radiocarbon-dated samples. *U.S. Geological Survey Open File Report 86-390*, 30 p., 1 sheet, scale 1:250,000.

Willis, J. B., Haeussler, P., Bruhn, R., & and Willis, G. (2007). Holocene slip rate for the western segment of the Castle Mountain fault, Alaska. *Bulletin of the Seismological Society of America*, 1019-1024.

Willis, J., & Bruhn, R. (2006). Active tectonics of the Susitna River basin, Alaska-intraplate deformation driven by microplate collision and subduction. *Geol. Soc. Am. Abstr. Programs, 38(5)*, 96.

Wilson, F. H., Schmoll, H., Haeussler, P., Schmidt, J., Yehle, L., & Labay, K. (2009). Preliminary Geologic Map of the Cook Inlet Region. *Alaska U.S. Geological Survey Open-File Report 2009-1108*, 54 p., 2 sheets.

Wilson, F., Dover, J., Bradley, D., Weber, F., Bundtzen, T., & Haeussler, P. (1998). Geologic map of central (interior) Alaska. *U.S. Geological Survey Open-File Report 98-0133-B*, 63. p, 3 sheets.

Wong, I., Thomas, P., & Abrahamson, N. (2004). The PEER-Lifelines validation of software used in probabilistic seismic hazard analysis. (M. Yegian, & E. Kavazanjian, Eds.) *American Society of Civil Engineers, Geotechnical Special Publication No. 126*, p. 807-815.

Woodward Clyde Consultants (WCC). (1982). *Final Report on Seismic Studies for Susitna Hydroelectric Project.*

Woodward-Clyde Consultants (WCC). (1980). *Interim Report on Seismic Studies at Susitna Hydroelectric Project: Report prepared for Acres America Inc.* Orange: Woodward-Clyde Consultants.

Yeats et al. (1997). Reservoir Triggered Seismicity. *USCOLD Committee on Earthquakes*.

Zhao, D., Christensen, D., & Pulpan, H. (1995). Tomographic imaging of the Alaskan Subduction Zone. *J. Geophys. Res., 100*, 6487-6504.

Zhao, D., Christensen, D., & Pulpan, H. (1995). Tomographic imaging of the Alaska subduction zone. *Journal of Geophysical Research, 100, B4*, p. 6487-6504.

Zhao, J., Zhang, J., Asano, A., Ohno, Y., Oouchi, T., Takahashi, T., et al. (2006). Attenuation relations of strong ground motion in Japan using site classification based on predominant period. *Bulletin of the Seismological Society of America, Vol. 96*, p. 898-913.